Panyasrivanit *et al.*, 2009) by using Western blotting to detect the increased formation of the autophagy-associated form of LC3, LC3-II, in response to DENV-3 infection. To verify the action of 3-MA, L-Asn and rapamycin on autophagy in control cells, we confirmed the reduction of LC3-II in response to 3-MA (Fig. 2f), as well as the increase of LC3-II in response to both rapamycin and L-Asn (Fig. 2g). In L-Asn-treated cells, the normal degradation of LC3-II that occurs upon fusion of autophagosomes with lysosomes is prevented as fusion with lysosomes is inhibited, resulting in accumulation of LC3-II (Eskelinen, 2005; Mizushima & Yoshimori, 2007). In response to DENV-3 infection, a significant increase in LC3-II was observed for up to 3 days p.i. (Fig. 2h) and examination of earlier time points showed that increased LC3-II was detectable as early as 6 h p.i. (Fig. 2i).

To confirm the induction of autophagy by DENV-3 infection, confocal microscopy was used to detect increased co-localization of LC3 and LAMP1. In this analysis, cells

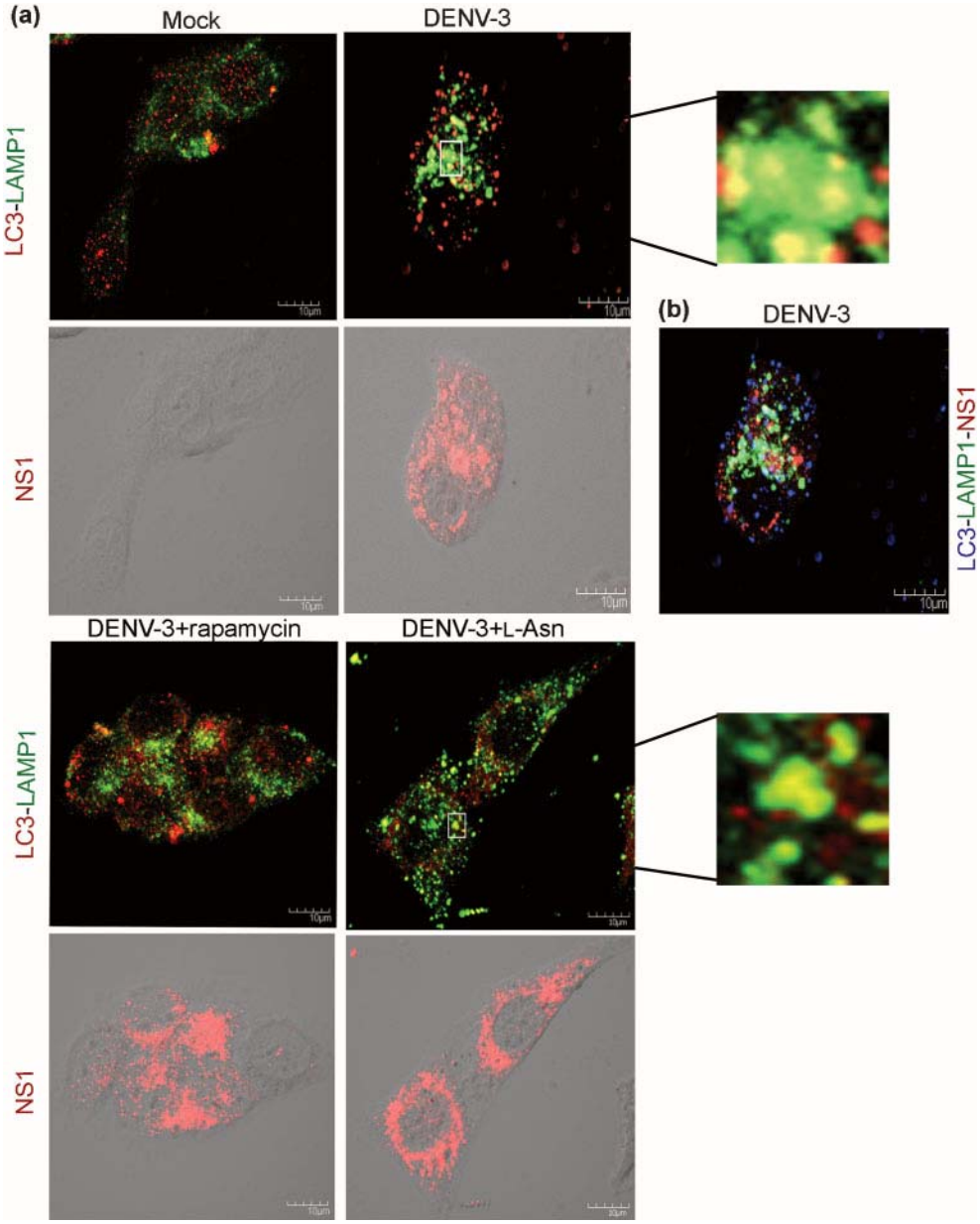

Fig. 3. Induction of autophagy in response to DENV-3 infection. (a) HepG2 cells were grown on glass coverslips and either mock-infected or infected with DENV-3 either directly or in the presence of rapamycin or L-Asn. Cells were examined simultaneously for the localization of LC3 (far-red), LAMP1 (green) and separately for NS1 (red) (a) or simultaneously for LC3 (blue), LAMP1 (green) and NS1 (red) in infected cells only (b).

Table 1. Summary of Pearson correlation coefficients of LC3, LAMP1, NS1, dsRNA and cathepsin D (CD) for DENV-3- and DENV-2-infected cells grown in the presence or absence of autophagy inhibitors

	Pearson correlation coefficient	
	DENV-3	DENV-2*
LC3–LAMP1	0.33 ± 0.04	0.34 ± 0.03
LC3–LAMP1 (rapamycin)	0.49 ± 0.01	0.55 ± 0.03
LC3–LAMP1 (L-Asn)	0.54 ± 0.05	0.46 ± 0.03
LC3–NS1	0.15 ± 0.08	0.44 ± 0.05
LC3–NS1 (L-Asn)	0.37 ± 0.03	0.51 ± 0.05
LC3–dsRNA	0.22 ± 0.03	0.35 ± 0.07
LC3–dsRNA (L-Asn)	0.47 ± 0.04	0.45 ± 0.06
CD–dsRNA	0.28 ± 0.05	0.19 ± 0.01
CD–dsRNA (L-Asn)	0.06 ± 0.05	–

*Data from Panyasrivanit *et al.* (2009).

were additionally stained with NS1 simultaneously to ensure that co-localization of LC3 and LAMP1 was assessed in infected cells. This experiment was undertaken in parallel with cells infected with DENV-3 in the presence of rapamycin or L-Asn and mock-infected cells. Results showed that co-localization between LC3 and LAMP1 significantly increased in DENV-3-infected cells (Pearson correlation coefficient 0.33, 95 % CI 0.29–0.37) compared with mock-infected cells (Pearson correlation coefficient 0.23, 95 % CI 0.21–0.25; $P=0.001$) (Fig. 3a). Significantly greater co-localization was seen in infected cells treated with rapamycin (Pearson correlation coefficient 0.49, 95 % CI 0.48–0.50; $P<0.001$ compared with DENV-3 infected cells) and in infected cells treated with L-Asn (Pearson correlation coefficient 0.54, 95 % CI 0.50–0.60; $P<0.001$ compared with DENV-3-infected cells). A degree of co-localization between LAMP1, LC3 and NS1 was observed in DENV-3-infected cells (Fig. 3b).

Both LC3-II analysis and confocal analysis of LC3–LAMP1 co-localization show that autophagy is induced in DENV-3-infected HepG2 cells. The degree of co-localization observed between LC3 and LAMP1 in DENV-3-infected cells was comparable to that previously observed in DENV-2-infected cells, as was the co-localization between LC3 and LAMP1 seen in either DENV-3- or DENV-2-infected cells treated with either rapamycin or L-Asn (Table 1 and Panyasrivanit *et al.*, 2009). We note that the level of LC3 and LAMP1 co-localization in mock-infected cells was slightly higher in this study than that determined previously (Panyasrivanit *et al.*, 2009), but it has been observed that the amount of LC3-II (the membrane-bound form which co-localizes with LAMP1) can fluctuate greatly when cells are cultured at different times, even when identical conditions are used (Mizushima & Yoshimori, 2007).

To determine whether the DENV-3 translation/replication complex is associated with autophagic vesicles, as seen with DENV-2 (Panyasrivanit *et al.*, 2009), infected cells were examined for the co-localization of LC3 and NS1 protein (Fig. 4a). A very low level of co-localization was observed between LC3 and NS1 in DENV-3-infected cells (Pearson correlation coefficient 0.15, 95 % CI 0.08–0.24), which is in contrast with results seen previously with DENV-2 (Table 1 and Panyasrivanit *et al.*, 2009). The level of co-localization between LC3 and NS1 was significantly increased when infection occurred in the presence of L-Asn (Pearson correlation coefficient 0.38, 95 % CI 0.35–0.41; $P<0.001$). The increase in co-localization of NS1 and LC3 in DENV-3-infected cells in the presence of L-Asn was coupled with increased levels of NS1 (Fig. 4b). A slight increase in NS1 levels was observed in DENV-2-infected cells in the presence of L-Asn compared with control infection (Fig. 4c). The low level of co-localization between NS1 and LC3 in DENV-3-infected cells and the increase in co-localization seen when lysosomal fusion is inhibited with L-Asn, suggests that, in contrast to DENV-2 where pre-lysosomal vacuoles (amphisomes or autophagosomes) are the site of translation/replication (Panyasrivanit *et al.*, 2009), post-lysosomal fusion vacuoles (autophagolysosomes) may play a role in DENV-3 infection (Fig. 1).

We therefore investigated whether autophagolysosomes were associated with NS1 in DENV-3-infected cells using cathepsin D, a constituent of mature autophagolysosomes (Eskelinen *et al.*, 2002). A similar level of co-localization between cathepsin D and NS1 was observed in DENV-3-infected cells as the level previously found between LC3 and NS1 (Fig. 4d; Pearson correlation coefficient 0.17, 95 % CI 0.12–0.22). Importantly, co-localization between Cathepsin D and NS1 was significantly reduced in the presence of L-Asn (Fig. 4d; Pearson correlation coefficient 0.084, 95 % CI 0.04–0.12; $P<0.05$). Therefore, both the increase in co-localization between LC3 and NS1 and the reduction of co-localization between cathepsin D and NS1 when DENV-3 infection occurs in the presence of L-Asn suggest that NS1 is divided between both pre- and post-lysosomal fusion autophagic vacuoles.

These results serve to differentiate between DENV-2 and DENV-3 infections. In DENV-2 infections, NS1 is predominantly associated with pre-lysosomal fusion vacuoles; treatment with L-Asn to inhibit lysosomal fusion and the formation of autophagolysosomes results in only a marginal and non-significant increase in co-localization between LC3 and NS1 (Panyasrivanit *et al.*, 2009) and only a marginal increase in the levels of NS1 (Fig. 4c). In contrast, in DENV-3-infected cells, NS1 is associated with both pre- and post-lysosomal fusion vacuoles and treatment with L-Asn results in a significant increase in the levels of NS1 (Fig. 4b), a significant increase in co-localization between LC3 and NS1 (Fig. 4a) and a decrease in co-localization between cathepsin D and NS1 (Fig. 4d).

To investigate the location of the DENV-3 replication complex on autophagic pre-lysosomal fusion vacuoles, the localization of dsRNA was investigated in relation to LC3

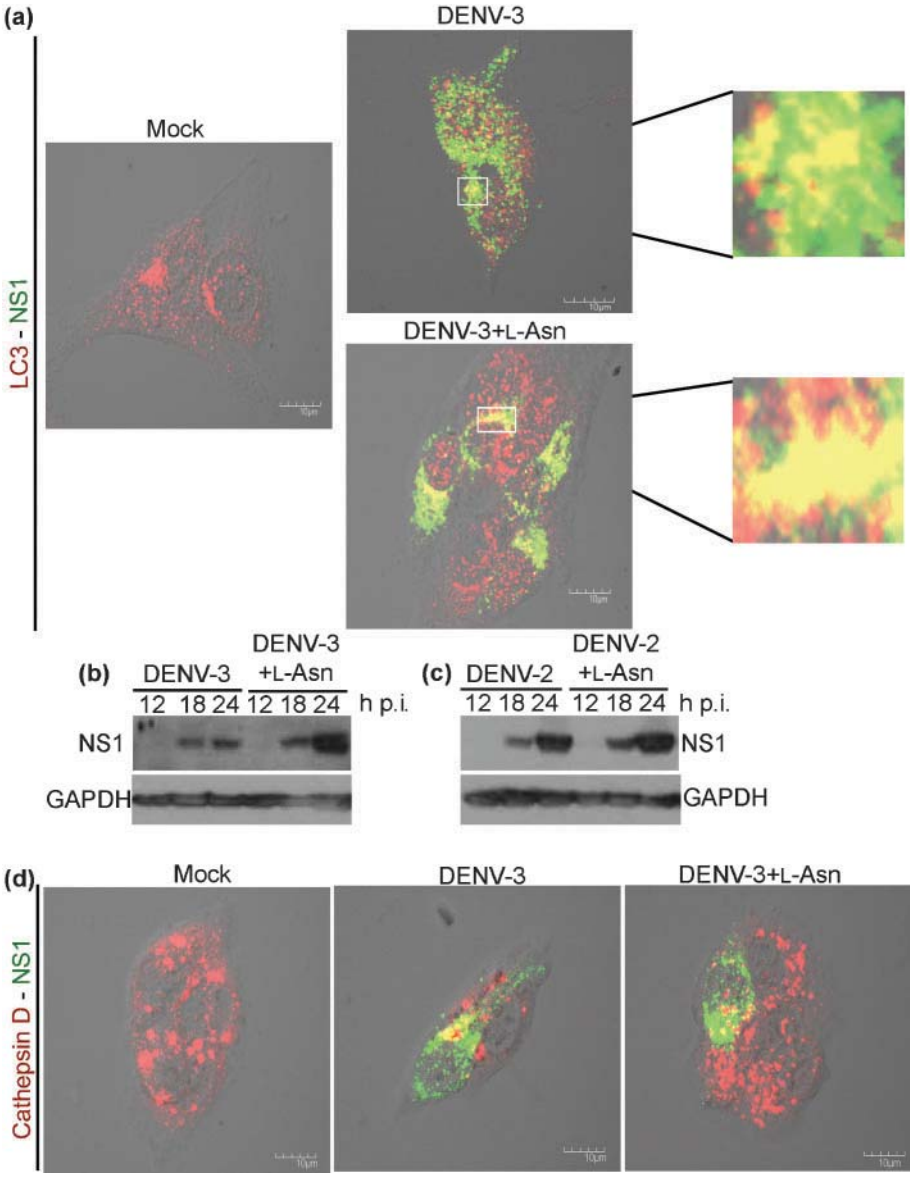

Fig. 4. NS1 in DENV-3-infected HepG2 cells. HepG2 cells grown on glass coverslips (a and d) or in culture (b and c) were either mock-infected or infected with DENV-3 (a, b and d) or DENV-2 (c) in the presence or absence of L-Asn. Cells were examined for co-localization of NS1 with LC3 (a) or NS1 with cathepsin D (d) or for the level of NS1 by Western blotting with GAPDH as a control (b and c). LC3 and cathepsin D are shown as red; NS1 is shown as green.

and to LC3 and MPR. Limited co-localization was observed between dsRNA and LC3 (Pearson correlation coefficient 0.22, 95 % CI 0.19–0.25) which significantly increased in the presence of L-Asn (Pearson correlation coefficient 0.48, 95 % CI 0.44–0.52; $P<0.001$) (Fig. 5a); triple localization of LC3, dsRNA and MPR identified the pre-lysosomal fusion structures as amphisomes (Fig. 5b), which is also seen in DENV-2 (Panyasrivanit *et al.*, 2009). As with DENV-2, ribosomal proteins were found to be co-localized with DENV-3 dsRNA (Fig. 5c), suggesting the capacity for translation exists at the replication complex on amphisomes.

To investigate the localization of the replication complex on post-lysosomal fusion vacuoles, the co-localization of cathepsin D and dsRNA was investigated at 24 h p.i. A degree of co-localization was observed between dsRNA and cathepsin D (Pearson correlation coefficient 0.28, 95 % CI 0.23–0.33); this decreased significantly when infection occurred in the presence of L-Asn (Pearson correlation coefficient 0.06, 95 % CI 0.01–0.11; $P<0.001$) (Fig. 6a), similar to the results seen for NS1. This again suggests that DENV-3 utilizes both pre- and post-lysosomal fusion vacuoles as translation/replication sites, in contrast with DENV-2, which has been proposed to use only pre-

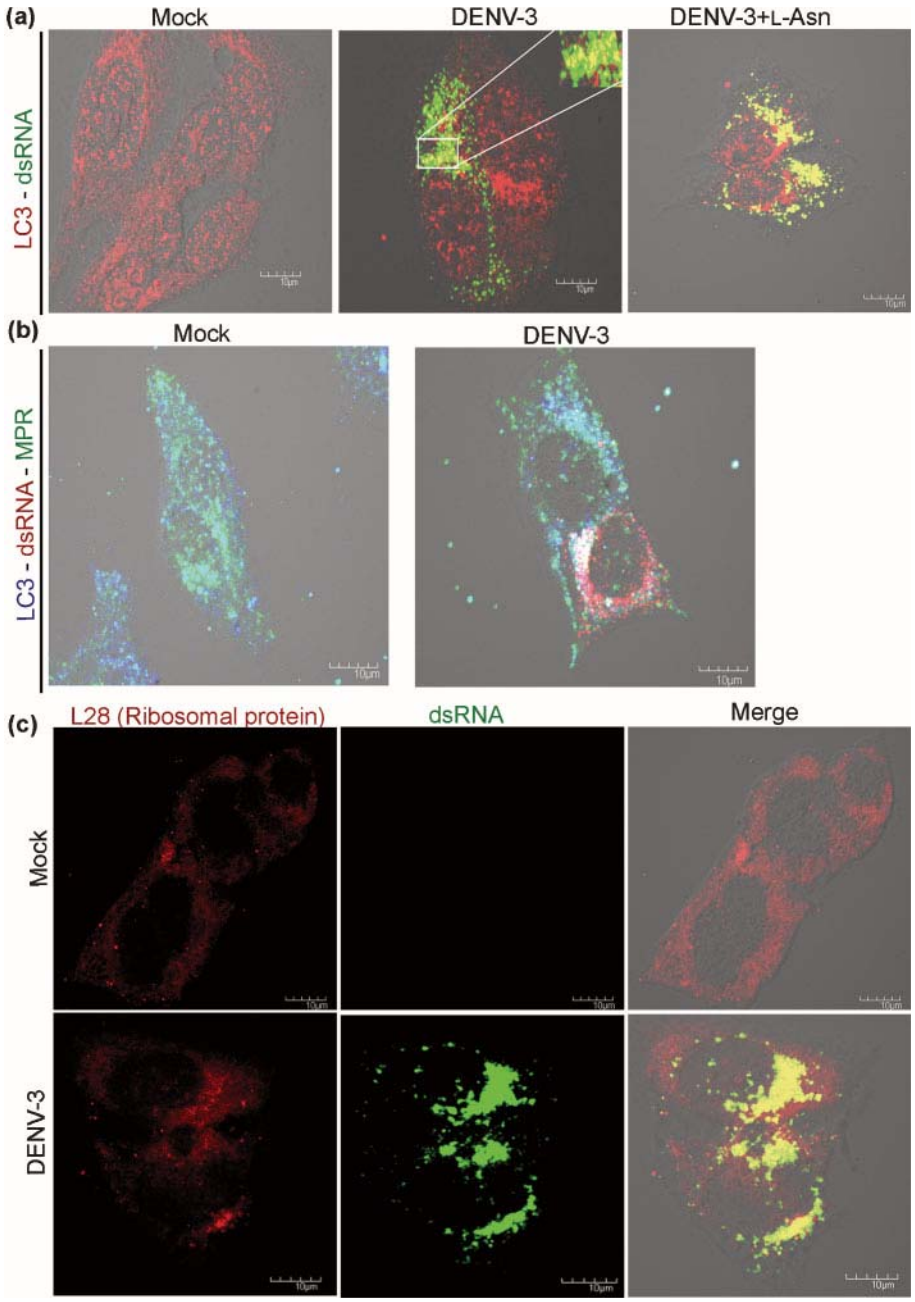

Fig. 5. Location of dsRNA in DENV-infected cells. HepG2 cells grown on glass coverslips were infected with DENV-3 in the presence or absence of L-Asn and examined for either the co-localization of LC3 (red) and dsRNA (green) (a), MPR (green), LC3 (far-red, false-coloured as blue in this figure) and dsRNA (red) (b) or ribosomal protein L28 (red) and dsRNA (green) (c).

lysosomal vacuoles. To provide further evidence to support this hypothesis, we investigated the co-localization of DENV-2 dsRNA and cathepsin D (Fig. 6a) and found, as expected, that DENV-2 dsRNA shows a significantly lower level of co-localization with cathepsin D (Pearson correlation coefficient 0.19, 95 % CI 0.18–0.20; $P=0.007$) compared with DENV-3 dsRNA. To provide further evidence, both earlier and later time points in the DENV replication cycle were examined. At 15 h p.i., co-localization between cathepsin D and dsRNA was significantly higher in DENV-3-infected samples (Pearson correlation coefficient 0.227, 95 % CI 0.19–0.27) than in DENV-2-infected samples (Pearson correlation coefficient 0.104, 95 % CI 0.07–0.13; $P<0.001$) (Fig. 6b). Similarly, at 36 h p.i., co-localization was higher in DENV-3-infected samples (Pearson correlation coefficient 0.229, 95 % CI 0.17–0.29) than in DENV-2-infected samples (Pearson correlation coefficient 0.093, 95 % CI 0.06–0.12; $P=0.003$) (Fig. 6b).

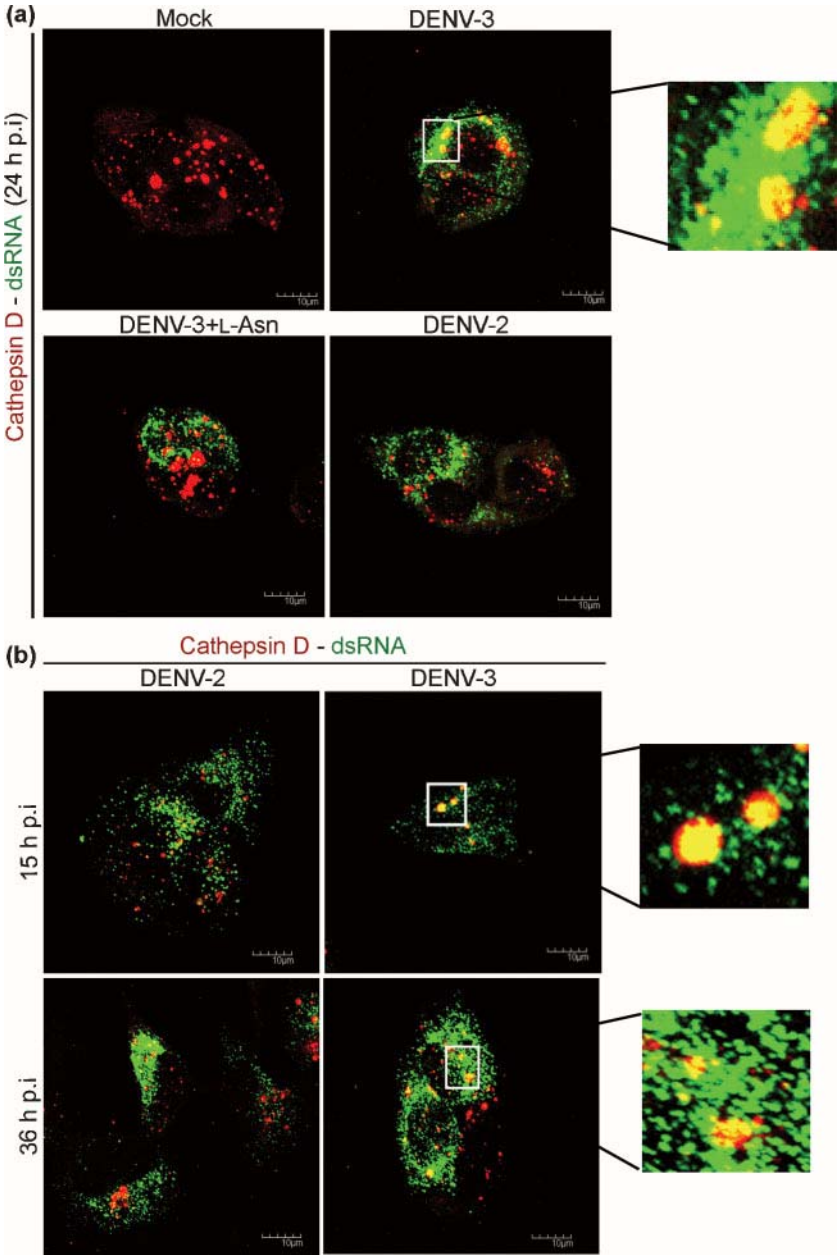

Fig. 6. Co-localization of cathepsin D and dsRNA in DENV-infected HepG2 cells. HepG2 cells grown on glass coverslips were infected with DENV-2 or DENV-3 in the presence or absence of L-Asn and examined for co-localization between cathepsin D (red) and dsRNA (green) at 24 h (a) and at 15 and 36 h (b) p.i.

We have previously shown that DENV-2 uses pre-lysosomal fusion amphisomes as a site for translation and replication, and that infection in the presence of L-Asn results in an increase of intracellular and extracellular virus, suggesting that lysosomal fusion results in loss of virus viability (Panyasrivanit *et al.*, 2009). As shown here, this is in contrast with DENV-3 which uses both amphisomes and autophagolysosomes as part of its replication strategy. Infection in the presence of L-Asn decreases both intracellular and extracellular virus yields, suggesting that interaction with the autophagolysosome is required for completion of the DENV-3 life cycle. However, while the interaction with the autophagolysosome is beneficial in terms of DENV-3 production, it is detrimental to the replication complexes, as demonstrated by the increase of NS1 in DENV-3 infections in the presence of L-Asn. Overall, our results are consistent with both DENV-2 and DENV-3 utilizing the endosomal–autophagosomal fusion pathway to gain entry into the cell and undertake translation and replication (Fig. 1). However, in detail, DENV-2 and DENV-3 employ significantly different translation/replication strategies.

Both this study and our previous study (Panyasrivanit *et al.*, 2009) have investigated the interaction between DENV and autophagy in liver cells. While the role of liver cells in the pathogenesis of the disease has been somewhat controversial, a significant body of work exists that supports the

involvement of the liver in dengue infections (Seneviratne *et al.*, 2006) and we have shown previously that human primary liver hepatocytes are able to be productively infected by DENV (Suksanpaisan *et al.*, 2007). However, studies on other cell types are urgently required, particularly cells of a monocyte/macrophage lineage, as these cells are the primary mediators of dengue infection.

ACKNOWLEDGEMENTS

This work was supported by grants from the Thailand Research Fund and Mahidol University. A. K. is supported by a Mahidol University Research Thesis Scholarship, M. P. is supported by a Thai Royal Golden Jubilee Research Scholarship and N. W. is supported by a scholarship from the National Center for Genetic Engineering and Biotechnology, National Science and Technology Development Agency. We thank Prida Malasit for kindly providing the anti-NS1 antibody and Yuvadee Siriyasub for assistance with the confocal microscopy.

REFERENCES

Acosta, E. G., Castilla, V. & Damonte, E. B. (2008). Functional entry of dengue virus into *Aedes albopictus* mosquito cells is dependent on clathrin-mediated endocytosis. *J Gen Virol* **89**, 474–484.

Bampton, E. T., Goemans, C. G., Niranjan, D., Mizushima, N. & Tolkovsky, A. M. (2005). The dynamics of autophagy visualized in live cells: from autophagosome formation to fusion with endo/lysosomes. *Autophagy* **1**, 23–36.

Clyde, K., Kyle, J. L. & Harris, E. (2006). Recent advances in deciphering viral and host determinants of dengue virus replication and pathogenesis. *J Virol* **80**, 11418–11431.

Dunn, W. A., Jr (1990a). Studies on the mechanisms of autophagy: formation of the autophagic vacuole. *J Cell Biol* **110**, 1923–1933.

Dunn, W. A., Jr (1990b). Studies on the mechanisms of autophagy: maturation of the autophagic vacuole. *J Cell Biol* **110**, 1935–1945.

Eskelinen, E. L. (2005). Maturation of autophagic vacuoles in mammalian cells. *Autophagy* **1**, 1–10.

Eskelinen, E. L., Illert, A. L., Tanaka, Y., Schwarzmann, G., Blanz, J., Von Figura, K. & Saftig, P. (2002). Role of LAMP-2 in lysosome biogenesis and autophagy. *Mol Biol Cell* **13**, 3355–3368.

Espert, L., Codogno, P. & Biard-Piechaczyk, M. (2007). Involvement of autophagy in viral infections: antiviral function and subversion by viruses. *J Mol Med* **85**, 811–823.

Gordon, P. B. & Seglen, P. O. (1988). Prelysosomal convergence of autophagic and endocytic pathways. *Biochem Biophys Res Commun* **151**, 40–47.

Guzman, M. G. & Kouri, G. (2002). Dengue: an update. *Lancet Infect Dis* **2**, 33–42.

Halstead, S. B. (1988). Pathogenesis of dengue: challenges to molecular biology. *Science* **239**, 476–481.

Heinz, F. X., Stiasny, K. & Allison, S. L. (2004). The entry machinery of flaviviruses. *Arch Virol Suppl* **18**, 133–137.

Holmes, E. C. & Twiddy, S. S. (2003). The origin, emergence and evolutionary genetics of dengue virus. *Infect Genet Evol* **3**, 19–28.

Kabeya, Y., Mizushima, N., Ueno, T., Yamamoto, A., Kirisako, T., Noda, T., Kominami, E., Ohsumi, Y. & Yoshimori, T. (2000). LC3, a mammalian homologue of yeast Apg8p, is localized in autophagosome membranes after processing. *EMBO J* **19**, 5720–5728.

Kihara, A., Kabeya, Y., Ohsumi, Y. & Yoshimori, T. (2001). Beclin-phosphatidylinositol 3-kinase complex functions at the trans-Golgi network. *EMBO Rep* **2**, 330–335.

Kimura, S., Noda, T. & Yoshimori, T. (2007). Dissection of the autophagosome maturation process by a novel reporter protein, tandem fluorescent-tagged LC3. *Autophagy* **3**, 452–460.

Ko, K. K., Igarashi, A. & Fukai, K. (1979). Electron microscopic observations on *Aedes albopictus* cells infected with dengue viruses. *Arch Virol* **62**, 41–52.

Krishnan, M. N., Sukumaran, B., Pal, U., Agaisse, H., Murray, J. L., Hodge, T. W. & Fikrig, E. (2007). Rab 5 is required for the cellular entry of dengue and West Nile viruses. *J Virol* **81**, 4881–4885.

Lee, H. K. & Iwasaki, A. (2008). Autophagy and antiviral immunity. *Curr Opin Immunol* **20**, 23–29.

Lee, Y. R., Lei, H. Y., Liu, M. T., Wang, J. R., Chen, S. H., Jiang-Shieh, Y. F., Lin, Y. S., Yeh, T. M., Liu, C. C. & Liu, H. S. (2008). Autophagic machinery activated by dengue virus enhances virus replication. *Virology* **374**, 240–248.

Lerena, C., Calligaris, S. D. & Colombo, M. I. (2008). Autophagy: for better or for worse, in good times or in bad times. *Curr Mol Med* **8**, 92–101.

Levine, B. & Klionsky, D. J. (2004). Development by self-digestion: molecular mechanisms and biological functions of autophagy. *Dev Cell* **6**, 463–477.

Malavige, G. N., Fernando, S., Fernando, D. J. & Seneviratne, S. L. (2004). Dengue viral infections. *Postgrad Med J* **80**, 588–601.

Meijer, A. J. & Codogno, P. (2006). Signalling and autophagy regulation in health, aging and disease. *Mol Aspects Med* **27**, 411–425.

Miller, S. & Krijnse-Locker, J. (2008). Modification of intracellular membrane structures for virus replication. *Nat Rev Microbiol* **6**, 363–374.

Mizushima, N. & Yoshimori, T. (2007). How to interpret LC3 immunoblotting. *Autophagy* **3**, 542–545.

Mizushima, N., Noda, T., Yoshimori, T., Tanaka, Y., Ishii, T., George, M. D., Klionsky, D. J., Ohsumi, M. & Ohsumi, Y. (1998). A protein conjugation system essential for autophagy. *Nature* **395**, 395–398.

Mizushima, N., Yoshimori, T. & Ohsumi, Y. (2002). Mouse Apg10 as an Apg12-conjugating enzyme: analysis by the conjugation-mediated yeast two-hybrid method. *FEBS Lett* **532**, 450–454.

Mizushima, N., Levine, B., Cuervo, A. M. & Klionsky, D. J. (2008). Autophagy fights disease through cellular self-digestion. *Nature* **451**, 1069–1075.

Modis, Y., Ogata, S., Clements, D. & Harrison, S. C. (2004). Structure of the dengue virus envelope protein after membrane fusion. *Nature* **427**, 313–319.

Mukhopadhyay, S., Kuhn, R. J. & Rossmann, M. G. (2005). A structural perspective of the flavivirus life cycle. *Nat Rev Microbiol* **3**, 13–22.

Noda, T. & Ohsumi, Y. (1998). Tor, a phosphatidylinositol kinase homologue, controls autophagy in yeast. *J Biol Chem* **273**, 3963–3966.

Ohsumi, Y. (2001). Molecular dissection of autophagy: two ubiquitin-like systems. *Nat Rev Mol Cell Biol* **2**, 211–216.

Panyasrivanit, M., Khakpoor, A., Wikan, N. & Smith, D. R. (2009). Co-localization of constituents of the dengue virus translation and replication machinery with amphisomes. *J Gen Virol* **90**, 448–456.

Puttikhunt, C., Kasinrerk, W., Srisa-ad, S., Duangchinda, T., Silakate, W., Moonsom, S., Sittisombut, N. & Malasit, P. (2003). Production of anti-dengue NS1 monoclonal antibodies by DNA immunization. *J Virol Methods* **109**, 55–61.

Salonen, A., Ahola, T. & Kääriäinen, L. (2005). Viral RNA replication in association with cellular membranes. *Curr Top Microbiol Immunol* **285**, 139–173.

Seglen, P. O. & Gordon, P. B. (1982). 3-Methyladenine: specific inhibitor of autophagic/lysosomal protein degradation in isolated rat hepatocytes. *Proc Natl Acad Sci U S A* **79**, 1889–1892.

Seglen, P. O., Berg, T. O., Blankson, H., Fengsrud, M., Holen, I. & Strømhaug, P. E. (1996). Structural aspects of autophagy. *Adv Exp Med Biol* **389**, 103–111.

Seneviratne, S. L., Malavige, G. N. & de Silva, H. J. (2006). Pathogenesis of liver involvement during dengue viral infections. *Trans R Soc Trop Med Hyg* **100**, 608–614.

Sithisarn, P., Suksanpaisan, L., Thepparit, C. & Smith, D. R. (2003). Behavior of the dengue virus in solution. *J Med Virol* **71**, 532–539.

Suksanpaisan, L., Cabrera-Hernandez, A. & Smith, D. R. (2007). Infection of human primary hepatocytes with dengue virus serotype 2. *J Med Virol* **79**, 300–307.

Taylor, P. R., Gordon, S. & Martinez-Pomares, L. (2005). The mannose receptor: linking homeostasis and immunity through sugar recognition. *Trends Immunol* **26**, 104–110.

Thepparit, C. & Smith, D. R. (2004). Serotype-specific entry of dengue virus into liver cells: identification of the 37-kilodalton/67-kilodalton high-affinity laminin receptor as a dengue virus serotype 1 receptor. *J Virol* **78**, 12647–12656.

Thepparit, C., Phoolcharoen, W., Suksanpaisan, L. & Smith, D. R. (2004). Internalization and propagation of the dengue virus in human hepatoma (HepG2) cells. *Intervirology* **47**, 78–86.

van der Schaar, H. M., Rust, M. J., Waarts, B. L., van der Ende-Metselaar, H., Kuhn, R. J., Wilschut, J., Zhuang, X. & Smit, J. M. (2007). Characterization of the early events in dengue virus cell entry by biochemical assays and single-virus tracking. *J Virol* **81**, 12019–12028.

Xie, Z. & Klionsky, D. J. (2007). Autophagosome formation: core machinery and adaptations. *Nat Cell Biol* **9**, 1102–1109.

Journal of General Virology (2009), **90**, 448–456 **DOI** 10.1099/vir.0.005355-0

Co-localization of constituents of the dengue virus translation and replication machinery with amphisomes

Mingkwan Panyasrivanit, Atefeh Khakpoor, Nitwara Wikan and Duncan R. Smith

Correspondence
Duncan R. Smith
duncan_r_smith@hotmail.com

Molecular Pathology Laboratory, Institute of Molecular Biology and Genetics, Mahidol University, Thailand

Received 3 July 2008
Accepted 13 October 2008

Infections with dengue virus (DENV) are a significant public health concern in tropical and subtropical regions. However, little detail is known about how DENV interacts with the host-cell machinery to facilitate its translation and replication. In DENV-infected HepG2 cells, an increase in the level of LC3-II (microtubule-associated protein 1 light chain 3 form II), the autophagosomal membrane-bound form of LC3, was observed, and LC3 was found to co-localize with dsRNA and DENV NS1 protein, as well as ribosomal protein L28, indicating the presence of at least some of the DENV translation/replication machinery on autophagic vacuoles. Inhibition of fusion of autophagic vacuoles with lysosomes resulted in an increase in both intracellular and extracellular virus, and co-localization observed between mannose-6-phosphate receptor (MPR) and dsRNA and between MPR and LC3 identified the autophagic vacuoles as amphisomes. Amphisomes are formed as a result of fusion between endosomal and autophagic vacuoles, and as such provide a direct link between virus entry and subsequent replication and translation.

INTRODUCTION

With an estimated 100 million infections per year worldwide, dengue virus (DENV), which is spread to humans by the bite of female *Aedes* mosquitoes, represents a significant public health threat in tropical and subtropical countries (Guzman & Kouri, 2002). The DENV complex comprises four antigenically distinct viruses termed DENV serotypes 1, 2, 3 and 4 (DENV-1 to -4), all of which can cause a wide spectrum of disease presentation, from a relatively mild febrile disease to a life-threatening haemorrhagic syndrome (Malavige *et al.*, 2004). DENV is an enveloped, positive-sense, single-stranded RNA virus of approximately 11 kb that encodes three structural proteins (core, pre-membrane and envelope) and seven non-structural proteins (NS1, NS2A, NS2B, NS3, NS4A, NS4B and NS5) in one open reading frame (Chang, 1997). Entry of DENV into a susceptible cell occurs primarily through receptor-mediated endocytosis via clathrin-coated pits (Krishnan *et al.*, 2007) and the virus is then trafficked to endosomes (Krishnan *et al.*, 2007; van der Schaar *et al.*, 2007) and fuses with the endosomal membranes (Heinz *et al.*, 2004) through a pH-dependent conformational change in the envelope protein (Modis *et al.*, 2004; Mukhopadhyay *et al.*, 2005). The fate of the released nucleocapsid is largely obscure, although it is known that, after uncoating of the virus genome, the host-cell translational machinery is utilized to synthesize a polyprotein precursor that is processed co- and post-translationally by a virus-encoded protease (NS3) and host signallases (Cahour *et al.*, 1992). Translation and subsequent replication of the DENV genome occur in tight association with intracellular membranous structures that are believed to be endoplasmic reticulum (ER)-derived (Clyde *et al.*, 2006; Miller & Krijnse-Locker, 2008; Salonen *et al.*, 2005), although the exact origin of these membranes remains unclear.

Autophagy is a lysosomal degradation pathway involved in the cellular turnover of macromolecules and organelles. It is conserved among eukaryotes and has been shown to be important for cellular development and remodelling (Levine & Klionsky, 2004; Meijer & Codogno, 2006), as well as being involved in a wide range of disease processes including cancer, neurodegeneration, innate and adaptive immunity, heart disease, liver disease and ageing (Lerena *et al.*, 2008; Mizushima *et al.*, 2008). Autophagy begins with the sequestration of an area of the cytoplasm within a crescent-shaped membrane called the isolation membrane, which probably arises from a pre-existing body (Hanada *et al.*, 2007; Kim *et al.*, 2002; Levine & Klionsky, 2004). This membrane has been suggested to originate from the ER (Dunn, 1990a) and/or from the *trans*-Golgi network (Kihara *et al.*, 2001). The isolation membrane then expands and matures into a large, characteristically double-membraned vesicle with a diameter of 500–1000 nm called an autophagosome (Dunn, 1990a). Among the key regulators

of this process are mTOR (a kinase target of rapamycin) and the beclin1–class III PI3k complex (Xie & Klionsky, 2007). The execution phase of autophagy is mediated primarily through two covalent conjugation pathways: the covalent linkage of Atg5 and Atg12 (Mizushima *et al.*, 1998, 2002; Ohsumi, 2001) and the covalent lipidation of Atg8 (called microtubule-associated protein 1 light chain 3, or LC3, in mammalian cells) by phosphatidylethanolamine (Kabeya *et al.*, 2000; Ohsumi, 2001). Lipidated LC3 eventually associates with the autophagy membranes (Kabeya *et al.*, 2000) and as such is the only creditable marker of autophagosomes in mammalian cells (Bampton *et al.*, 2005; Kimura *et al.*, 2007). Fusion of the autophagosome with endosomes forms structures called amphisomes (Gordon & Seglen, 1988), whilst subsequent fusion with lysosomes forms autophagolysosomes (Dunn, 1990b).

Recently, it has been shown that autophagy is induced upon DENV-2 infection of Huh7 cells (Lee *et al.*, 2008). Biochemical inhibition of autophagy resulted in a reduction in the number of virus progeny produced, and infection was significantly inhibited in Atg5-knockout MEF cells, suggesting that DENV subverts the autophagic process (Lee *et al.*, 2008). However, the details of how DENV affects the autophagic process remain unknown. Given that double-membrane vesicle structures have been associated with DENV replication (Miller & Krijnse-Locker, 2008) and that such double-membrane structures are a classic hallmark of autophagosomes (Dunn, 1990a), it is possible that, similar to poliovirus (Jackson *et al.*, 2005), equine arteritis virus (Pedersen *et al.*, 1999), coronavirus and mouse hepatitis virus (Lee & Iwasaki, 2008), DENV uses autophagic membranes as sites for virus replication.

METHODS

Cells, viruses and infection. The human hepatoma cell line HepG2 (ATCC HB-8065) was cultivated at 37 °C under 10 % CO_2 in Dulbecco's modified Eagle's medium (Gibco) supplemented with 10 % heat-inactivated fetal bovine serum (Gibco) (DMEM/FBS) and 100 U penicillin/streptomycin ml^{-1} (PAA). For characterization of autophagy, HepG2 cells were seeded onto glass coverslips and grown for 24 h under standard conditions after which the growth medium was replaced with complete growth medium or growth medium supplemented with either 100 nM rapamycin (Sigma-Aldrich) or 100 nM rapamycin and 10 mM 3-methyladenine (3-MA; Sigma-Aldrich).

DENV-2 strain 16681 was propagated in the *Aedes albopictus*-derived cell line C6/36 (ATCC CRL-1660). The virus was partially purified by centrifugation to remove cell debris and stored at −80 °C.

For infection of HepG2 cells, cells were grown to subconfluency and pre-treated for 3 h with 10 mM 3-MA in DMEM/FBS or for 1 h with 100 nM rapamycin or 30 mM L-asparagine (L-Asn; Sigma-Aldrich) in DMEM/FBS, or left untreated, and were then infected with DENV-2 at 10 p.f.u. per cell for 2 h in DMEM with or without an autophagy modulator as appropriate. After 2 h, normal growth medium (with or without autophagy modulator as appropriate) was added and cells were incubated under normal conditions until harvesting of the cells or medium. Virus titres were determined by standard plaque assay as described previously (Sithisarn *et al.*, 2003) and intracellular virus levels were determined as described elsewhere (Thepparit & Smith, 2004).

Indirect immunofluorescence. Approximately 3×10^4 HepG2 cells were seeded and grown on 1 cm^2 coverslips under standard conditions for 24 h, followed directly by infection with DENV-2 at 10 p.f.u. per cell for 2 h or pre-incubated for 3 h with 10 mM 3-MA in DMEM/FBS or for 1 h with 100 nM rapamycin or 30 mM L-Asn in DMEM/FBS before virus infection at 10 p.f.u. per cell. At various time points, cells were washed twice with PBS and then fixed in 100 % ice-cold methanol for 20 min. Cells were subsequently permeabilized with 0.3 % Triton X-100 in PBS for 10 min and then washed with

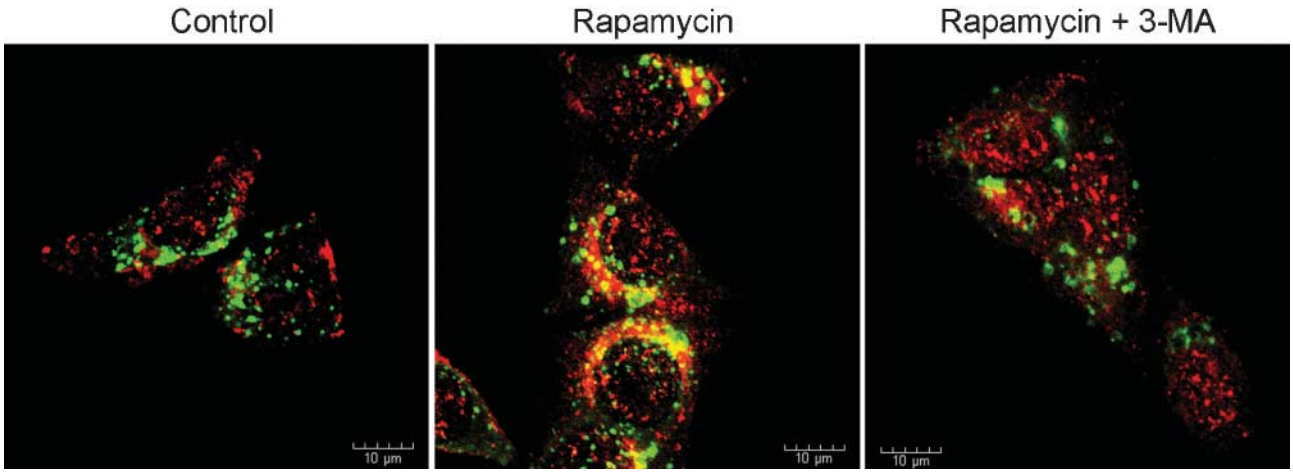

Fig. 1. Induction of autophagy in HepG2 cell. HepG2 cells were grown on glass coverslips and then incubated in complete medium (control) or in the presence of rapamycin or rapamycin and 3-MA for 15 min and subsequently incubated with appropriate primary and secondary antibodies to detect LC3 (red) and LAMP1 (green). Fluorescent signals were observed using an Olympus FluoView 1000 confocal microscope. At least 15 fields were examined, and representative, non-contrast-adjusted merged images are shown.

0.03 % Triton X-100 in PBS or permeabilized, washed and then blocked for 1 h at room temperature with 5 % FBS in 0.03 % Triton X-100 in PBS (for anti-NS1 antibody). The cells were then incubated with two or three primary antibodies at 4 °C overnight. Following incubation, cells were washed four times with 0.03 % Triton X-100 in PBS and incubated with two or three appropriate secondary antibodies for 1 h at room temperature. Subsequently, coverslips were washed with 0.03 % Triton X-100 in PBS six times and then mounted onto glass slides. The cells were observed under a confocal microscope.

The primary antibodies used were a rabbit polyclonal anti-MAP-LC3 antibody (Santa Cruz Biotechnology), a goat polyclonal anti-MAP-LC3 antibody (Santa Cruz Biotechnology), a mouse monoclonal anti-CD107a (LAMP1) antibody (BD Transduction), a rabbit polyclonal anti-LAMP1 antibody (Abcam), a mouse monoclonal anti-DENV NS1 antibody (Puttikhunt *et al.*, 2003), a mouse monoclonal anti-dsRNA antibody (J2; English and Scientific Consulting), a goat polyclonal anti-ribosomal protein L28 antibody (Santa Cruz Biotechnology) and a rabbit polyclonal anti-mannose-6-phosphate receptor antibody (Abcam).

Secondary antibodies used as appropriate were rhodamine Red X-conjugated goat anti-rabbit IgG (Jackson ImmunoResearch), fluorescein isothiocyanate (FITC)-conjugated donkey anti-rabbit IgG

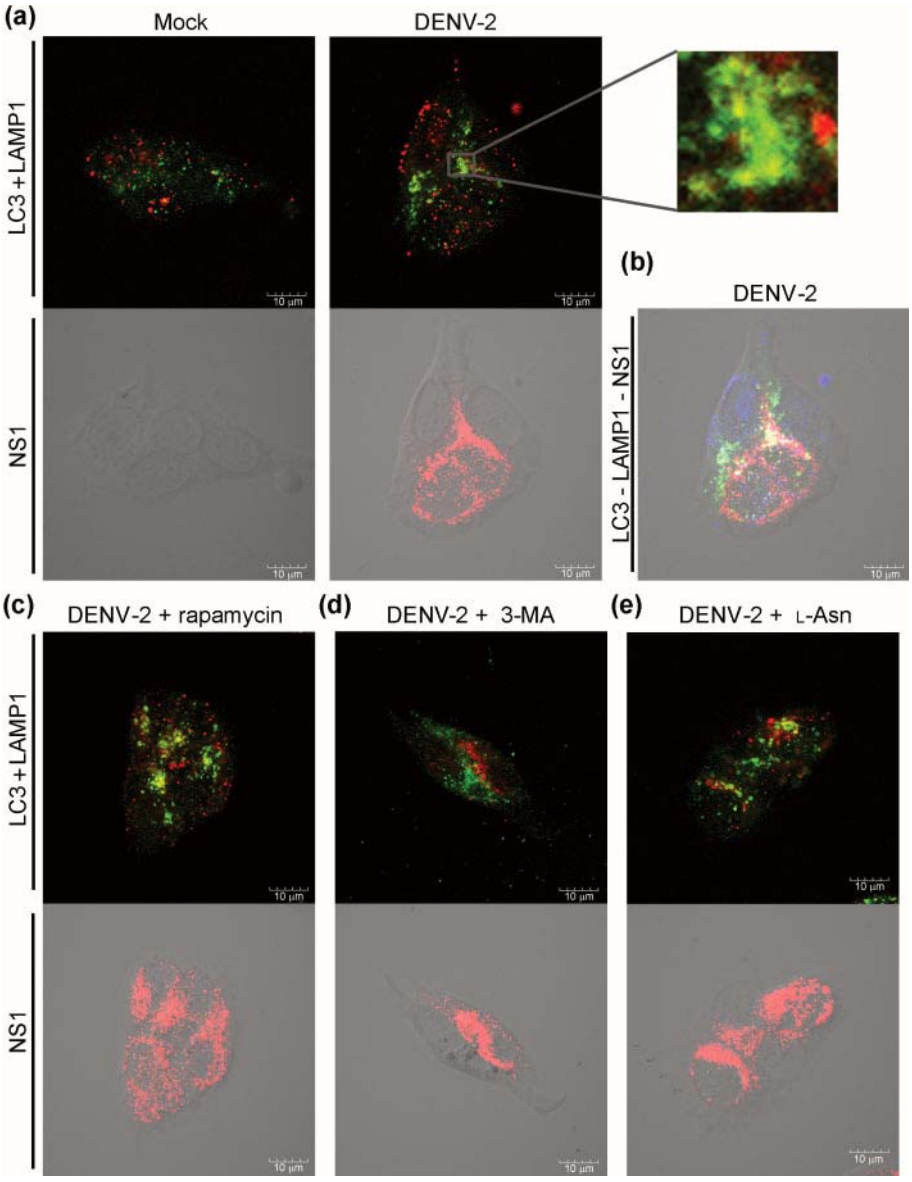

Fig. 2. Induction of autophagy in response to DENV-2 infection. HepG2 cells were grown on glass coverslips and either mock infected or infected with DENV-2 either directly (a, b) or in the presence of rapamycin (c), 3-MA (d) or L-Asn (e). Cells were examined simultaneously for the localization of LC3 (far red) and LAMP1 (green) and separately for NS1 (red) (a, c–e) or simultaneously for LC3 (blue), LAMP1 (green) and NS1 (red) (b), in uninfected or infected cells as indicated. Fluorescent signals were observed using an Olympus FluoView 1000 confocal microscope. At least 15 fields were examined. Images were merged for LC3 and LAMP1, with the NS1 signal from the same field shown merged with the bright-field view.

(Santa Cruz Biotechnology), Cy5-conjugated rabbit anti-goat IgG (Invitrogen), FITC-conjugated goat anti-mouse IgG (KPL) and Alexa Fluor 594-conjugated chicken anti-mouse IgG (Molecular Probes).

Fluorescence confocal microscope imaging and analysis. Fluorescently labelled samples were observed under an Olympus FluoView 1000 microscope equipped with Olympus FluoView software version 1.6. For samples stained with two primary antibodies, images were captured in the red (rhodamine-labelled secondary antibodies), far-red (Cy5-labelled secondary antibodies) or green (FITC-labelled secondary antibodies) channels. For samples stained with three primary antibodies, images were captured in the green (FITC-labelled secondary antibodies), red (Alexa Fluor 594-labelled secondary antibodies) and far-red (Cy5-labelled secondary antibodies) channels. Final images were a non-contrast-adjusted merge of two or three channels. Where three channels were merged, far-red images were shown as blue. Some images had a bright-field image included in the final merge. At least 15 fields from each coverslip were examined and a minimum of two independent experiments was undertaken for each condition. Representative images of selected fields are shown.

Image analysis was undertaken using the ImageJ analysis program (Abramoff *et al.*, 2004) using the PSC co-localization plug-in (French *et al.*, 2008) to calculate co-localization. At least 20 cells were analysed for each condition. Results are presented in terms of Pearson correlation coefficients, which represent the linear relationship of the signal intensity from the green and red channels of the analysed image. The program allowed masking of areas to be excluded from the analysis, and uninfected cells were masked prior to analysis. Statistical analysis of significance between datasets was undertaken by a paired sample test using SPSS (SPSS Inc.) using a value of $P<0.05$ for significance.

Western blot analysis. Total proteins from mock-infected or DENV-infected HepG2 cells were extracted and separated by PAGE before transfer to a solid support. Membranes were blocked with 5 % skimmed milk in TBS for 2 h at room temperature, followed by incubation with antibodies against LC3 in 5 % BSA in TBS or glyceraldehyde-3-phosphate dehydrogenase (GAPDH) in 5 % skimmed milk in TBS at 4 °C overnight. The membranes were then incubated with appropriate secondary antibodies in 5 % skimmed milk in TBS at room temperature for 1 h. The antibodies used were a 1 : 3000 dilution for rabbit polyclonal anti-LC3 antibody (Novus Biological) and a 1 : 800 dilution for mouse monoclonal anti-GAPDH antibody (Santa Cruz Biotechnology), followed by a 1 : 3000 dilution of horseradish peroxidase-conjugated goat anti-rabbit IgG (Pierce) or a 1 : 4000 dilution of horseradish peroxidase-conjugated anti-mouse IgG (Sigma Chemical Co.). Signals were developed using an ECL-Plus Western Blotting Analysis kit (GE Healthcare).

Statistical analysis. Virus production data were analysed using the GraphPad Prism program (GraphPad Software). Statistical analysis of significance was undertaken by a paired sample test using SPSS with a value of $P<0.05$ for significance.

RESULTS

Autophagy in HepG2 cells

Lee *et al.* (2008) showed that autophagy is induced in response to DENV infection, but the study was undertaken in Huh7 cells. This study therefore sought initially to establish that autophagy could be induced in HepG2 cells and that this pathway was susceptible to manipulation in these cells. To establish that the autophagy pathway is viable in HepG2 cells, the localization of LC3 (a specific marker of autophagic vacuoles) and LAMP1 (a marker of endosomal and lysosomal membranes) was examined in control cells, in cells treated with the autophagy inducer rapamycin (Noda & Ohsumi, 1998) and in cells treated

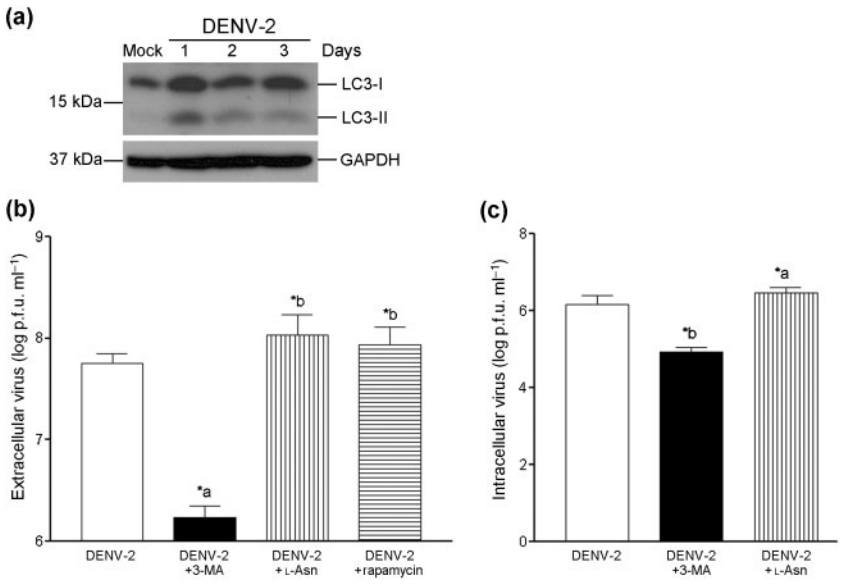

Fig. 3. Induction of autophagy in response to DENV-2 infection and effects of autophagy modulation. (a) Western blot analysis of LC3 and GAPDH expression in mock-infected or DENV-2-infected HepG2 cells on days 1–3 p.i. (b) Extracellular virus production of HepG2 cells infected with DENV-2 in the presence or absence of 3-MA, rapamycin or L-Asn. Virus yield is plotted as log virus titre ± SD. Data were derived from six independent replicates, with duplicate assays of each replicate. The statistical significance of virus output compared with the control is shown. *a, $P<0.001$; *b, $P=0.012$. (c) Intracellular virus production of HepG2 cells infected with DENV-2 in the presence or absence of 3-MA or L-Asn. Virus yield is plotted as log virus titre ± SD. Data were derived from six independent replicates, with duplicate assays of each replicate. The statistical significance of virus yield compared with the control is shown. *a, $P<0.001$; *b, $P=0.001$.

with both rapamycin and the PI3k kinase class III inhibitor 3-MA, which inhibits autophagy (Seglen & Gordon, 1982). Little if any co-localization was seen in control cells, whilst co-localization was observed in rapamycin-treated cells by 15 min after the addition of rapamycin. Co-localization of LAMP1 and LC3 in response to rapamycin treatment was completely abolished by 3-MA treatment (Fig. 1).

Induction of autophagy in response to DENV infection

To confirm that autophagy was induced in response to DENV-2 infection using strain 16681 as opposed to strain PL0146 as used by Lee *et al.* (2008), HepG2 cells were infected with DENV-2 strain 16681 at 10 p.f.u. per cell in parallel with samples treated with rapamycin, 3-MA and L-Asn, which inhibits fusion of lysosomes with autophagosomes and amphisomes (Gordon & Seglen, 1988). An m.o.i. of 10 had been determined separately to give infection rates of greater than 90 % at 24 h post-infection (p.i.) (data not shown). At 24 h p.i., samples were simultaneously stained with antibodies directed against LC3, LAMP1 and NS1. The co-localization of LC3 and LAMP1 was examined only in cells positive for NS1 staining to ensure that only DENV-infected cells were analysed.

The results showed an increased co-localization between LC3 and LAMP1 in response to DENV-2 infection [mean Pearson correlation coefficient 0.34, 95 % confidence interval (CI) 0.31–0.37] compared with mock-infected cells (mean Pearson correlation coefficient 0.14, 95 % CI 0.13–0.15; $P<0.001$; Fig. 2a). The level of co-localization between LC3 and LAMP1 in infected cells was significantly increased in the presence of the autophagy inducer rapamycin (mean Pearson correlation coefficient 0.55, 95 % CI 0.52–0.58; $P<0.001$; Fig. 2c) and abolished in the presence of 3-MA (Fig. 2d). An increase in the co-localization of LC3 and LAMP1 over and above that seen in infected cells was observed in cells infected in the presence of L-Asn (mean Pearson correlation coefficient 0.46, CI 0.43–0.49; $P<0.001$; Fig. 2e). Western blotting demonstrated the formation of the autophagy-associated form of LC3, LC3-II, in response to DENV infection (Fig. 3a). Virus yield at 24 h p.i. as determined by standard plaque assay was significantly reduced in response to 3-MA treatment ($P<0.001$) and increased by the presence of both rapamycin ($P=0.012$) and L-Asn ($P=0.012$), with all experiments undertaken six times independently, with duplicate assays of titre (Fig. 3b). The increase in virus yield seen in the presence of L-Asn suggested that fusion with lysosomes resulted in a degree of virus degradation. The yield of intracellular virus, determined as described elsewhere (Thepparit & Smith, 2004), was similarly increased in the presence of L-Asn ($P<0.001$) and decreased in the presence of 3-MA ($P=0.001$) (Fig. 3c).

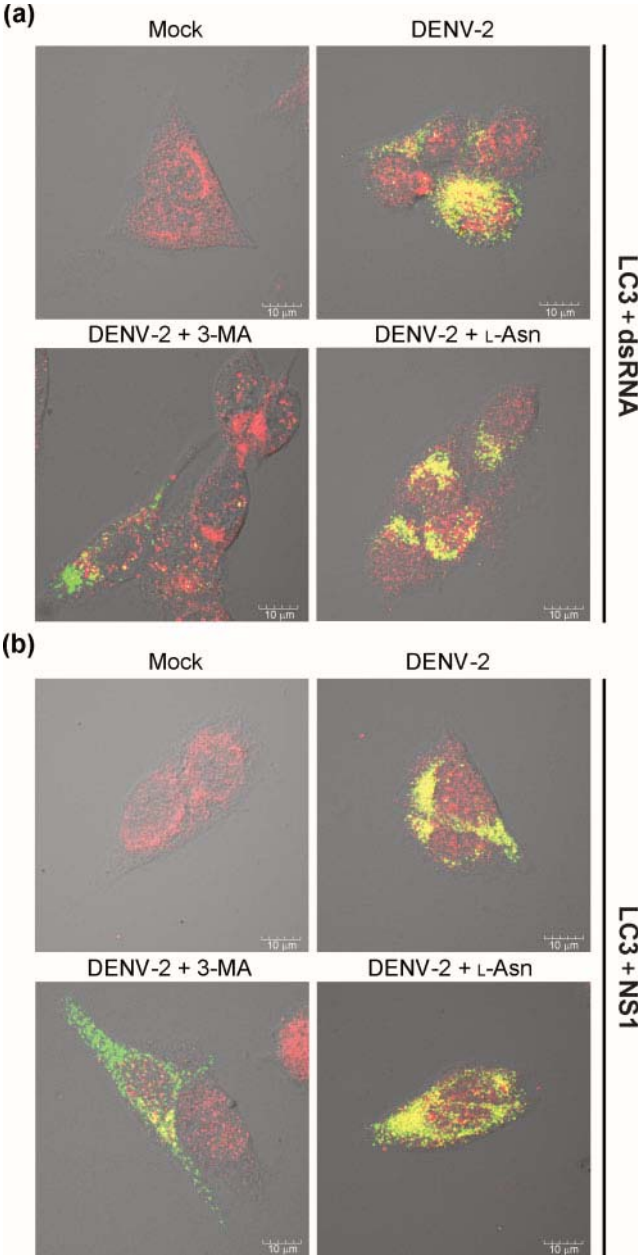

Fig. 4. Localization of the DENV replication complex. HepG2 cells were grown on glass coverslips and either mock infected or infected with DENV-2 either directly or in the presence of 3-MA or L-Asn, and examined for the localization of LC3 (red) and either dsRNA (green) (a) or NS1 (green) (b). Fluorescent signals were observed using an Olympus FluoView 1000 confocal microscope. At least 15 fields were examined, and representative, non-contrast-adjusted merged images are shown.

Autophagy and DENV replication and translation

To investigate whether parts of the replication/translation machinery of DENV co-localized with LC3, DENV-2-infected cells were examined for the localization of DENV

NS1 protein and dsRNA in relation to LC3. The location of dsRNA was detected using the antibody J2, which has previously been established as being able to detect flavivirus dsRNA (Weber *et al.*, 2006), whilst NS1 protein was detected using a well-characterized monoclonal antibody (Puttikhunt *et al.*, 2003).

At 24 h p.i., significant levels of co-localization were observed between dsRNA and LC3 (mean Pearson correlation coefficient 0.35, 95 % CI 0.28–0.42), which was largely eliminated by treatment with 3-MA, whilst L-Asn treatment significantly increased the co-localization between dsRNA and LC3 (mean Pearson correlation coefficient 0.45, 95 % CI 0.39–0.51; P=0.001; Fig. 4a). NS1 protein similarly co-localized with LC3 in DENV-2-infected cells (mean Pearson correlation coefficient 0.44, 95 % CI 0.39–0.49), and co-localization was again largely eliminated by treatment with 3-MA and increased when DENV-2-infected cells were treated with L-Asn (mean Pearson correlation coefficient 0.51, 95 % CI 0.46–0.56; Fig. 4b), again suggesting degradation of virus or viral proteins upon fusion of the autophagic vacuole with lysosomes. NS1 protein also co-localized with both LC3 and LAMP1 (Fig. 2b).

We further investigated the co-localization of ribosomal proteins with the presence of dsRNA to determine whether there was translational capacity at the site of RNA replication and found significant co-localization between dsRNA and ribosomal proteins using an antibody directed against ribosomal protein L28 (Fig. 5).

As a marker of both endosomes and lysosomes, LAMP1 co-localization is unable to discriminate between the formation of autophagolysosomes (fusion of autophagosomes with lysosomes) and amphisomes (fusion of autophagosomes with endosomes). We therefore investigated whether the endosomal marker mannose-6-phosphate receptor (MPR) co-localized with dsRNA. High levels of MPR signal were observed in mock-infected cells, and co-localization between MPR and LC3 was more evident than co-localization between LC3 and LAMP1 in mock-infected cells. This may reflect either a higher level of MPR in HepG2 cells or may simply result from differences in antibody avidity. However, clear co-localization between MPR and dsRNA (Fig. 6a) was observed, as well as increased co-localization between MPR and LC3 in infected cells (Fig. 6b), suggesting amphisomes as the site of DENV-2 replication and translation.

To confirm amphisomes as a site of at least part of the DENV replication complex, triple staining using antibodies directed against MPR, LC3 and dsRNA was undertaken in infected cells. The results (Fig. 7) showed co-localization of these three markers.

DISCUSSION

Whilst entry of DENV into target cells by receptor-mediated endocytosis into clathrin-coated pits and subsequent pH-dependent fusion of the virus structural envelope protein with membranes of the late endosomes

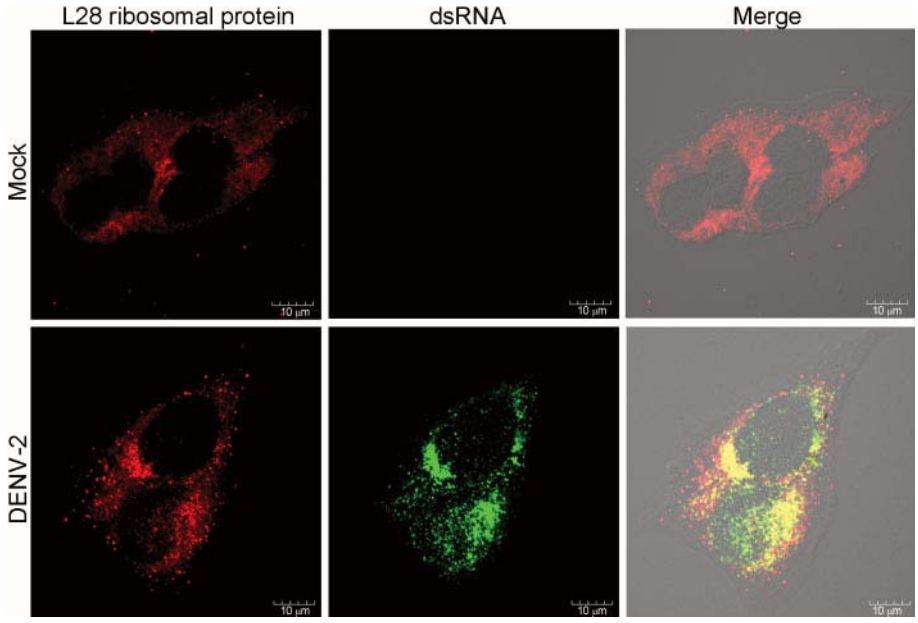

Fig. 5. Co-localization of ribosomes with DENV dsRNA. HepG2 cells were grown on glass coverslips and either mock infected or infected with DENV-2 and examined for the localization of L28 (red) and dsRNA (green). Fluorescent signals were observed using an Olympus FluoView 1000 confocal microscope. At least 15 fields were examined, and representative single-channel and merged non-contrast-adjusted images are shown.

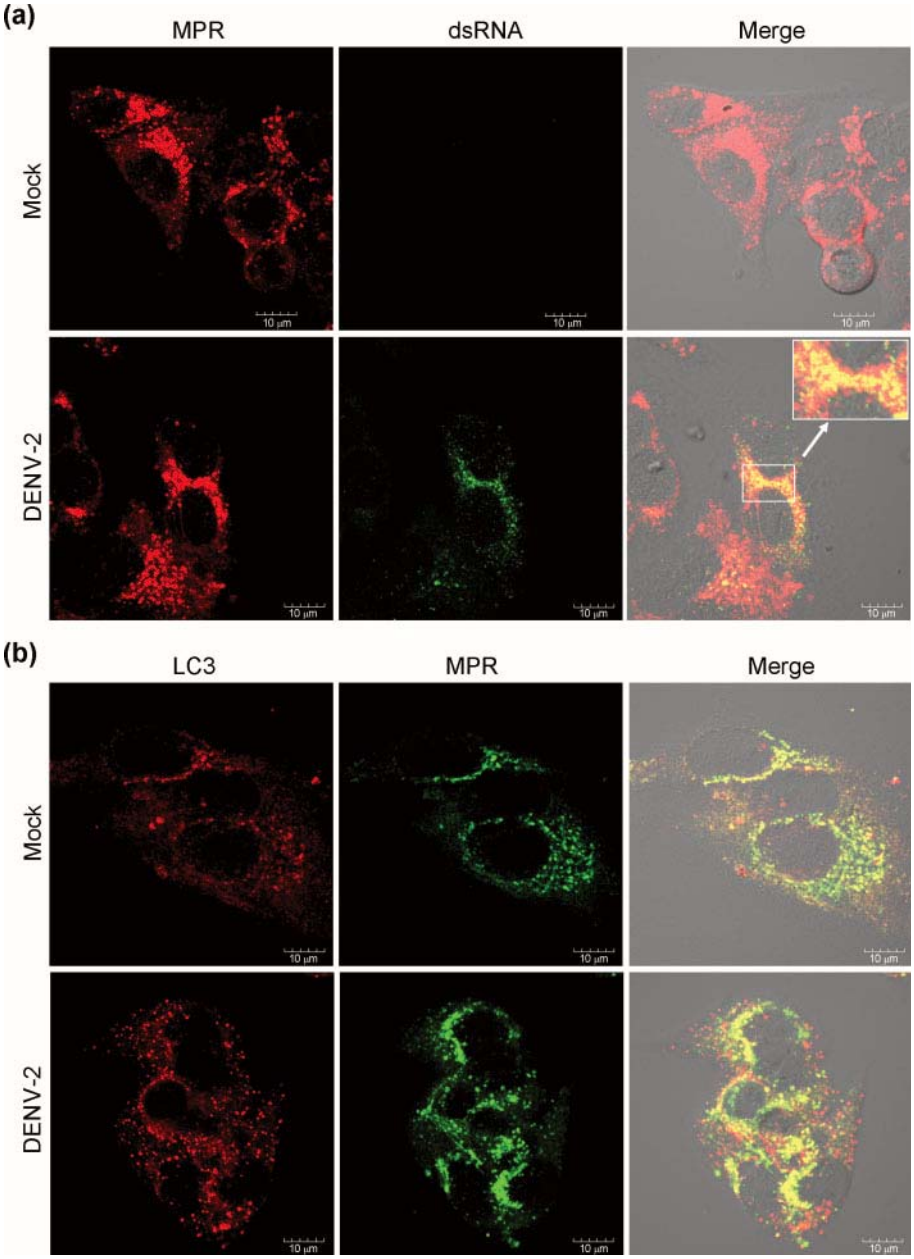

Fig. 6. Investigation of amphisomes as sites of DENV replication. HepG2 cells were grown on glass coverslips and either mock infected or infected with DENV-2 and examined for the localization of MPR (red) and dsRNA (green) (a) or MPR (green) and LC3 (red) (b). Fluorescent signals were observed using an Olympus FluoView 1000 confocal microscope. At least 15 fields were examined, and representative single-channel and merged non-contrast-adjusted images are shown.

has been well documented (Allison *et al.*, 1995; Mukhopadhyay *et al.*, 2005), subsequent events are less well characterized. It is currently believed that flavivirus genomes are released into and replicate in the cytoplasm in close association with intracellular membranous structures that possibly derive from the ER (Clyde *et al.*, 2006; Miller & Krijnse-Locker, 2008). Consistently, flavivirus infections characteristically result in significant proliferation of rough ER membranes, and the flavivirus replication complex has been partly correlated with these ER membranes (Boulton & Westaway, 1976) and with cytoplasmic vesicles and vacuoles (Mackenzie *et al.*, 1996), and it has been proposed that flaviviruses bud from ER membranes and transit the Golgi body before release from the cell (Clyde *et al.*, 2006; Yoshii *et al.*, 2004).

More recently, Lee *et al.* (2008) showed that autophagy is induced by DENV-2 infection in Huh7 cells, and that the

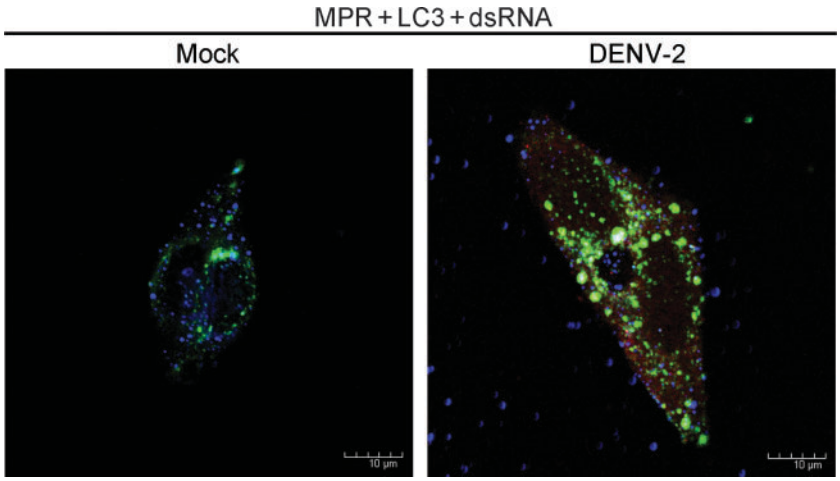

Fig. 7. Identification of amphisomes as sites of DENV replication. HepG2 cells were grown on glass coverslips and either mock infected or infected with DENV-2 and examined simultaneously for the localization of MPR (green), LC3 (blue) and dsRNA (red). The LC3 signal was originally collected in the far-red channel and is coloured blue for this figure. Co-localization of all three markers is shown as white.

induction of autophagy serves to enhance DENV replication. Inhibition of autophagy, either by biochemical treatment with 3-MA or by knockout of Atg5 (in MEF cells) serves to reduce the levels of infectious virus produced (Lee *et al.*, 2008). Similarly, as shown here, DENV-2 induced autophagy in HepG2 cells and biochemical inhibition of autophagy with 3-MA reduced virus yield, whilst induction of autophagy with rapamycin enhanced virus yield.

The process of autophagy initially generates double-membraned structures called autophagosomes (Dunn, 1990a), which are capable of fusing with endosomes to form amphisomes (Gordon & Seglen, 1988). Both autophagosomes and amphisomes can subsequently fuse with lysosomes to form autophagolysosomes, the primary degradative vesicle (Dunn, 1990b). Interestingly, however, the inhibition of lysosomal fusion with L-Asn served to increase both intracellular and extracellular virus yield, suggesting that lysosomal fusion of autophagic vacuoles to form autophagolysosomes has a deleterious effect on DENV replication. This consequently suggests that viable virus is produced prior to lysosomal fusion on either autophagosomes or amphisomes.

The co-localizations observed between LC3 and LAMP1, LC3 and dsRNA, LC3 and NS1, and between NS1, LC3 and LAMP1, as well as between ribosomal proteins and dsRNA, located the DENV translation/replication complex on autophagosomes, and the co-localization seen between MPR and dsRNA, MPR and LC3, and between MPR, LC3 and dsRNA would indicate that these structures are amphisomes, formed by the fusion of autophagosomes and endosomes. Given the localization of the DENV replication/translation complex on amphisomes, it is unsurprising that subsequent fusion with lysosomes (and their proteolytic contents) to form autophagolysosomes results in a decrease in the number of virus progeny.

The induction of autophagic structures and the location of part of the DENV replication/translation complex on these structures is consistent with a considerable body of work that locates the DENV replication complex on induced membranes and vacuoles (Boulton & Westaway, 1976; Mackenzie *et al.*, 1996) and explains why modulation of autophagy serves to modulate DENV output, as seen by Lee *et al.* (2008) and ourselves in this study. As amphisomes are formed by the fusion of endosomes and autophagosomes (Gordon & Seglen, 1988; Gordon *et al.*, 1992), the identification of these structures as the sites of at least part of the DENV replication/translation complex provides a basis for a unified model linking DENV entry and replication in terms of an ongoing and continual association with membranes of an endosomal–autophagic lineage.

ACKNOWLEDGEMENTS

This work was supported by grants from Mahidol University and the Thailand Research Fund. M. P. is supported by a Thai Royal Golden Jubilee Research Scholarship, A. K. is supported by a Mahidol University Research Thesis Scholarship and N. W. is supported by a scholarship from the National Center for Genetic Engineering and Biotechnology, National Science and Technology Development Agency. We thank Prida Malasit for kindly providing the anti-NS1 antibody and Yuvadee Siriyasub for considerable help and assistance with the confocal microscopy.

REFERENCES

Abramoff, M. D., Magelhaes, P. J. & Ram, S. J. (2004). Image processing with ImageJ. *Biophotonics International* **11**, 36–42.

Allison, S. L., Schalich, J., Stiasny, K., Mandl, C. W., Kunz, C. & Heinz, F. X. (1995). Oligomeric rearrangement of tick-borne encephalitis virus envelope proteins induced by an acidic pH. *J Virol* **69**, 695–700.

Bampton, E. T., Goemans, C. G., Niranjan, D., Mizushima, N. & Tolkovsky, A. M. (2005). The dynamics of autophagy visualized in live cells: from autophagosome formation to fusion with endo/lysosomes. *Autophagy* **1**, 23–36.

Boulton, R. W. & Westaway, E. G. (1976). Replication of the flavivirus Kunjin: proteins, glycoproteins, and maturation associated with cell membranes. *Virology* **69**, 416–430.

Cahour, A., Falgout, B. & Lai, C. J. (1992). Cleavage of the dengue virus polyprotein at the NS3/NS4A and NS4B/NS5 junctions is

mediated by viral protease NS2B–NS3, whereas NS4A/NS4B may be processed by a cellular protease. *J Virol* **66**, 1535–1542.

Chang, G. J. (1997). Molecular biology of dengue viruses. In *Dengue and Dengue Hemorrhagic Fever*, pp. 175–198. Edited by D. J. Gubler & G. Kuno. Wallingford: CAB International.

Clyde, K., Kyle, J. L. & Harris, E. (2006). Recent advances in deciphering viral and host determinants of dengue virus replication and pathogenesis. *J Virol* **80**, 11418–11431.

Dunn, W. A., Jr (1990a). Studies on the mechanisms of autophagy: formation of the autophagic vacuole. *J Cell Biol* **110**, 1923–1933.

Dunn, W. A., Jr (1990b). Studies on the mechanisms of autophagy: maturation of the autophagic vacuole. *J Cell Biol* **110**, 1935–1945.

French, A. P., Mills, S., Swarup, R., Bennett, M. J. & Pridmore, T. P. (2008). Colocalization of fluorescent markers in confocal microscope images of plant cells. *Nat Protoc* **3**, 619–628.

Gordon, P. B. & Seglen, P. O. (1988). Prelysosomal convergence of autophagic and endocytic pathways. *Biochem Biophys Res Commun* **151**, 40–47.

Gordon, P. B., Hoyvik, H. & Seglen, P. O. (1992). Prelysosomal and lysosomal connections between autophagy and endocytosis. *Biochem J* **283**, 361–369.

Guzman, M. G. & Kouri, G. (2002). Dengue: an update. *Lancet Infect Dis* **2**, 33–42.

Hanada, T., Noda, N. N., Satomi, Y., Ichimura, Y., Fujioka, Y., Takao, T., Inagaki, F. & Ohsumi, Y. (2007). The Atg12–Atg5 conjugate has a novel E3-like activity for protein lipidation in autophagy. *J Biol Chem* **282**, 37298–37302.

Heinz, F. X., Stiasny, K. & Allison, S. L. (2004). The entry machinery of flaviviruses. *Arch Virol Suppl* **18**, 133–137.

Jackson, W. T., Giddings, T. H., Jr, Taylor, M. P., Mulinyawe, S., Rabinovitch, M., Kopito, R. R. & Kirkegaard, K. (2005). Subversion of cellular autophagosomal machinery by RNA viruses. *PLoS Biol* **3**, e156.

Kabeya, Y., Mizushima, N., Ueno, T., Yamamoto, A., Kirisako, T., Noda, T., Kominami, E., Ohsumi, Y. & Yoshimori, T. (2000). LC3, a mammalian homologue of yeast Apg8p, is localized in autophagosome membranes after processing. *EMBO J* **19**, 5720–5728.

Kihara, A., Kabeya, Y., Ohsumi, Y. & Yoshimori, T. (2001). Beclin–phosphatidylinositol 3-kinase complex functions at the *trans*-Golgi network. *EMBO Rep* **2**, 330–335.

Kim, J., Huang, W. P., Stromhaug, P. E. & Klionsky, D. J. (2002). Convergence of multiple autophagy and cytoplasm to vacuole targeting components to a perivacuolar membrane compartment prior to *de novo* vesicle formation. *J Biol Chem* **277**, 763–773.

Kimura, S., Noda, T. & Yoshimori, T. (2007). Dissection of the autophagosome maturation process by a novel reporter protein, tandem fluorescent-tagged LC3. *Autophagy* **3**, 452–460.

Krishnan, M. N., Sukumaran, B., Pal, U., Agaisse, H., Murray, J. L., Hodge, T. W. & Fikrig, E. (2007). Rab 5 is required for the cellular entry of dengue and West Nile viruses. *J Virol* **81**, 4881–4885.

Lee, H. K. & Iwasaki, A. (2008). Autophagy and antiviral immunity. *Curr Opin Immunol* **20**, 23–29.

Lee, Y. R., Lei, H. Y., Liu, M. T., Wang, J. R., Chen, S. H., Jiang-Shieh, Y. F., Lin, Y. S., Yeh, T. M., Liu, C. C. & Liu, H. S. (2008). Autophagic machinery activated by dengue virus enhances virus replication. *Virology* **374**, 240–248.

Lerena, C., Calligaris, S. D. & Colombo, M. I. (2008). Autophagy: for better or for worse, in good times or in bad times. *Curr Mol Med* **8**, 92–101.

Levine, B. & Klionsky, D. J. (2004). Development by self-digestion: molecular mechanisms and biological functions of autophagy. *Dev Cell* **6**, 463–477.

Mackenzie, J. M., Jones, M. K. & Young, P. R. (1996). Immunolocalization of the dengue virus nonstructural glycoprotein NS1 suggests a role in viral RNA replication. *Virology* **220**, 232–240.

Malavige, G. N., Fernando, S., Fernando, D. J. & Seneviratne, S. L. (2004). Dengue viral infections. *Postgrad Med J* **80**, 588–601.

Meijer, A. J. & Codogno, P. (2006). Signalling and autophagy regulation in health, aging and disease. *Mol Aspects Med* **27**, 411–425.

Miller, S. & Krijnse-Locker, J. (2008). Modification of intracellular membrane structures for virus replication. *Nat Rev Microbiol* **6**, 363–374.

Mizushima, N., Noda, T., Yoshimori, T., Tanaka, Y., Ishii, T., George, M. D., Klionsky, D. J., Ohsumi, M. & Ohsumi, Y. (1998). A protein conjugation system essential for autophagy. *Nature* **395**, 395–398.

Mizushima, N., Yoshimori, T. & Ohsumi, Y. (2002). Mouse Apg10 as an Apg12-conjugating enzyme: analysis by the conjugation-mediated yeast two-hybrid method. *FEBS Lett* **532**, 450–454.

Mizushima, N., Levine, B., Cuervo, A. M. & Klionsky, D. J. (2008). Autophagy fights disease through cellular self-digestion. *Nature* **451**, 1069–1075.

Modis, Y., Ogata, S., Clements, D. & Harrison, S. C. (2004). Structure of the dengue virus envelope protein after membrane fusion. *Nature* **427**, 313–319.

Mukhopadhyay, S., Kuhn, R. J. & Rossmann, M. G. (2005). A structural perspective of the flavivirus life cycle. *Nat Rev Microbiol* **3**, 13–22.

Noda, T. & Ohsumi, Y. (1998). Tor, a phosphatidylinositol kinase homologue, controls autophagy in yeast. *J Biol Chem* **273**, 3963–3966.

Ohsumi, Y. (2001). Molecular dissection of autophagy: two ubiquitin-like systems. *Nat Rev Mol Cell Biol* **2**, 211–216.

Pedersen, K. W., van der Meer, Y., Roos, N. & Snijder, E. J. (1999). Open reading frame 1a-encoded subunits of the arterivirus replicase induce endoplasmic reticulum-derived double-membrane vesicles which carry the viral replication complex. *J Virol* **73**, 2016–2026.

Puttikhunt, C., Kasinrerk, W., Srisa-ad, S., Duangchinda, T., Silakate, W., Moonsom, S., Sittisombut, N. & Malasit, P. (2003). Production of anti-dengue NS1 monoclonal antibodies by DNA immunization. *J Virol Methods* **109**, 55–61.

Salonen, A., Ahola, T. & Kaariainen, L. (2005). Viral RNA replication in association with cellular membranes. *Curr Top Microbiol Immunol* **285**, 139–173.

Seglen, P. O. & Gordon, P. B. (1982). 3-Methyladenine: specific inhibitor of autophagic/lysosomal protein degradation in isolated rat hepatocytes. *Proc Natl Acad Sci U S A* **79**, 1889–1892.

Sithisarn, P., Suksanpaisan, L., Thepparit, C. & Smith, D. R. (2003). Behavior of the dengue virus in solution. *J Med Virol* **71**, 532–539.

Thepparit, C. & Smith, D. R. (2004). Serotype-specific entry of dengue virus into liver cells: identification of the 37-kilodalton/67-kilodalton high-affinity laminin receptor as a dengue virus serotype 1 receptor. *J Virol* **78**, 12647–12656.

van der Schaar, H. M., Rust, M. J., Waarts, B. L., van der Ende-Metselaar, H., Kuhn, R. J., Wilschut, J., Zhuang, X. & Smit, J. M. (2007). Characterization of the early events in dengue virus cell entry by biochemical assays and single-virus tracking. *J Virol* **81**, 12019–12028.

Weber, F., Wagner, V., Rasmussen, S. B., Hartmann, R. & Paludan, S. R. (2006). Double-stranded RNA is produced by positive-strand RNA viruses and DNA viruses but not in detectable amounts by negative-strand RNA viruses. *J Virol* **80**, 5059–5064.

Xie, Z. & Klionsky, D. J. (2007). Autophagosome formation: core machinery and adaptations. *Nat Cell Biol* **9**, 1102–1109.

Yoshii, K., Konno, A., Goto, A., Nio, J., Obara, M., Ueki, T., Hayasaka, D., Mizutani, T., Kariwa, H. & Takashima, I. (2004). Single point mutation in tick-borne encephalitis virus prM protein induces a reduction of virus particle secretion. *J Gen Virol* **85**, 3049–3058.

[Autophagy 5:3, 434-435; 1 April 2009]; ©2009 Landes Bioscience

Autophagic Punctum

Linking dengue virus entry and translation/replication through amphisomes

Mingkwan Panyasrivanit, Atefeh Khakpoor, Nitwara Wikan and Duncan R. Smith*

Molecular Pathology Laboratory; Institute of Molecular Biology and Genetics; Mahidol University; Nakorn Pathom, Thailand

Key words: amphisome, autophagy, dengue, endosome, replication, translation

Amphisomes are preautolysosomal vacuoles formed upon the fusion of autophagosomes with endosomes, and as such represent a critical meeting point between endocytic and autophagic pathways. Dengue virus enters into susceptible cells by clathrin-mediated endocytosis, and colocalization of dengue markers with markers of both autophagic and endosomal vesicles demonstrates that amphisomes are a site of dengue virus replication and translation. This work links for the first time the processes of dengue virus entry and translation/replication, and allows for interpretation of the early part of the dengue virus life cycle in terms of a continual association with membranes of an endosomal-autophagosomal lineage.

Dengue virus (DENV) is the most significant arbovirus worldwide, with some 2.5 billion people living at risk of infection. It has been estimated that some 50 million to 100 million infections occur each year, and infection with dengue virus is the most common cause of hospitalizations among children in Southeast Asia. The disease has emerged worldwide throughout tropical and subtropical regions which are the habitat of the principal transmission vector, Aedes mosquitoes (principally *Aedes aegypti*, *A. albopictus* and *A. polynesiensis*), and dengue has emerged as a critical globally endemic disease. To date there is no specific treatment or vaccine.

DENV is a mosquito-borne single-stranded RNA virus that belongs to the genus Flavivirus (family Flaviviridae), a genus that includes many important human pathogenic viruses including yellow fever virus, West Nile virus, Japanese encephalitis virus and tick-borne encephalitis virus. Dengue virus is comprised of four antigenically-related serotypes called dengue serotypes 1, 2, 3 and 4 (DEN1 to DEN 4) and infection by any one of the four serotypes can cause either a relatively benign fever, namely dengue fever, or a more serious disease such as dengue hemorrhagic fever (DHF) or dengue shock syndrome (DSS).

Autophagy (macroautophagy) is a lysosomal degradative pathway primarily functioning to turn over macromolecules and organelles in eukaryotic cells. However, autophagy is also involved in a number of processes including the response to cellular starvation and defense against invading pathogens. In cases of virus infection, the interaction between the autophagy mechanism and the invading virus is thought to follow one of two routes: defense or subversion. In the case of autophagy as a cellular defense mechanism, autophagy is induced to clear the cell of the invading virus. However, some viruses have adapted to evade the autophagy mechanism, by downregulating the pathway (as occurs with herpes simplex virus). More recently it has become clear that some viruses have evolved to subvert the autophagy process by using the autophagic membranes as sites for viral replication (as occurs with poliovirus) and downregulation of autophagy results in a reduction of virus production.

Dengue virus induces autophagy in mammalian cells, and biochemical downregulation of autophagy results in a reduction in the amount of extracellular and intracellular virus produced. By colocalizing a dengue virus nonstructural protein (NS1) as well as double-stranded RNA (an essential part of the dengue replication complex) with LC3, we identified autophagic vacuoles as a site for at least a part of the dengue virus replication complex. In addition, extensive colocalization between L28 (a ribosomal protein) and dsRNA provide evidence of translational capacity, and provide a rational explanation as to why downregulation of autophagy results in reductions in extracellular and intracellular virus levels. Interestingly, inhibition of fusion between preautolysosomal vacuoles and lysosomes with L-asparagine results in a significant increase in extracellular and intracellular virus yield, suggesting that fusion of these vacuoles with lysosomes is detrimental to dengue virus production, and further suggesting that autophagic structures prior to lysosomal fusion are the critical site of dengue virus replication/translation. Autophagic vacuoles prior to lysosomal fusion include both autophagosomes and amphisomes, with amphisomes being formed by fusion of autophagosomes with endosomes. Colocalization of LC3, dsRNA and the endosomal marker mannose-6-phosphate receptor (MPR) provide evidence that the dengue virus replication/translation complex is associated with amphisomes.

Entry of DENV into mammalian cells through clathrin coated pit-mediated endocytosis and pH-mediated uncoating of the virus

*Correspondence to: Duncan R. Smith; Molecular Pathology Laboratory, Institute of Molecular Biology and Genetics; Mahidol University; 25/25 Phuttamontol Sai 4; Salaya, Nakorn Pathom 73170 Thailand; Tel.: 662.800.3624; Fax: 662.441.9906; Email: duncan_r_smith@hotmail.com

Submitted: 01/20/09; Revised: 01/22/09; Accepted: 01/23/09

Previously published online as an *Autophagy* E-publication: http://www.landesbioscience.com/journals/autophagy/article/7925

Punctum to: Panyasrivanit M, Khakpoor A, Wikan N, Smith DR. Co-localization of constituents of the dengue virus translation and replication machinery with amphisomes. J Gen Virol 2009; 90:448-56; PMID: 19141455; DOI: 10.1099/vir.0.005355-0.

in endosomes has been well characterized, but subsequent events remain poorly understood. In particular, the process by which the released nucleocapsid is targeted to the previously presumed site of dengue virus replication (the endoplasmic reticulum) had not been addressed. In light of our results however, it is possible to reinterpret the early part of the dengue virus life cycle by proposing that virus entry and replication/translation occur in a tight and continuing association with membranes of an endosomal-autophagosomal lineage.

While the identification of amphisomes as a site for dengue virus replication/translation complex answers some questions, a great deal of further work remains to be done. In particular, while we have examined the interaction between DEN2 and the autophagic machinery, it is unclear as to whether all four dengue serotypes interact in the same manner. Moreover our study was undertaken in liver cells, which, as shown in much previous work, are involved in the pathology of dengue; however, they do not represent the critical cell type in dengue infections. More work will need to be undertaken to determine the nature of the interaction in other cell types (in particular cells of a monocytes/macrophage lineage) which may or may not be similar to that seen in liver cells.

In addition to the induction of autophagy, the dengue virus induces both ER stress and apoptosis in infected cells. Given that both of these processes have considerable crosstalk with the autophagy pathway, a reevaluation of those processes may be required. At this point, whereas entry of the virus and replication/translation have been linked, further attention to the latter stages of the dengue life cycle will be needed.

Acknowledgements

This work is supported by grants from Mahidol University and the Thailand Research Fund. M.P. is supported by a Thai Royal Golden Jubilee Research Scholarship, A.K. is supported by a Mahidol University Research Thesis Scholarship and N.W. is supported by a Scholarship from the NSTDA, BIOTEC.

Journal of Medical Virology 79:300–307 (2007)

Infection of Human Primary Hepatocytes With Dengue Virus Serotype 2

Lukkana Suksanpaisan, Arturo Cabrera-Hernandez, and Duncan R. Smith*

Molecular Pathology Laboratory, Institute of Molecular Biology and Genetics, Mahidol University, Thailand

While the impact of the dengue viruses on liver function is prominent as shown by hepatomegaly, liver enzyme abnormality, occasional fulminant hepatic failure and histological changes including hepatocellular necrosis, significant debate exists as to the possible involvement of the predominant cell type in the liver, hepatocytes, in the disease process. To address this issue purified human primary hepatocytes were exposed to dengue virus serotype 2 and the production of de novo viral progeny was established by standard plaque assay, RT-PCR and immunocytochemistry. To investigate the response of the primary hepatocytes to infection, the expression of a panel of 9 cytokine genes (IFN-β, TRAIL, MCP-1, IL-6, IL-1β, IL-8, MIP-1α, MIP-1β, and RANTES) was semi-quantitatively investigated by RT-PCR and up-regulation of TRAIL, MIP-1α, IFN-β, MIP-1β, IL-8, and RANTES was observed in response to infection. The induction of IL-8 in response to infection was accompanied by the secretion of IL-8 as verified by ELISA assay. The ability of hepatocytes to be infected with dengue virus serotype 2 in vitro support evidence implicating human hepatocytes as a target cell in cases of dengue virus infection, and provide the first experimental evidence to support the large number of clinical studies that implicate the liver as a critical target organ in severe cases of dengue infection. ***J. Med. Virol. 79:300–307, 2007.***

KEY WORDS: cytokine; flavivirus; IL-8; liver

INTRODUCTION

Approximately 2.5 billion people live in areas at risk of infection with the dengue viruses, and up to 100 million infections are believed to occur annually [Guzman and Kouri, 2002]. While the majority of these infections are believed to be asymptomatic, infection may result in a febrile disease termed dengue fever (DF) or it may result in hemorrhagic manifestations which are classified as either dengue hemorrhagic fever (DHF), or dengue shock syndrome (DSS) dependent upon severity [Halstead, 1989]. The causative agent of DF, DHF, and DSS are the dengue viruses. These viruses are classified in the family *Flaviviridae*, genus *Flavivirus*, and species *Dengue virus*. There are four antigenically distinct viruses, termed dengue serotypes 1, 2, 3, and 4. The dengue viruses are enveloped positive-sense single-stranded RNA viruses of approximately 11 kb and encode three structural proteins (core, pre-membrane and envelope) and seven non-structural proteins (NS1, NS2A, NS2B, NS3, NS4A, NS4B, and NS5) in one open reading frame [Chang, 1997].

While the impact of the dengue viruses on liver function is prominent as shown by high rates of hepatomegaly [Mohan et al., 2000], liver enzyme abnormality [Kuo et al., 1992; Nguyen et al., 1997; Mohan et al., 2000; Wahid et al., 2000], occasional fulminant hepatic failure [Subramanian et al., 2005] and histological changes including hepatocellular necrosis [Bhamarapravati, 1989] significant debate exists as to the possible involvement of the liver in the disease process. The liver is predominantly (80%) composed of hepatocytes, although other cells include Kupffer, endothelial, stellate and biliary cells. Kupffer cells have been previously shown to be infectable by the dengue viruses, and although the infection is not productive, cell death occurs [Marianneau et al., 1999]. While liver cell lines are broadly permissive to dengue infection [Lin et al., 2000b], the transformed nature of these cells makes interpretation of the significance of their infectablity problematic.

To address the question of whether primary human hepatocytes can be infected, we sought to infect viable

Grant sponsor: Thailand Research Fund; Grant number: BRG4980010; Grant sponsor: Mahidol University; Grant sponsor: Royal Golden Jubilee Scholarship; Grant sponsor: Consejo Nacional de Ciencia y Tecnología, México.

*Correspondence to: Duncan R. Smith, Molecular Pathology Laboratory, Institute of Molecular Biology and Genetics, Mahidol University, Salaya Campus, 25/25 Phuttamonthol Sai 4, Salaya, Nakorn Pathom, Thailand 73170.
E-mail: duncan_r_smith@hotmail.com

Accepted 16 October 2006

DOI 10.1002/jmv.20798

Published online in Wiley InterScience (www.interscience.wiley.com)

human primary hepatocytes with dengue virus serotype 2 and to establish infection through the assay of progeny viruses, the detection of both dengue virus polarity strands as well as through indirect immunocytochemistry to detect the products of dengue virus translation. When productive dengue virus infection of human primary hepatocytes was established, the study further sought to determine the cellular response of the primary hepatocytes to infection by examining the expression of a panel of cytokine genes as well as the specific up-regulation and secretion of the chemotactic cytokine IL-8, a primary mediator of the inflammatory response [Remick, 2005].

MATERIALS AND METHODS

Cells and Viruses

Primary human hepatocytes from two different donors (batches 4F0011 and 5F0063; $\geq$95% hepatocytes) were purchased and maintained strictly as recommended by the manufacturer (Cambrex Bio Science Walkersville, Inc., Walkersville, MD) using the appropriate media and reagents purchased from the same manufacturer (HCM BulletKit, Cambrex Bio Science Walkersville, Inc.). Approximately 2.2×10^5 cells were seeded onto individual 12 mm diameter collagen coated PTFE membranes in 12 well polystyrene plates (Transwell-Col, Corning Incorporated, Corning, NY) and incubated under 5% CO_2 at 37°C overnight.

The human hepatoma cell line HepG2 was cultured in DMEM (HyClone, Logan, UT) containing 10% FCS (PAA, Pasching, Austria) 100 U/ml penicillin and 100 μg/ml streptomycin. The cells were incubated at 37°C/10% CO_2. Dengue virus serotype 2 (strain 16681) was propagated in the *Aedes albopictus* derived cell line, C6/36. For infection, stock virus, prepared as described elsewhere [Suksanpaisan and Smith, 2003] was diluted in DMEM. Cells were incubated with virus at MOI of 5 for 1.5 hr following which the cells were washed twice and maintained in growth medium.

RNA Extraction and RT-PCR

Total RNA was extracted with Trizol reagent (Molecular research center, Inc., Cincinnati, OH) according to the manufacturer's instructions. cDNA was synthesized from total cellular RNA using Improm II™ reverse transcriptase (Promega, Madison, WI) and primer D2_R (Table I) for dengue virus positive strand or D1_F (Table I) for dengue virus negative strand or with oligo $(dT)_{15}$ primer (Promega) for cytokine genes. For PCR of dengue virus positive and negative strands, first strand cDNA was amplified for 35 cycles with D1_F and D2_R primers using Taq DNA polymerase (Promega). Cycling condition were as follows: denaturation at 94°C for 10 sec, annealing at 57°C for 30 sec, and extension at 72°C for 1 min. Cytokine genes and 18S RNA were amplified with 7 pmol each of specific primers pairs as shown in Table I in a total reaction volume of 10 μl. Cycling condition were as follows: denaturation at 94°C for 15 sec (for IFN-β, IL-1β, MIP1-α, MCP-1, IL-8, MIP1-β, TRAIL, RANTES, and 18S) or for 20 sec (IL-6), annealing at 55°C for 20 sec (for IFN-β, IL-1β, MIP1-α, MCP-1, IL-8, MIP1-β, TRAIL, IL-6, and 18S) or for 12 sec (RANTES) and extension at 72°C for 30 sec (for IFN-β, IL-1β, MIP1-α, MCP-1, IL-8, MIP1-β, TRAIL, and 18S) or for 18 sec (RANTES) or for 1 min (IL-6). Cytokine gene first strand cDNAs were amplified for 35 cycles while control 18S was amplified for 28 cycles. All PCR products were separated on 1.8% agarose gels and visualized by ethidium bromide staining.

TABLE I. Gene Specific Oligonucleotide Primers

Primer	Sequence	Product size	References
D1_F	5′-TCAATATGCTGAAACGCGCGAGAAACCG-3′	511	Lanciotti et al. [1992]
D2_R	5′-TTGCACCAACAGTCAATGTCTTCAGGTTC-3′		
IFN-β	5′-GATTCATCTAGCACTGGCTGG-3′	186	Li et al. [2005]
	5′-CTTCAGGTAATGCAGAATCC-3′		
IL-1β	5′-AAGCTTGGTGATGTCTGG-3′	330	Bosch et al. [2002]
	5′-TGAGAGGTGCTGATGTACCA-3′		
MIP-1α	5′-CGCCTGCTGCTTCAGCTACACCTCCCGGCAGA-3′	195	Dumoulin et al. [1999]
	5′-TGGACCCCTCAGGCACTCAGCTCCAGGTCGCT-3′		
MCP-1	5′-TTCTCAAACTGAAGCTCGCACTCTCGCC-3′	348	Nordskog et al. [2005]
	5′-TGTGGAGTGAGTGTTCAAGTCTTCGGAGTT-3′		
RANTES	5′-CCACATCAAGGAGTATTTCTACACC-3′	101	Lin et al. [2000a]
	5′-TCTTCTCTGGGTTGGCACACAC-3′		
IL-8	5′-AAGAGAGCTCTGTCTGGACC-3′	408	Bosch et al. [2002]
	5′-GATATTCTCTTGGCCCTTGG-3′		
MIP1-β	5′-GGAAGCTTCCTCGCAACTTTG-3′	200	Chiba et al. [2004]
	5′-GCTCAGGTGACCTTCCCTGAA-3′		
TRAIL	5′-CAATGACGAAGAGAGTATGA-3′	537	Matsuda et al. [2005]
	5′-CCCCCTTGATAGATGGAATA-3′		
IL-6	5′-CCACACAGACAGCCACTCACCTC-3′	313	Abdallah et al. [2005]
	5′-CTGGCTTGTTCCTCACTACTCTC-3′		
Actin	5′-GAAGATGACCCAGATCATGT-3′	330	
	5′-ATCTCTTGCTCGAAGTCCAG-3′		
18s RNA	5′-AAACGGCTACCACATCCAAG-3′	155	
	5′-CCTCCAATGGATCCTCGTTA-3′		

Indirect Immunofluorescence Microscopy

HepG2 cells were grown onto standard glass coverslips while human hepatocytes were grown on collagen type I coated coverslips (Becton Dickinson, Bedford, MA). Cells were infected with the dengue virus at MOI 5 for 1.5 hr and the cells were subsequently fixed at 0, 24, and 36 hr post-infection with 4% paraformaldehyde at room temperature for 30 min. The cells were then permeabilized by incubation with 0.3% Triton X-100 in PBS for 10 min and methanol for 5 min at room temperature followed by incubation with 5% BSA in PBS for 1 hr. Cells were subsequently incubated with either a 1:10 dilution of mouse anti-dengue monoclonal antibody HB114 [Henchal et al., 1982] or directly with a mouse anti-dengue NS1 protein monoclonal antibody [Puttikhunt et al., 2003] at 4°C overnight, follow by six wash with 0.03% Triton X-100 in PBS. Samples were then incubated with a 1:500 dilution of an anti-mouse IgG monoclonal antibody conjugated with Alexa594 (Molecular Probes, Eugene, OR) and 20μg/μl DAPI (4′-6-Diamidino-2-phenylindole) in 1% BSA (Molecular Probes) for 1 hr at room temperature, follow by six washes with 0.03% Triton X-100 in PBS. Coverslips were mounted on glass slides with Vectashield (Vector Laboratories, Burlingame, CA).

Human IL-8 ELISA

The concentration of IL-8 was determined using a commercial ELISA kit (ID Labs, Inc., ON, Canada). Culture medium from either control mock infected or cells infected with the dengue virus at MOI 5 was collected at 0, 12, 18, 24, and 36 hr post-infection. The assays were performed as recommend by the manufacturer, and IL-8 concentration was determined by spectrometry at 450 nm.

RESULTS

To establish if primary human hepatocytes are able to be productively infected with the dengue virus, approximately 2.2×10^5 primary hepatocytes were seeded onto individual 12 mm diameter collagen coated PTFE membranes in two 12 well polystyrene plates and incubated under 5% CO_2 at 37°C overnight. At the same time approximately 3×10^5 HepG2 cells were seeded into individual wells of a 12 well tissue culture plate and incubated overnight under 10% CO_2 at 37°C. Following overnight incubation, one well of HepG2 cells was trypsinized and cells counted and the well was shown to contain 3×10^5 cells. Primary hepatocytes and HepG2 cells were incubated with dengue virus serotype 2 at an MOI of 5 and cells incubated for a further 60 hr. Over this time assays of cell number showed that infected primary hepatocytes decreased from 1×10^5 to 1×10^4, or a drop of 90% (see Fig. 1a). Loss of viable cells occurred by the hepatocytes rounding up and detaching from the matrix support. In comparison mock infected primary hepatocytes declined from 7×10^4 to 4×10^4 over the same time period, a decline of some 40%, while infected HepG2 cells showed a 60% increase in cell number due to cell proliferation. Over the 60 hr of the experiment growth medium was sampled at 0, 6, 12, 18, 24, 36, 48, and 60 hr post-infection and levels of infectious progeny viruses established by standard plaque assay on LLC-MK_2 cells. Experiment was undertaken independently in duplicate with duplicate plaque assay of samples. By 60 hr a tenfold increase in virus titer over input was observed for both primary hepatocytes and HepG2 cells (Fig. 1b) strongly suggestive of de novo virus replication and productive infection. The genome of dengue is a positive sense RNA strand which can be translated directly [White and Fenner, 1994]. As part of the replication process an antisense (negative sense) strand is produced that is subsequently used as a template for further positive strand production [White and Fenner, 1994]. To establish the presence of both the positive (sense) and negative (antisense) strands of the dengue virus genome human primary hepatocytes and HepG2 cells were infected with dengue virus serotype 2 for 48 hr after which total RNA was extracted and cDNA was synthesized from total cellular RNA and subjected to RT-PCR using dengue specific primers (Table I) as well as primers directed against actin. Results (Fig. 1c) show the presence of both dengue polarity strands in the hepatocytes as well as in HepG2 cells.

As a final confirmation of productive dengue virus infection of primary hepatocytes, translation of the dengue genome was investigated through the detection of both structural and non-structural dengue proteins. While structural proteins may be present in the infected cell as a result of the original infecting virus, the presence of non-structural proteins would confirm dengue virus genome translation. For this reason, primary hepatocytes and HepG2 cells were grown separately on microscope cover slips overnight and cells were then infected with dengue virus serotype 2 at an MOI of 5 and the cells were incubated for a further 0, 24, or 36 hr after which they were subsequently fixed and incubated with either mouse anti-dengue monoclonal antibody HB114 [Henchal et al., 1982] or a mouse anti dengue NS1 monoclonal antibody [Puttikhunt et al., 2003] followed by a further incubation with an anti-mouse IgG monoclonal antibody conjugated with Alexa594. Samples were incubated further with DAPI before visualization under a fluorescent microscope. Results (Fig. 1d) show that both primary hepatocytes and HepG2 cells show the synthesis of E protein and NS1 protein by 24 hr post-infection. Nuclear staining with DAPI confirmed the presence of many fragmented nuclei in the primary hepatocytes and fragmentation patterns were consistent with the induction of cellular apoptosis (Fig. 2). Counting of multiple fields of cells double stained cells (either DAPI and NS1 or DAPI and E protein) at 24 hr gave cell infection rates of $67.74\% \pm 26.21$ for NS1 and $76.57\% \pm 18.94$ for E protein, suggesting that the majority of the primary hepatocytes were infected by 24 hr.

Having confirmed the productive infection of primary hepatocytes by the dengue virus the study sought to

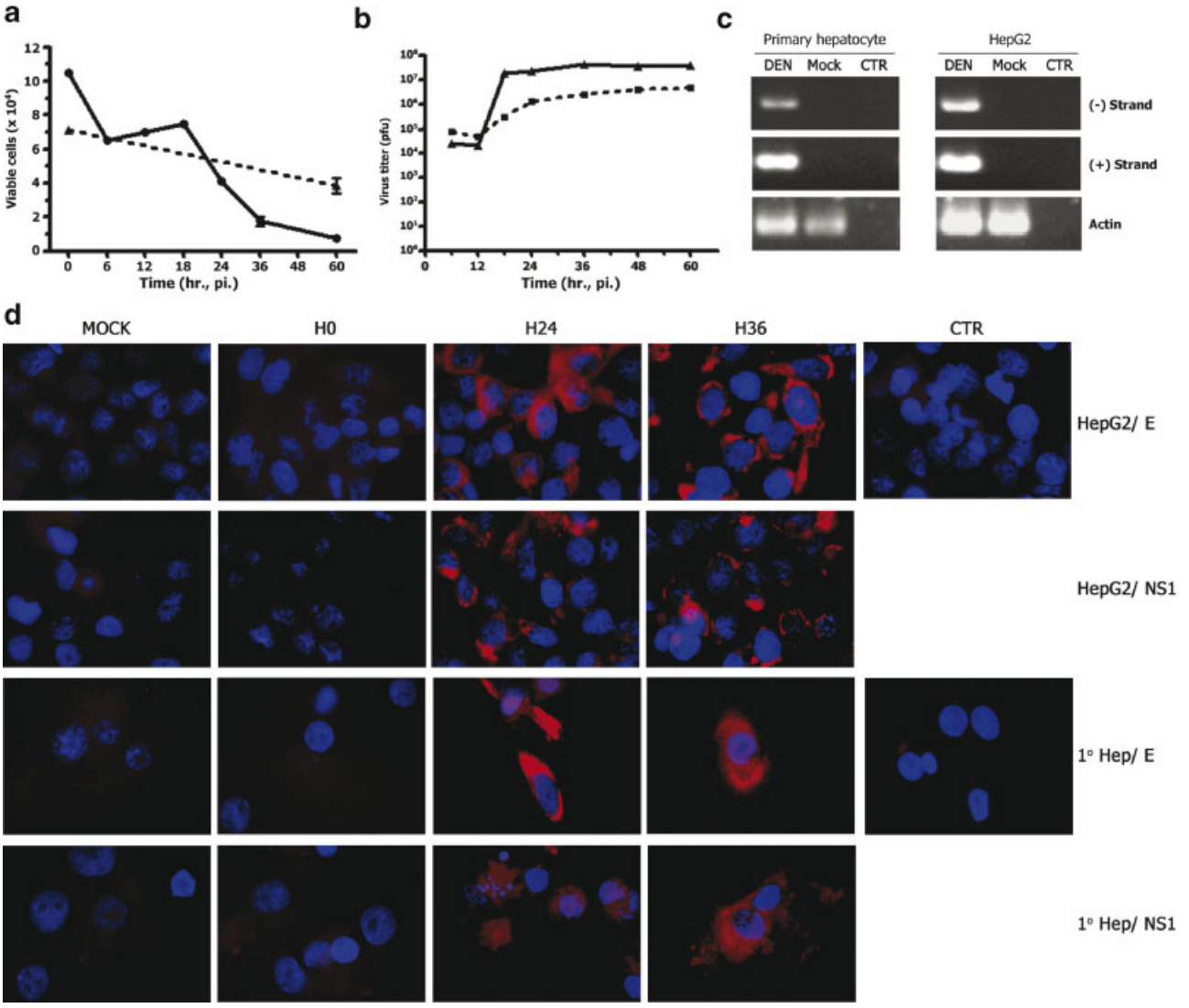

Fig. 1. Infection of human primary hepatocytes with the dengue virus. **Panel a**: Human primary hepatocytes were infected with the dengue virus at MOI 5 (solid line) or mock infected (broken line) and cell number counted for up to 60 hr post-infection. Error bars are s.e.m. of two independent experiments counted in quadruplet. **Panel b**: Human primary hepatocytes (broken line) or HepG2 cells (solid line) were infected with the dengue virus and media assayed by standard plaque assay for infectious progeny viruses. Experiment was undertaken in duplicate with duplicate assay of virus titers, error bars represent s.e.m. **Panel c**: RT-PCR analysis of dengue virus infected and mock infected human primary hepatocytes and HepG2 cells to detect positive (sense) and negative (anti-sense) dengue strands. CTR: control reaction with no template. **Panel d**: Merged images of immunoflourescent staining of dengue virus infected human primary hepatocytes (1° Hep) and HepG2 cells using monoclonal antibodies directed against either dengue virus E protein or dengue virus NS1 protein. Positive signal shows red, while DAPI staining shows nuclei as blue. CTR: no primary antibody.

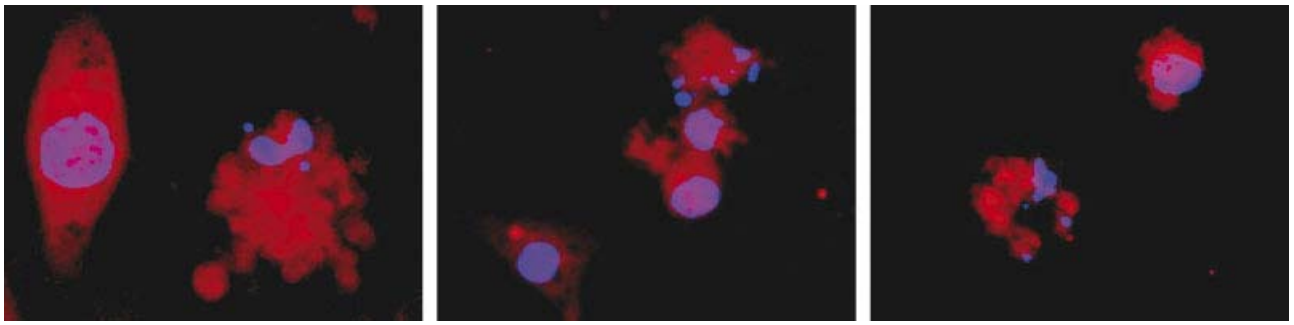

Fig. 2. Primary human hepatocyte nuclei fragmentation in response to dengue virus infection. Merged images of immunoflourescent staining of dengue virus infected human primary hepatocytes showing nuclear fragmentation using monoclonal antibodies directed against dengue virus NS1 protein and DAPI staining at 24 hr post-infection.

investigate the cellular response of the primary hepatocytes to dengue virus infection and multiple parallel wells of hepatocytes were infected with dengue virus serotype 2 at an MOI of 5 for 1.5 hr. At times of 0, 12, 18, 24, and 36 hr post-infection cells were harvested and RNA extracted and cDNA prepared. Semi-quantitative expression profiles for IFN-β, TRAIL, MCP-1, IL-6, IL-1β, IL-8, MIP-1α, MIP-1β, and RANTES were determined by RT-PCR using the primers given in Table I, together with 18S RNA levels as a control. All PCR products were separated on 1.8% agarose gels and visualized by ethidium bromide staining. The experiment was conducted in parallel with HepG2 cells, and undertaken twice independently.

Results (Fig. 3) show similar, but not identical induction profiles between primary hepatocytes and HepG2 cells. In particular a significant induction of IL-6 was observed in HepG2 cells, but no message for IL-6 was detectable in primary hepatocytes. Similarly, MCP-1 was observed to be expressed in hepatocytes, but not HepG2 cells. IL-1β was apparently down-regulated in primary hepatocytes, but induced in HepG2 cells. In both cell types a significant induction of TRAIL, MIP-1α, IFN-β, MIP-1β IL-8, and RANTES was observed. Quantitation of the signal intensities of the various PCR products against the 18S signal (Fig. 4) showed that in HepG2 cells a peak of induction was observed between 18 and 24 hr post-infection while contrast induction in primary hepatocytes was generally lower and without a significant peak, except for RANTES and IL-8 which showed a sharp increase in signal between 24 and 36 hr. Accurate quantitation of bands also revealed that the IL-1β profile was identical in both HepG2 cells and primary hepatocytes.

From the cytokine profile it was noted that IL-8, an important regulator of the acute inflammatory response [Remick, 2005], was up-regulated significantly and as IL-8 has been shown to be significantly higher in the serum of dengue hemorrhagic patients than in DF patients [Raghupathy et al., 1998] we sought to determine if the increase in the message was accompanied by the release of IL-8 protein and so primary hepatocytes were again infected at an MOI of 5 in parallel with HepG2 cells. Samples of the growth medium were sampled at 0, 12, 18, 24, and 36 hr post-infection and assayed for immunoreactive human IL-8 using the ELISA assay. Experiment was undertaken independently in duplicate with triplicate assay of each sample together with control (mock infected) cells. Results (Fig. 5) show that significant amounts of IL-8 are released from both primary hepatocytes and HepG2 cells in response to dengue virus infection. In contrast no IL-8 was detected in either mock infected human primary cells or mock infected HepG2 cells.

DISCUSSION

The involvement of the liver in the pathogenesis of dengue virus infections is the subject of some controversy. While several studies have shown the presence of high rates of hepatomegaly [Mohan et al., 2000] as well as significant disorder of the levels of serum liver

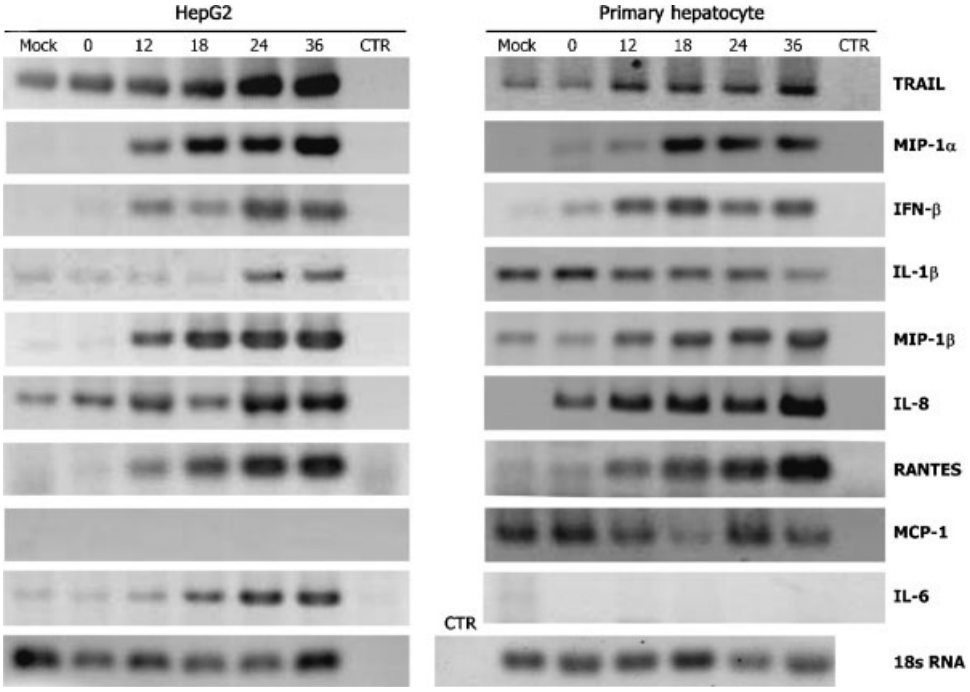

Fig. 3. Cytokine response of dengue virus infected human primary hepatocytes. Human primary hepatocytes or HepG2 cells were infected with the dengue virus at MOI 5 and the expression of nine cytokines (IFN-β, TRAIL, MCP-1, IL-6, IL-1β, IL-8, MIP-1α, MIP-1β, and RANTES) examined by RT-PCR for up to 36 hr post-infection. 18S ribosomal RNA was used as a control.

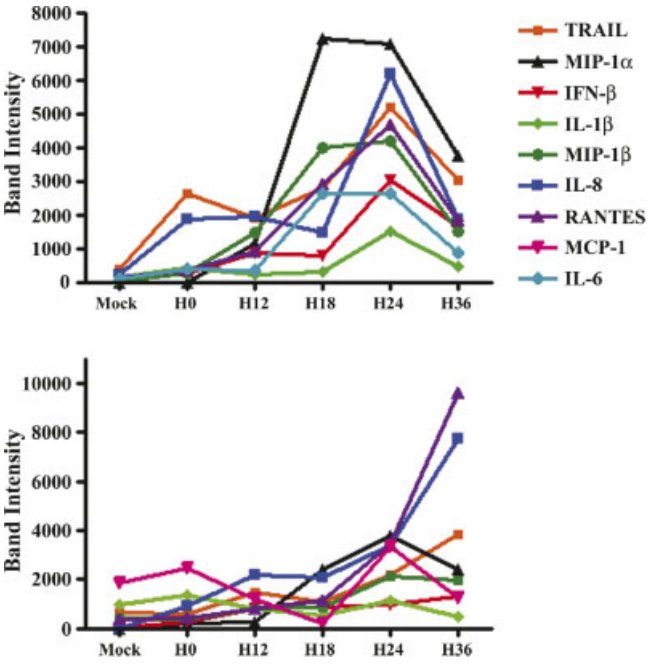

Fig. 4. Quantification of cytokine gene response in dengue infected HepG2 cells and primary hepatocytes. Band intensities of cytokine gene expression from Figure 2 were calculated relative to the 18S ribosomal intensity using the ImageJ program and plotted as a function of time. **Top**, HepG2; **bottom**, primary human hepatocytes.

enzymes [Kuo et al., 1992; Nguyen et al., 1997; Mohan et al., 2000; Wahid et al., 2000], whether these occur as a result from the direct infection of cells of the liver or result from a bystander effect possibly as a result of dysregulation of the host immune responses is unclear. Further uncertainty arises from the nature of the cell or cells in the liver affected by the infection process.

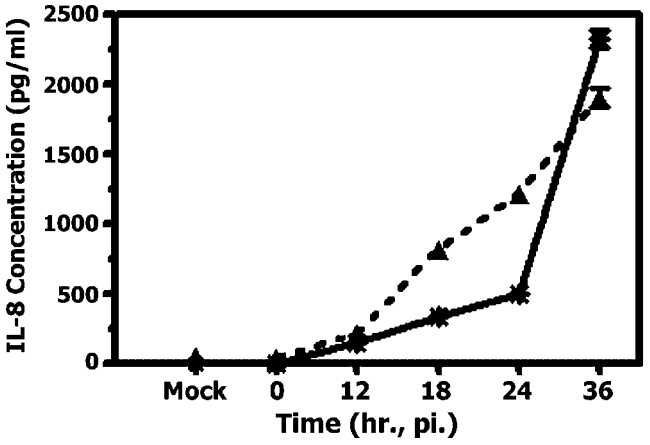

Fig. 5. Production of IL-8 from infected primary hepatocytes and HepG2 cells. Human primary hepatocytes and HepG2 cells were infected with dengue virus serotype 2 at MOI 5 and culture medium sampled over 36 hr post-infection and levels of immunoreactive human IL-8 assayed by ELISA assay. Solid line: HepG2 cells, broken line: human primary hepatocytes. Mock: Mock infected primary hepatocytes and HepG2 cells at 0 hr post-infection. Experiment was undertaken in duplicate with triplicate sample assay. Error bars represent s.e.m.

The direct involvement of the liver in the pathogenesis of dengue has been suggested by the demonstration of the dengue virus RNA by reverse transcription (RT)-PCR in liver tissue samples obtained from children with fatal DF [Rosen et al., 1999; Huerre et al., 2001], the demonstration of dengue virus antigens in hepatocytes [Couvelard et al., 1999; Huerre et al., 2001] as well as the recovery of the virus from liver samples from fatal cases of dengue [Rosen et al., 1989]. While earlier studies based upon autopsy specimens have suggested the involvement of both hepatocytes and Kupffer cells [Couvelard et al., 1999; Rosen et al., 1999; Huerre et al., 2001], this is contradicted by more recent studies that report only the involvement of Kupffer cells [Jessie et al., 2004]. Animal studies have similarly been contradictory. Using BALB/c mice injected interperitonealy with dengue serotype 2 obtained from a human patient, Paes et al. [2005] found results consistent with the involvement of hepatocytes including the detection of viral antigens in hepatocytes as well as morphological changes of hepatocytes and hepatocyte necrosis. In contrast to this, an earlier study by Chen et al. [2004] using immunocompetent C57BL/6 mice injected with a high titer inoculation of Dengue 2 strain 16681 (the same strain type as used in this study) found little if any direct involvement of hepatocytes and the authors concluded that liver injury primarily arose though the infiltration of activated lymphocytes, especially CD8+ T cells [Chen et al., 2004]. Other authors have suggested that CD4+ cytotoxic T cells (CTL's) may mediate liver damage through bystander lysis after activation by dengue virus infected Kupffer cells through the Fas/FasL pathway [Gagnon et al., 1999]. Antibodies directed against dengue virus proteins [Lin et al., 2002, 2003], or autoantibodies [Chaturvedi et al., 2001; Lin et al., 2001; Oishi et al., 2003] may also play a role in mediating liver damage through mechanisms independent of direct infection of hepatocytes. As such the question of whether hepatocytes can be directly infected is of critical importance in understanding the pathogenesis of dengue virus infections.

Using isolated purified human primary hepatocytes, this study has demonstrated that human primary hepatocytes in vitro are able to be productively infected with dengue virus serotype 2, and that infection results in a significant cytokine response. There was a marked and rapid loss of infected hepatocytes, significantly over and above the loss seen for uninfected hepatocytes and cells from infection experiments were observed to round up and detach from the matrix support. In addition, infected hepatocytes with fragmented nuclei were observed frequently and both observations are morphologically consistent with the induction of apoptosis in infected hepatocytes. Although the induction of apoptosis was not verified formally in this study, the induction of apoptosis in infected transformed hepatocytes has been well established [Marianneau et al., 1997, 1998; Thongtan et al., 2004] and evidence suggests that in transformed hepatocytes induction of apoptosis occurs through the up-regulation of TRAIL [Matsuda et al.,

2005]. TRAIL (TNF-related apoptosis-inducing ligand or Apo2 ligand) is a type II transmembrane protein that triggers apoptosis mainly in tumor cells [Ashkenazi and Dixit, 1999; Walczak et al., 1999] but has a minimal proapoptotic effect in most normal human cells in vitro and in TRAIL-treated animals [Wiley et al., 1995; Pitti et al., 1996; Gura, 1997; Rieger et al., 1998; French and Tschopp, 1999; Walczak et al., 1999]. TRAIL mRNA is constitutively present in many tissues, unlike the restricted expression of other proapoptotic members of the TNF family [Wiley et al., 1995; Pitti et al., 1996]. Interestingly though, in contrast to many other cell types hepatocytes are highly sensitive to the action of TRAIL [Jo et al., 2000], and as such while the induction of TRAIL seen in dengue infected transformed hepatocytes [Matsuda et al., 2005] may reflect the transformed nature of these cells, the induction of TRAIL seen here in dengue infected primary hepatocytes may well represent a bone fide pathway of apoptotic induction in dengue infected hepatocytes.

In addition to the transcriptional up-regulation of TRAIL, we also noted a significant up-regulation of IL-8 which was associated with the secretion of immunoreactive IL-8. IL-8 is a chemotactic cytokine responsible for inducing chemotaxis, which is the directed migration of cells to a site of inflammation and IL-8 is a chemoattractant for neutrophils, basophils, and lymphocytes [Mantovani et al., 1992]. Up-regulation of IL-8, together with RANTES, MIP-1α, MIP-1β, has been reported previously for dengue infected HepG2 cells [Medin et al., 2005] consistent with the results found here for both HepG2 and primary hepatocytes. IL-8 has been reported to be found at significantly higher levels in the serum of DHF patients with severe grade fever than in DF patients [Raghupathy et al., 1998].

As such, these results suggest that the role of the liver in severe DF infections may well be underestimated. It is likely that the combination of a significant cytokine response, coupled with the early induction of cell death will serve to limit the spread of the virus both by the direct removal of apoptotic cells by recruited phagocytic cells as well as the provision of a dead end host cell for free viruses [Marianneau et al., 1999]. In particular these results may serve to explain the discrepancy between the high proportion of liver abnormality as evidenced by liver enzyme levels [Kuo et al., 1992; Nguyen et al., 1997; Mohan et al., 2000; Wahid et al., 2000] and the low levels of liver damage seen in classical autopsy studies [Bhamarapravati, 1989; Subramanian et al., 2005]. Given that fatalities occur commonly 7–10 days after infection [Malavige et al., 2004] the evidence of significant hepatocyte loss may not be detectable without significantly more refined studies, leading to an underestimation of the effects of liver involvement in the pathobiology of dengue infections.

ACKNOWLEDGMENTS

This work was supported by Grant BRG4980010 (D.R.S) from the Thailand Research Fund and by Mahidol University. L.S is supported by a Royal Golden Jubilee Scholarship and a Research Assistantship from Mahidol University. A. C.-H. was supported by the Consejo Nacional de Ciencia y Tecnología, México. The authors thank Prida Malasit, Sirirat Hospital, Thailand for kindly providing the anti-dengue NS1 protein monoclonal antibody used in this study.

REFERENCES

Abdallah BM, Stilgren LS, Nissen N, Kassem M, Jorgensen HR, Abrahamsen B. 2005. Increased RANKL/OPG mRNA ratio in iliac bone biopsies from women with hip fractures. Calcif Tissue Int 76: 90–97.

Ashkenazi A, Dixit VM. 1999. Apoptosis control by death and decoy receptors. Curr Opin Cell Biol 11:255–260.

Bhamarapravati N. 1989. Hemostatic defects in dengue hemorrhagic fever. Rev Infect Dis 11:S826–S829.

Bosch I, Xhaja K, Estevez L, Raines G, Melichar H, Warke RV, Fournier MV, Ennis FA, Rothman AL. 2002. Increased production of interleukin-8 in primary human monocytes and in human epithelial and endothelial cell lines after dengue virus challenge. J Virol 76:5588–5597.

Chang GJ. 1997. Molecular biology of dengue viruses. In: Gubler DJ, Kuno G, editors. Dengue and dengue hemorrhagic fever. Wallingford: CAB International. pp 175–198.

Chaturvedi UC, Elbishbishi EA, Agarwal R, Mustafa AS. 2001. Cytotoxic factor-autoantibodies: Possible role in the pathogenesis of dengue haemorrhagic fever. FEMS Immunol Med Microbiol 30: 181–186.

Chen HC, Lai SY, Sung JM, Lee SH, Lin YC, Wang WK, Chen YC, Kao CL, King CC, Wu-Hsieh BA. 2004. Lymphocyte activation and hepatic cellular infiltration in immunocompetent mice infected by dengue virus. J Med Virol 73:419–431.

Chiba K, Zhao W, Chen J, Wang J, Cui HY, Kawakami H, Miseki T, Satoshi H, Tanaka J, Asaka M, Kobayashi M. 2004. Neutrophils secrete MIP-1 beta after adhesion to laminin contained in basement membrane of blood vessels. Br J Haematol 127:592–597.

Couvelard A, Marianneau P, Bedel C, Drouet MT, Vachon F, Henin D, Deubel V. 1999. Report of a fatal case of dengue infection with hepatitis: Demonstration of dengue antigens in hepatocytes and liver apoptosis. Hum Pathol 30:1106–1110.

Dumoulin FL, Altfeld M, Rockstroh JK, Leifeld L, Sauerbruch T, Spengler U. 1999. Semiquantitation of human chemokine mRNA levels with a newly constructed multispecific competitor fragment. J Immunol Methods 224:61–67.

French LE, Tschopp J. 1999. The TRAIL to selective tumor death. Nat Med 5:146–147.

Gagnon SJ, Ennis FA, Rothman AL. 1999. Bystander target cell lysis and cytokine production by dengue virus-specific human CD4(+) cytotoxic T-lymphocyte clones. J Virol 73:3623–3629.

Gura T. 1997. How TRAIL kills cancer cells, but not normal cells. Science 277:768.

Guzman MG, Kouri G. 2002. Dengue: An update. Lancet Infect Dis 2: 33–42.

Halstead SB. 1989. Antibody, macrophages, dengue virus infection, shock, and hemorrhage: A pathogenetic cascade. Rev Infect Dis 11: S830–S839.

Henchal EA, Gentry MK, McCown JM, Brandt WE. 1982. Dengue virus-specific and flavivirus group determinants identified with monoclonal antibodies by indirect immunofluorescence. Am J Trop Med Hyg 31:830–836.

Huerre MR, Lan NT, Marianneau P, Hue NB, Khun H, Hung NT, Khen NT, Drouet MT, Huong VT, Ha DQ, Buisson Y, Deubel V. 2001. Liver histopathology and biological correlates in five cases of fatal dengue fever in Vietnamese children. Virchows Arch 438:107–115.

Jessie K, Fong MY, Devi S, Lam SK, Wong KT. 2004. Localization of dengue virus in naturally infected human tissues, by immunohistochemistry and in situ hybridization. J Infect Dis 189:1411–1418.

Jo M, Kim TH, Seol DW, Esplen JE, Dorko K, Billiar TR, Strom SC. 2000. Apoptosis induced in normal human hepatocytes by tumor necrosis factor-related apoptosis-inducing ligand. Nat Med 6:564–567.

Kuo CH, Tai DI, Chang-Chien CS, Lan CK, Chiou SS, Liaw YF. 1992. Liver biochemical tests and dengue fever. Am J Trop Med Hyg 47:265–270.

Lanciotti RS, Calisher CH, Gubler DJ, Chang GJ, Vorndam AV. 1992. Rapid detection and typing of dengue viruses from clinical samples by using reverse transcriptase-polymerase chain reaction. J Clin Microbiol 30:545–551.

Li K, Chen Z, Kato N, Gale M, Jr., Lemon SM. 2005. Distinct poly(I-C) and virus-activated signaling pathways leading to interferon-beta production in hepatocytes. J Biol Chem 280:16739–16747.

Lin YL, Liu CC, Chuang JI, Lei HY, Yeh TM, Lin YS, Huang YH, Liu HS. 2000a. Involvement of oxidative stress, NF-IL-6, and RANTES expression in dengue-2-virus-infected human liver cells. Virology 276:114–126.

Lin YL, Liu CC, Lei HY, Yeh TM, Lin YS, Chen RM, Liu HS. 2000b. Infection of five human liver cell lines by dengue-2 virus. J Med Virol 60:425–431.

Lin CF, Lei HY, Liu CC, Liu HS, Yeh TM, Wang ST, Yang TI, Sheu FC, Kuo CF, Lin YS. 2001. Generation of IgM anti-platelet autoantibody in dengue patients. J Med Virol 63:143–149.

Lin CF, Lei HY, Shiau AL, Liu HS, Yeh TM, Chen SH, Liu CC, Chiu SC, Lin YS. 2002. Endothelial cell apoptosis induced by antibodies against dengue virus nonstructural protein 1 via production of nitric oxide. J Immunol 169:657–664.

Lin CF, Lei HY, Shiau AL, Liu CC, Liu HS, Yeh TM, Chen SH, Lin YS. 2003. Antibodies from dengue patient sera cross-react with endothelial cells and induce damage. J Med Virol 69:82–90.

Malavige GN, Fernando S, Fernando DJ, Seneviratne SL. 2004. Dengue viral infections. Postgrad Med J 80:588–601.

Mantovani A, Bussolino F, Dejana E. 1992. Cytokine regulation of endothelial cell function. FASEB J 6:2591–2599.

Marianneau P, Cardona A, Edelman L, Deubel V, Despres P. 1997. Dengue virus replication in human hepatoma cells activates NF-kappaB which in turn induces apoptotic cell death. J Virol 71:3244–3249.

Marianneau P, Flamand M, Deubel V, Despres P. 1998. Induction of programmed cell death (apoptosis) by dengue virus in vitro and in vivo. Acta Cient Venez 49:13–17.

Marianneau P, Steffan AM, Royer C, Drouet MT, Jaeck D, Kirn A, Deubel V. 1999. Infection of primary cultures of human Kupffer cells by dengue virus: No viral progeny synthesis, but cytokine production is evident. J Virol 73:5201–5206.

Matsuda T, Almasan A, Tomita M, Tamaki K, Saito M, Tadano M, Yagita H, Ohta T, Mori N. 2005. Dengue virus-induced apoptosis in hepatic cells is partly mediated by Apo2 ligand/tumour necrosis factor-related apoptosis-inducing ligand. J Gen Virol 86:1055–1065.

Medin CL, Fitzgerald KA, Rothman AL. 2005. Dengue virus nonstructural protein NS5 induces interleukin-8 transcription and secretion. J Virol 79:11053–11061.

Mohan B, Patwari AK, Anand VK. 2000. Hepatic dysfunction in childhood dengue infection. J Trop Pediatr 46:40–43.

Nguyen TL, Nguyen TH, Tieu NT. 1997. The impact of dengue haemorrhagic fever on liver function. Res Virol 148:273–277.

Nordskog BK, Fields WR, Hellmann GM. 2005. Kinetic analysis of cytokine response to cigarette smoke condensate by human endothelial and monocytic cells. Toxicology 212:87–97.

Oishi K, Inoue S, Cinco MT, Dimaano EM, Alera MT, Alfon JA, Abanes F, Cruz DJ, Matias RR, Matsuura H, Hasebe F, Tanimura S, Kumatori A, Morita K, Natividad FF, Nagatake T. 2003. Correlation between increased platelet-associated IgG and thrombocytopenia in secondary dengue virus infections. J Med Virol 71:259–264.

Paes MV, Pinhao AT, Barreto DF, Costa SM, Oliveira MP, Nogueira AC, Takiya CM, Farias-Filho JC, Schatzmayr HG, Alves AM, Barth OM. 2005. Liver injury and viremia in mice infected with dengue-2 virus. Virology 338:236–246.

Pitti RM, Marsters SA, Ruppert S, Donahue CJ, Moore A, Ashkenazi A. 1996. Induction of apoptosis by Apo-2 ligand, a new member of the tumor necrosis factor cytokine family. J Biol Chem 271:12687–12690.

Puttikhunt C, Kasinrerk W, Srisa-ad S, Duangchinda T, Silakate W, Moonsom S, Sittisombut N, Malasit P. 2003. Production of anti-dengue NS1 monoclonal antibodies by DNA immunization. J Virol Methods 109:55–61.

Raghupathy R, Chaturvedi UC, Al-Sayer H, Elbishbishi EA, Agarwal R, Nagar R, Kapoor S, Misra A, Mathur A, Nusrat H, Azizieh F, Khan MA, Mustafa AS. 1998. Elevated levels of IL-8 in dengue hemorrhagic fever. J Med Virol 56:280–285.

Remick DG. 2005. Interleukin-8. Crit Care Med 33:S466–S467.

Rieger J, Naumann U, Glaser T, Ashkenazi A, Weller M. 1998. APO2 ligand: A novel lethal weapon against malignant glioma? FEBS Lett 427:124–128.

Rosen L, Khin MM, Tin U. 1989. Recovery of virus from the liver of children with fatal dengue: Reflections on the pathogenesis of the disease and its possible analogy with that of yellow fever. Res Virol 140:351–360.

Rosen L, Drouet MT, Deubel V. 1999. Detection of dengue virus RNA by reverse transcription-polymerase chain reaction in the liver and lymphoid organs but not in the brain in fatal human infection. Am J Trop Med Hyg 61:720–724.

Subramanian V, Shenoy S, Joseph AJ. 2005. Dengue hemorrhagic fever and fulminant hepatic failure. Dig Dis Sci 50:1146–1147.

Suksanpaisan L, Smith DR. 2003. Analysis of saturation binding and saturation infection for dengue serotypes 1 and 2 in liver cells. Intervirology 46:50–55.

Thongtan T, Panyim S, Smith DR. 2004. Apoptosis in dengue virus infected liver cell lines HepG2 and Hep3B. J Med Virol 72:436–444.

Wahid SF, Sanusi S, Zawawi MM, Ali RA. 2000. A comparison of the pattern of liver involvement in dengue hemorrhagic fever with classic dengue fever. Southeast Asian J Trop Med Public Health 31:259–263.

Walczak H, Miller RE, Ariail K, Gliniak B, Griffith TS, Kubin M, Chin W, Jones J, Woodward A, Le T, Smith C, Smolak P, Goodwin RG, Rauch CT, Schuh JC, Lynch DH. 1999. Tumoricidal activity of tumor necrosis factor-related apoptosis-inducing ligand in vivo. Nat Med 5:157–163.

White DO, Fenner FJ. 1994. Flaviviridae. Medical virology, 4th edn. San Diego. pp 433–450.

Wiley SR, Schooley K, Smolak PJ, Din WS, Huang CP, Nicholl JK, Sutherland GR, Smith TD, Rauch C, Smith CA, et al. 1995. Identification and characterization of a new member of the TNF family that induces apoptosis. Immunity 3:673–682.

Journal of Biomedical Science

BioMed Central

Research

Open Access

Characterization of dengue virus entry into HepG2 cells

Lukkana Suksanpaisan[1,2], Tharinee Susantad[1,3] and Duncan R Smith*[1]

Address: [1]Molecular Pathology Laboratory, Institute of Molecular Biology and Genetics, Mahidol University, Salaya campus, 25/25 Phuttamontol Sai 4, Salaya, Nakorn Pathom, 73170, Thailand, [2]Molecular Medicine Program, Mayo Clinic College of Medicine, Guggenheim 18, 200 First street SW, Rochester, MN, 55905, USA and [3]National Science and Development Agency (NSTDA), 111 Thailand Science Park, Phahonyothin Road, Klong 1, Klong Luang, Pathumthani, 12120, Thailand

Email: Lukkana Suksanpaisan - tataat@hotmail.com; Tharinee Susantad - jomjam_aus@hotmail.com; Duncan R Smith* - duncan_r_smith@hotmail.com

* Corresponding author

Published: 4 February 2009

Journal of Biomedical Science 2009, **16**:17 doi:10.1186/1423-0127-16-17

Received: 29 June 2008
Accepted: 4 February 2009

This article is available from: http://www.jbiomedsci.com/content/16/1/17

Abstract

Background: Despite infections by the dengue virus being a significant problem in tropical and sub-tropical countries, the mechanism by which the dengue virus enters into mammalian cells remains poorly described.

Methods: A combination of biochemical inhibition, dominant negative transfection of Eps15 and siRNA mediated gene silencing was used to explore the entry mechanism of dengue into HepG2 cells.

Results: Results were consistent with entry via multiple pathways, specifically via clathrin coated pit mediated endocytosis and macropinocytosis, with clathrin mediated endocytosis being the predominant pathway.

Conclusion: We propose that entry of the dengue virus to mammalian cells can occur by multiple pathways, and this opens the possibility of the virus being directed to multiple cellular compartments. This would have significant implications in understanding the interaction of the dengue virus with the host cell machinery.

Background

While most animal viruses enter into cells by receptor mediated endocytosis in clathrin coated pits [1,2], evidence to date suggests that the normal mechanism of dengue virus entry into both insect and mammalian cells is by direct fusion of the virus with the cell membrane [3-6], although endocytosis of dengue viruses has been observed with neutralization escape mutants [5], in the presence of neutralizing antibodies [6] as well as in the non-target cell line Hela [7]. These results are somewhat contradictory to results with other flaviviruses, and both Japanese encephalitis virus (JEV) and West Nile virus have been shown to enter cells via clathrin coated pits [8-10]. However, the majority of the studies undertaken to date on the dengue viruses have been based upon electron microscopy ultrastructural studies [4-6] or non-target cells [7] and as such no comprehensive direct biochemical or genetic analysis of the entry mechanism of the dengue virus has yet been undertaken.

Methods

Cells and viruses

HepG2 and Vero cells were maintained as previously described [11-13] Dengue serotypes 1 (strain 16007), 2

(strain 16681), 3 (strain 16562) and 4 (strain 1036) were propagated in Vero cells and purified as described previously [11,12].

Cytotoxicity assessment by Annexin V staining

Confluent HepG2 cells were pretreated at 37°C with either 20 μM cytochalasin D or 30 μg/ml nystatin for 2 hr, or with 15 μg/ml chlorpromazine or 3 mM amiloride or 50 μM LY294002 or 0.2 μM wortmannin for 1.5 hr with 80% DMSO for 20 hours as a positive control. Cells were then trysinized and subsequently washed twice with cold-PBS. Cells were then washed with binding buffer (BD Biosciences Pharmingen, San Diego, CA) and resuspended in binding buffer. Annexin V-FITC (BD Biosciences Pharmingen, San Diego, CA) was added to the cell suspensions and samples were incubated in the dark for 15 min before analysis by flow cytometry (BD FACSCalibur # E6361).

Biochemical inhibition of dengue entry

Confluent HepG2 cells were pretreated at 37°C with chlorpromazine, amiloride, wortmannin or LY294002 for 30 min or with cytochalasin D or nystatin for 1 hr. The cells were infected with each dengue serotype in either in the presence or absence of the appropriate inhibitor at an MOI of 1, for 1 hr at 37°C. The extracellular viruses were then inactivated by acid glycine (pH3) treatment [14]. The infected cells were further grown for one propagation cycle minus two hours with the exact time dependent upon the dengue serotype as determined previously [12], and the number of infected cells determined by our adaptation of the standard plaque assay [15]. Experiments were undertaken independently in triplicate with duplicate plaque assay of samples.

Eps15 transfection, infection and indirect immunofluorescence microscopy

Plasmid constructs of dominant negative (DIII and EH29) and control (D3Δ2) Eps15 were kindly provided by A. Benmerah (Department of Infectious Diseases, Institut Cochin, Paris, France). Transfections of HepG2 cells were undertaken using lipofectamine2000 (Invitrogen, OR., USA). Briefly, 3 μg of the appropriate plasmid DNA was complexed with 4 μl of lipofectamine2000 for 30 min at room temperature and then added to HepG2 cells pregrown to 70–80% confluency on glass coverslips. The cell/complex mix was incubated at 37°C, 10% CO_2 for 2 days. Transfection efficiencies routinely exceeded 70% efficiency as determined by counting of multiple fields. Transfected cells were subsequently infected with dengue virus serotype 1, 2, 3 or 4 at an MOI of 20 for 1.5 hr followed by acid glycine (pH3) treatment to inactivate uninternalized viruses [14] and incubated for 15 hr at 37°C, 10% CO_2. A further set of cells were serum starved for 30 min and incubated with 5 μg transferrin conjugated with Alexa 594 (Molecular Probes, OR) at 37°C for 30 min follow by acid glycine treatment.

Both dengue infected and transferrin treated transfected cells were fixed with 4% paraformaldehyde for 30 min at room temperature. Transferrin control cells were directly mounted with Vectashield (Vector Laboratories, Inc., CA) while dengue virus infected cells were further permeabilized with 0.3% TritonX-100 and methanol. Nonspecific binding was blocked by incubation with 5% BSA for 1 hr at room temperature. Cells were incubated with an anti-dengue E protein monoclonal antibody, HB-114 [16] at 4°C overnight. After six washes with 0.03% TritonX-100 in PBS cells were incubated with a chicken anti-mouse IgG conjugated with Alexa 594 (Molecular Probes, OR) for 1 hr at room temperature and subsequently washed with six washes of 0.03% TritonX-100 in PBS before mounting with Vectashield (Vector Laboratories, Inc., CA).

siRNA design and generation

Target sites on clathrin heavy chain (GenBank accession number NM_004859) and the green fluorescent protein (GFP; GenBank accession number U50974) were determined using the on-line tool from Ambion, Austin, TX http://www.ambion.com/techlib/misc/siRNA_finder.html and the selected sequences were subjected to siRNA template design to generate DNA oligonucleotide sequences for use with the Silencer™ siRNA Construction kit (Ambion). Six templates for siRNA generation were selected:

siCHC1: 298-AACCCAGCAACATTGGCTTC-318

siCHC2: 411-AAGTAATCCAATTCGAAGACC-431

siCHC3: 484-AAAGCTGGGAAAACTCTTCAG-504

siCHC4: 1951-AATAATCGCCCATCTGAAGGT-1971

siCHC5:3544-AATGAACCTGCGGTCTGGAGT-3564

siGFP: 295-AAAGATGACGGGAACTACAAG-315

Numbering indicates the corresponding position of the selected 21 nucleotide sequence in the open reading frame of NM_004859 (siCHC1 to siCHC5) or U50974 (siGFP). All sequences were searched against the NCBI's database to confirm specificity. Sense and antisense DNA templates were chemically synthesized (BioBasic, Canada) and following the kit instructions based on *in-vitro* transcription, the siRNAs were produced and quantified by spectrophotometry.

siRNA transfection

HepG2 cells were maintained in Dulbecco's modified Eagle's medium (DMEM) supplemented with 10% heat-inactivated fetal bovine serum without antibiotics. Reverse transfections according to the manufacturers protocols were performed with Lipofectamine™RNAiMAX (Invitrogen, Carlsbad, CA) by mixing the respective siRNA and 1.2 μl of Lipofectamine™RNAiMAX and adding to a single well of a 24 well plate. After 20 minutes of incubation at room temperature, a suspension of 5×10^4 HepG2 cells was added and cell: complex mixtures incubated under standard conditions. Mock transfections (lipofectamine only) were performed in parallel. All transfections were undertaken in a final volume of 600 μl with siRNA at a final concentration at 50 nM. Transfections were harvested at 1 to 4 days post-transfection.

RNA extraction and RT-PCR analysis

Transfected cells from a single well of a 24-well plate were homogenized in 0.5 ml Trizol reagent (Molecular Research Center, Cincinnati, OH) and RNA purified as recommended by the manufacturer. For the RT-PCR analysis, an oligo$(dT)_{17}$ primer was used to synthesize first strand cDNA using ImpromII™ reverse transcriptase (Promega, Madison, WI). The cDNA was then amplified in a multiplex reaction with 2 specific primer pairs for CHC (CHCf: 5'-AAGCTCATCTTTGGGCAGAA-3'; CHCr: 5-GAGACAGCACCATCAGCAAA-3') and GAPDH (GAPDHf: TTGGTATCGTGGAAGGACTCA-3'; GAPDHr: 5'-ACCACCTGGTGCTCAGTGTAG-3') as an internal control. Expected products were 343 bp (GAPDH) and 222 bp (CHC) Cycle conditions were 94°C for 3 minutes followed by 20 cycles of 94°C for 30 seconds, 58°C for 45 seconds and 72°C for 45 seconds followed by a final extension of 72°C for 7 minutes. PCR products were analyzed on 1.8% agarose gels containing ethidium bromide.

Infection of siRNA silenced HepG2 cells

HepG2 cells (5×10^4) were grown on coverslips in single wells of a 24 well plate and transfected as above with either siRNAs as stated or mock transfected. At day 3 post transfection cells were infected with dengue virus serotype 2 MOI 20 for 2 hours followed by an acid glycine wash and subsequently incubated for 15 hours under standard conditions. Dengue virus E protein was detected as described above except that cells were also stained with DAPI. Parallel non-infected samples were incubated with transferrin as described above and were additionally stained with DAPI. Where biochemical inhibition was used in conjunction with siRNA silencing, samples were treated with 0.2 μM wortmannin for 30 minutes immediately preceding dengue virus infection.

Results

Effect of endocytosis inhibitors on dengue virus entry

To investigate the mechanism of dengue virus internalization into HepG2 cells, cells were pre-treated with cytochalasin D, amiloride, LY294002 or wortmannin to inhibit macropinocytosis, nystatin to inhibit caveolae mediated entry or chlorpromazine to inhibit clathrin-coated pit mediated. Prior to the infection experiment cells were incubated with a range of concentrations of the inhibitors to assess cytotoxicity. Cytotoxicity was initially assessed by cellular morphological changes under light microscopy (data not shown). Working concentrations (the highest concentration without apparent cytotoxicity) were established as: cytochalasin D at 20 μM, amiloride at 3 mM, LY294002 at 50 μM, wortmannin at 0.2 μM, nystatin 20 μM at 30 μM and chlorpromazine at 15 μM (HepG2). The lack of cytotoxicity at these concentrations was confirmed by Annexin V staining and flow cytometry (Figure 1).

To determine the effects of the various inhibitors on dengue virus entry, cells were pre-incubated for 1 hr with cytochalasin D or nystatin and for 30 min with chlorpromazine, amiloride, wortmannin or LY294002 at the concentrations determined above, following which the cells were incubated separately with all four dengue virus serotypes individually at an MOI of 1 for 1 hr following which the virus: cell mixtures were treated with acid glycine pH3 to inactivate any uninternalized viruses [14]. Cells were incubated under optimal growth conditions for a time equivalent to one virus replication cycle minus 2 hr based on our previous data for each serotype in HepG2 cells [12] following which the cells were briefly trypsinized, serially diluted and plated onto pre-grown cell monolayers and overlaid with agarose/nutrient medium as previously described for this adaptation of the standard plaque assay [15]. All experiments were undertaken independently in triplicate with duplicate assay of infected cell number.

Results (Figure 2) show that inhibition of caveolae mediated endocytosis with nystatin results in a relatively uniform increase in the number of dengue virus infected cells for all serotypes, while inhibition of clathrin coated pit mediated endocytosis with chlorpromazine results in a significant reduction in the number of dengue infected cells for all four serotypes although the magnitude of the effect is variable. Inhibition of macropinocytosis with cytochalasin D, amiloride, LY294002 or wortmannin showed a broad range of effects depending upon the specific inhibitor used, as well as to some extent the serotype of the dengue virus (Figure 2).

Given that this study as well as our previous studies investigating dengue virus entry into HepG2 cells [11-13,15,17-20] have routinely employed acid glycine

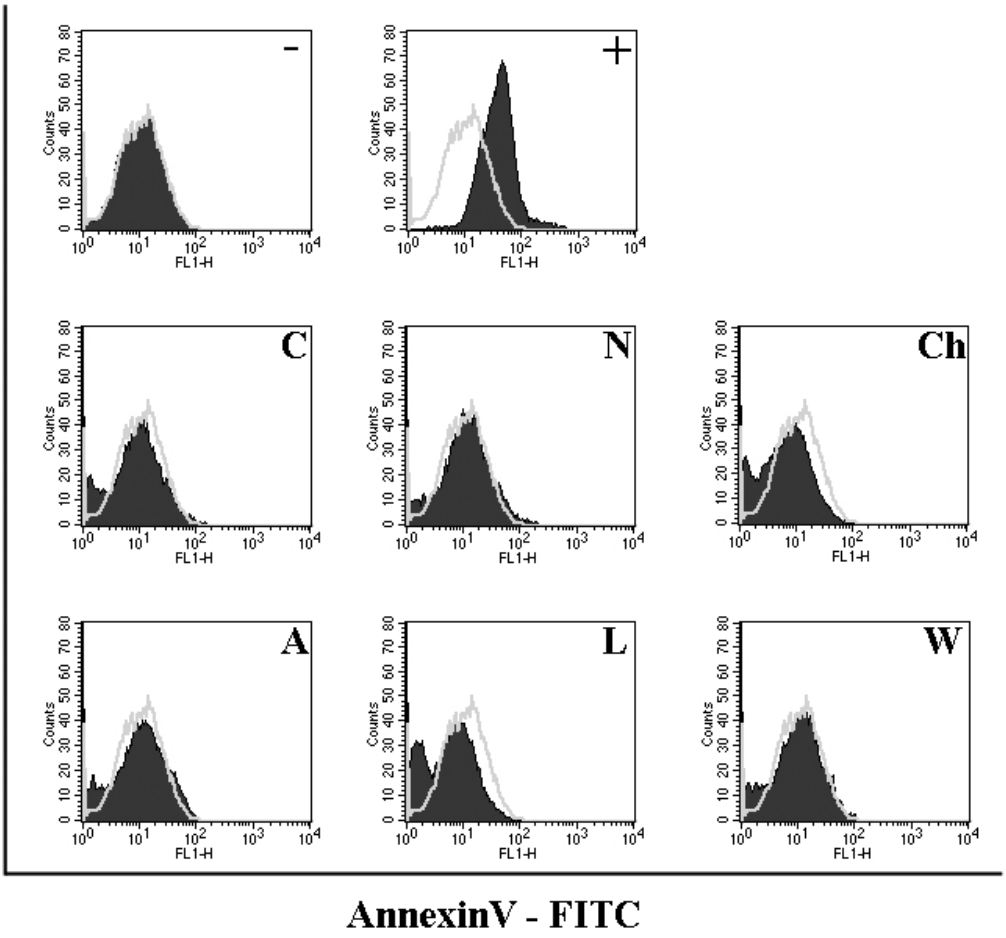

Figure 1
Cytotoxicity assessement of biochemical inhibitors. Flow cytometry histograms of HepG2 cells treated with working concentrations of cytochalasin D (C); amiloride (A); nystatin (N); chlorpromazine (Ch) LY294002 (L); wortmannin (W) or treated with 80% DMSO (+) or untreated (-).

washes [14] to inactivate uninternalized viruses, we sought to determine whether this would materially affect the inhibition studies. The effect of acid glycine treatment was assessed by pre-incubating HepG2 cells with one the inhibitors (15 μM chlorpromazine) or with medium alone as a control. Cells were then infected with dengue virus serotype 2 at MOI of 1 in presence or absence of the inhibitor following which cells were either treated with acid glycine (pH3) or subjected to three washes with PBS. Numbers of infected cells were determined by our adaptation of standard plaque assay [15]. Results showed that washes with acid glycine did not increase virus entry due to promoting viral fusion at the cell surface (Figure 3).

Dominant negative inhibition of clathrin coated pit endocytosis

Given that biochemical inhibitors can cause broad spectrum effects, we further sought to specifically knock out clathrin-dependent endocytosis using over-expressing dominant negative mutants of Eps-15 [21-23] which are able to effectively inhibit clathrin-mediated endoctyosis without affecting non-clathrin pathways [24]. HepG2 cells were transfected with either control (D3Δ2) or dominant negative mutants (DIII and EH29) of the Eps15 protein fused to GFP as well as the vector containing GFP only. Transfection with Lipofectamine2000 routinely resulted in transfection efficiencies of greater than 70% (data not shown). Transfected cultures were either infected with each of the four dengue virus serotype indi-

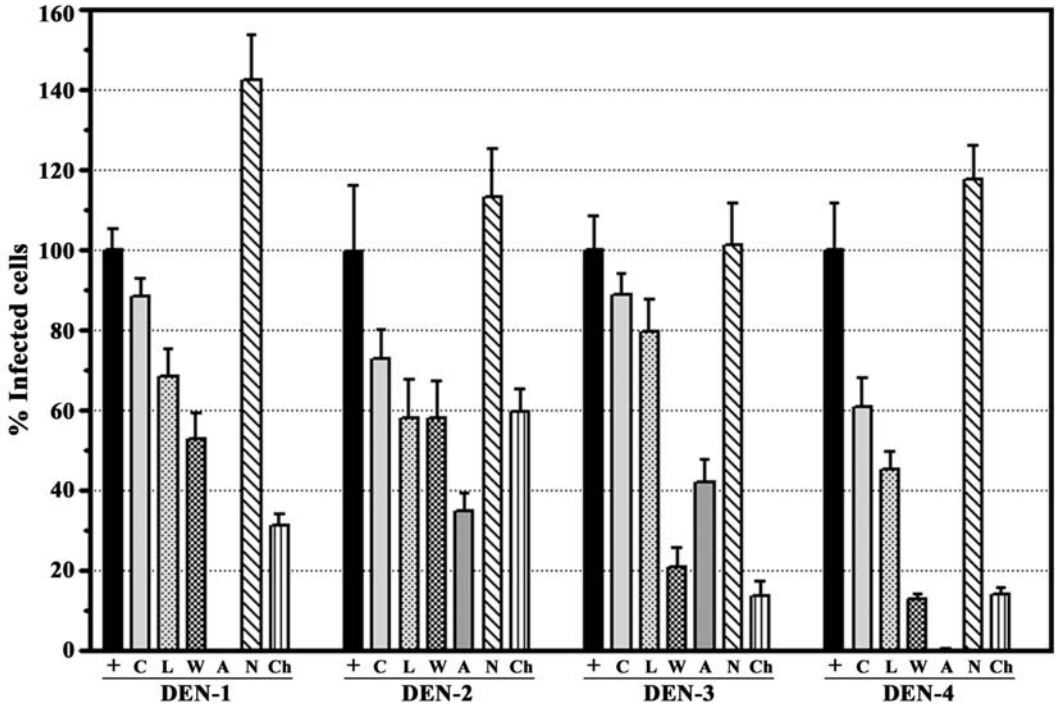

Figure 2
Effects of biochemical inhibitors of endocytosis on dengue virus entry. HepG2 cells were pre-incubated with cytochalasin D (C); amiloride (A); nystatin (N); chlorpromazine (Ch) LY294002 (L); wortmannin (W) or not pre-incubated (+) and subsequently infected with each serotype of the dengue viruses in the presence or absence of the respective treatment. Results are shown as a percentage of infected cells compared to control (100%). Error bar represent SEM of three independent experiments assayed in duplicate.

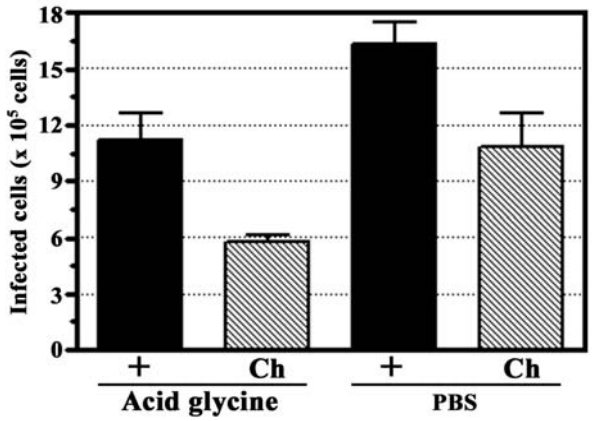

Figure 3
Effect of acid glycine wash. HepG2 cells were infected in the presence or absence of chlorpromazine (Ch) with our without an acid glycine wash. Results are shown as number of infected cells. Error bars represent SEM of three independent experiments assayed in duplicate.

vidually at MOI of 20, or incubated with Alexa 594 conjugated-transferrin before incubation and fixation. Visualization of signal was undertaken by incubating dengue infected samples with a primary monoclonal antibody directed against dengue E protein followed by incubation with a chicken anti-mouse IgG conjugated with Alexa 594.

Results show that both dominant negative Eps15 mutants (DIII and EH29) significantly excluded the entry of transferrin (Figure 4). However, while the two mutants predominantly excluded entry of all four dengue serotypes (Figure 4), numerous examples of dengue virus entry in the presence of expression of the dominant negative mutants were observed (Figure 5). Quantitation by counting multiple fields (n > 30) suggested that 15- to 20% of cells expressing either of the mutants were positive for dengue virus entry for each serotype. In contrast, only scattered cells were seen to be potentially positive for transferrin entry in the presence of the mutants, and these were possibly due to cells overlaying each other.

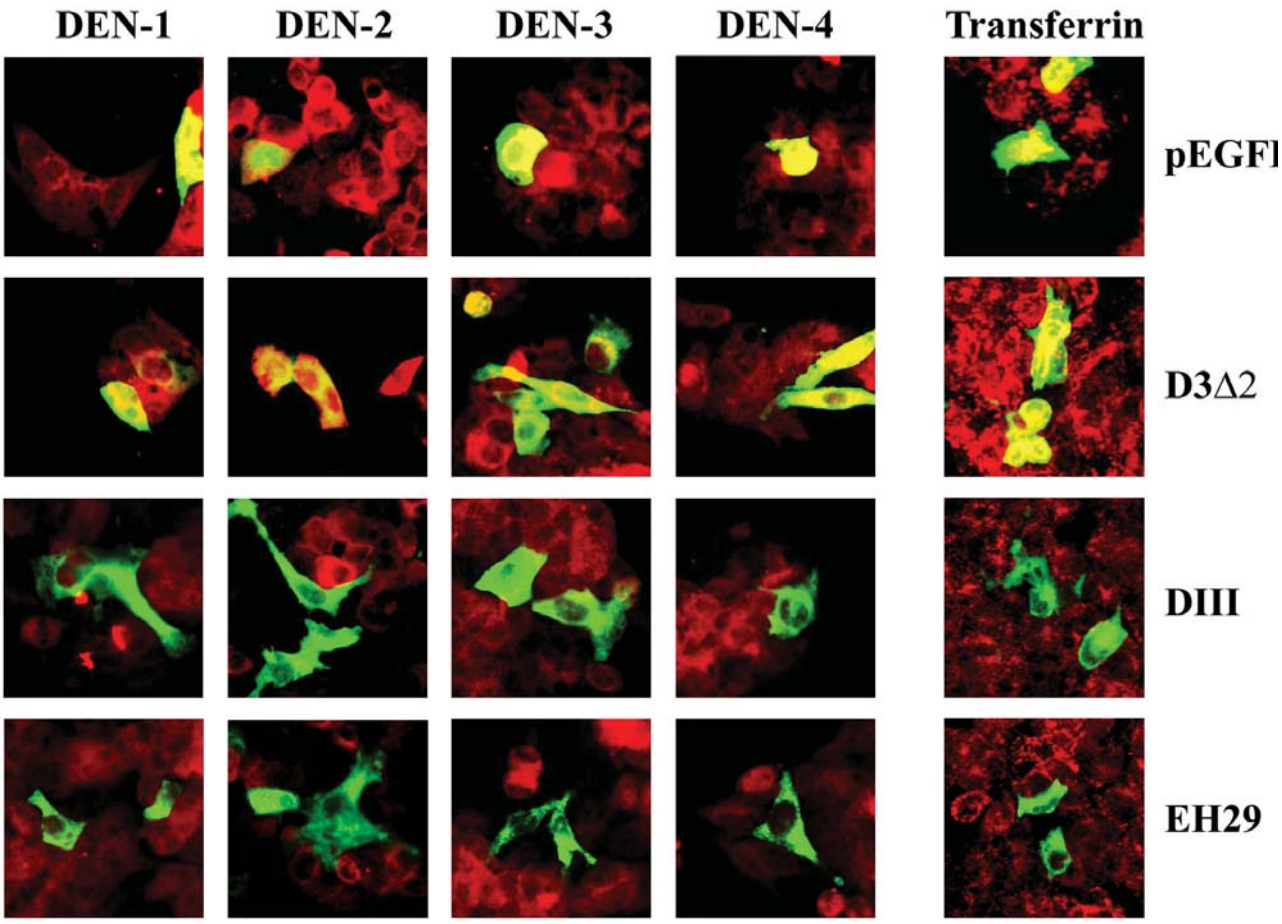

Figure 4
Immunofluorescence of dengue infection and dominant negative mutant of Eps15. HepG2 cell were transfected with either of two dominant negative Eps15 mutants (DIII or EH29) or a wild type Eps15 clone (D3Δ2) all fused to GFP or pEGFP as control, followed by infection with each dengue virus serotype individually or Alexa 594 conjugated-transferrin. Dengue infected samples were subsequently incubated with a mouse monoclonal antibody directed against dengue E protein and an Alexa 594 conjugated chicken anti-mouse IgG antibody. Signal from Alexa 594 (red) and GFP (green) were observed under a fluorescent microscope. Merged images are shown.

siRNA mediated inhibition of clathrin heavy chain expression

Given the significant entry of the dengue virus in the presence of over-expressing dominant negative mutants of Eps15, it is possible that either entry was occurring via multiple pathways, or the Eps15 mutants were not completely inhibiting clathrin mediated entry. To further explore this, RNA interference was used to down regulate the expression of clathrin heavy chain, an integral part of the clathrin vesicle [25]. Five different siRNAs (siCHCs) against human clathrin heavy chain (GenBank accession number NM_004859) were generated using in vitro transcription together with 1 siRNA targeted to the green fluorescent protein (GFP; GenBank accession number U50974) for use as a control. To confirm all siRNAs were double-stranded, an aliquot of each siRNA was treated with RNaseIII which digests double-stranded RNA or RNaseA which digests single-stranded RNA. All siRNA constructs were confirmed to be off the appropriate size and to consist of dsRNA (data not shown).

To optimize the silencing of the expression of the clathrin heavy chain, the 5 different siCHCs were transfected into HepG2 cells in parallel with transfections of siGFP and lipofectamine alone (mock). On days 1 to 4 days post-transfection, cells were harvested and RNA extracted. Multiplex RT-PCR was undertaken to detect messages from GAPDH and clathrin heavy chain (CHC) simultaneously

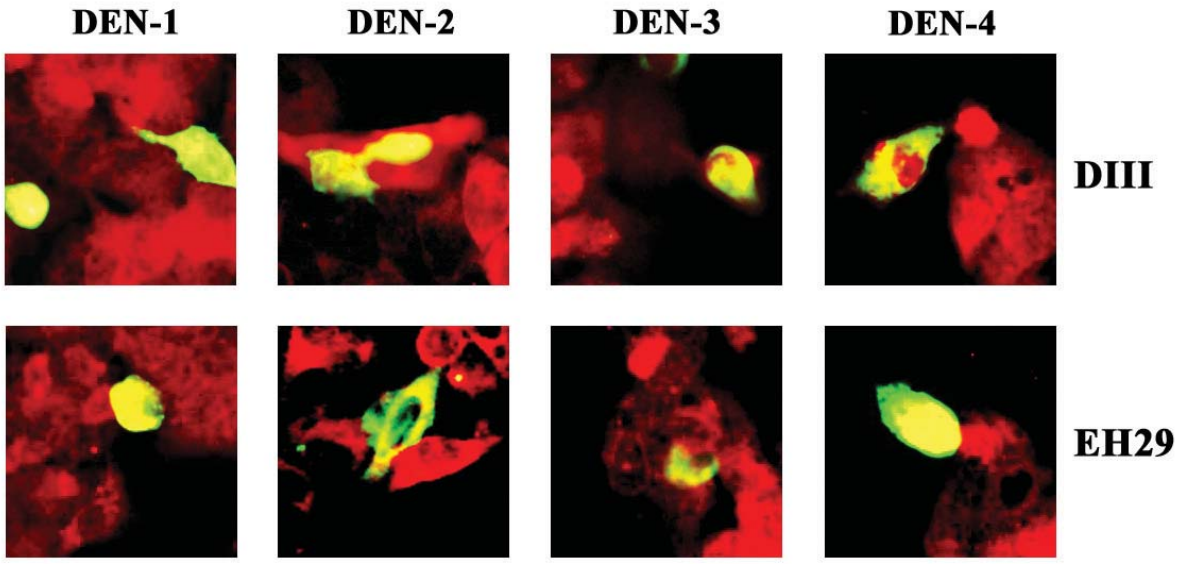

Figure 5
Entry of the dengue virus in the presence of dominant negative mutants of Eps15. Examples of cells positive for both dominant negative mutants of Eps15 (DIII or EH29)-GFP (green) and dengue virus infection (red). Merged images are shown.

and results analyzed by agarose gel electrophoresis. Experiments were undertaken independently in triplicate.

Results showed a constant signal for GAPDH and the clathrin heavy chain (CHC) for mock and siGFP transfection (Figure 6). Message for clathrin heavy chain was seen to be significantly reduced for all transfections, with the greatest signal reduction being seen on day 3 post infection and for siCHC3 and siCHC5 (Figure 6).

Dengue virus serotype 2 infection of clathrin heavy chain silenced HepG2 cells

Optimal silencing of clathrin heavy chain expression was noted at day 3 post transfection with siRNA constructs siCHC3 and siCHC5. These two siRNAs were again transfected into HepG2 cells as above in parallel with transfections of siGFP and mock (transfection agent only) and on day 3 post transfection cells were infected with dengue virus serotype 2 and an MOI of 20 and cells allowed to grow for 15 hours (the time for one replication cycle of dengue serotype 2 minus two hours) under optimal conditions. At 15 hours cells were either analyzed by microscopy or by our adaptation of the standard plaque assay [15] to determine the number of infected cells. Both microscopy and determination of infected cell number were undertaken independently in triplicate.

Consistent with our results with transfections of dominant negative constructs of Eps15, a significant reduction of transferrin entry was seen with siCHC transfections, but not with mock or siGFP (Figure 7). Dengue virus serotype 2 entry was observed for mock and siGFP transfections (Figure 7). While transfections of siCHC constructs again reduced dengue virus entry significantly, entry of the virus was still observed. Levels of entry of the dengue virus serotype 2 in siCHC transfected cells was again observed to be on the order of 15 to 20% of cells as determined by counting multiple microscope fields ($n > 30$).

Results of dengue virus entry as seen by our adaptation of the standard plaque assay [15] were consistent with the results observed by microscopy. We observed a slight reduction of dengue virus entry in siGFP transfected cells as compared to wild type (mock transfected) suggesting that transfection of even irrelevant siRNAs may marginally affect the viability of the HepG2 cells. A significant reduction in the number of dengue virus infected cells was observed with the siCHC transfections (Figure 8, Panel A), with the number of infected cells again being some 20% of wild type (mock transfected) cells.

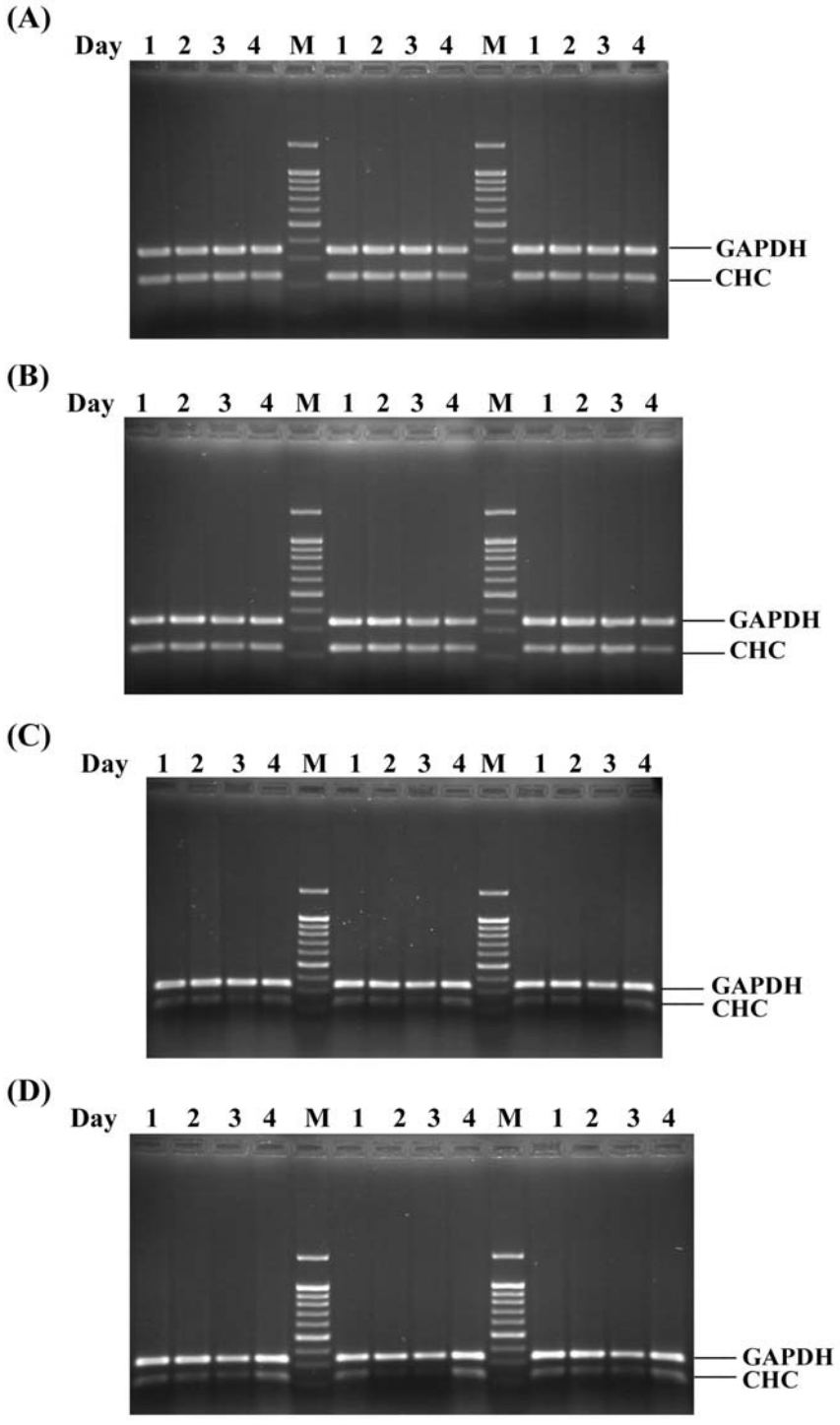

Figure 6
Silencing of Clathrin heavy chain in HepG2 cells. Multiplex RT-PCR products for GAPDH or clathrin heavy chain (CHC) of HepG2 cells either mock transfected (A); transfected with siGFP (B); transfected with siCHC3 (C) or transfected with siCHC5 (D). Samples represent day 1 to 4 post transfection and transfections were undertaken independently in triplicate.

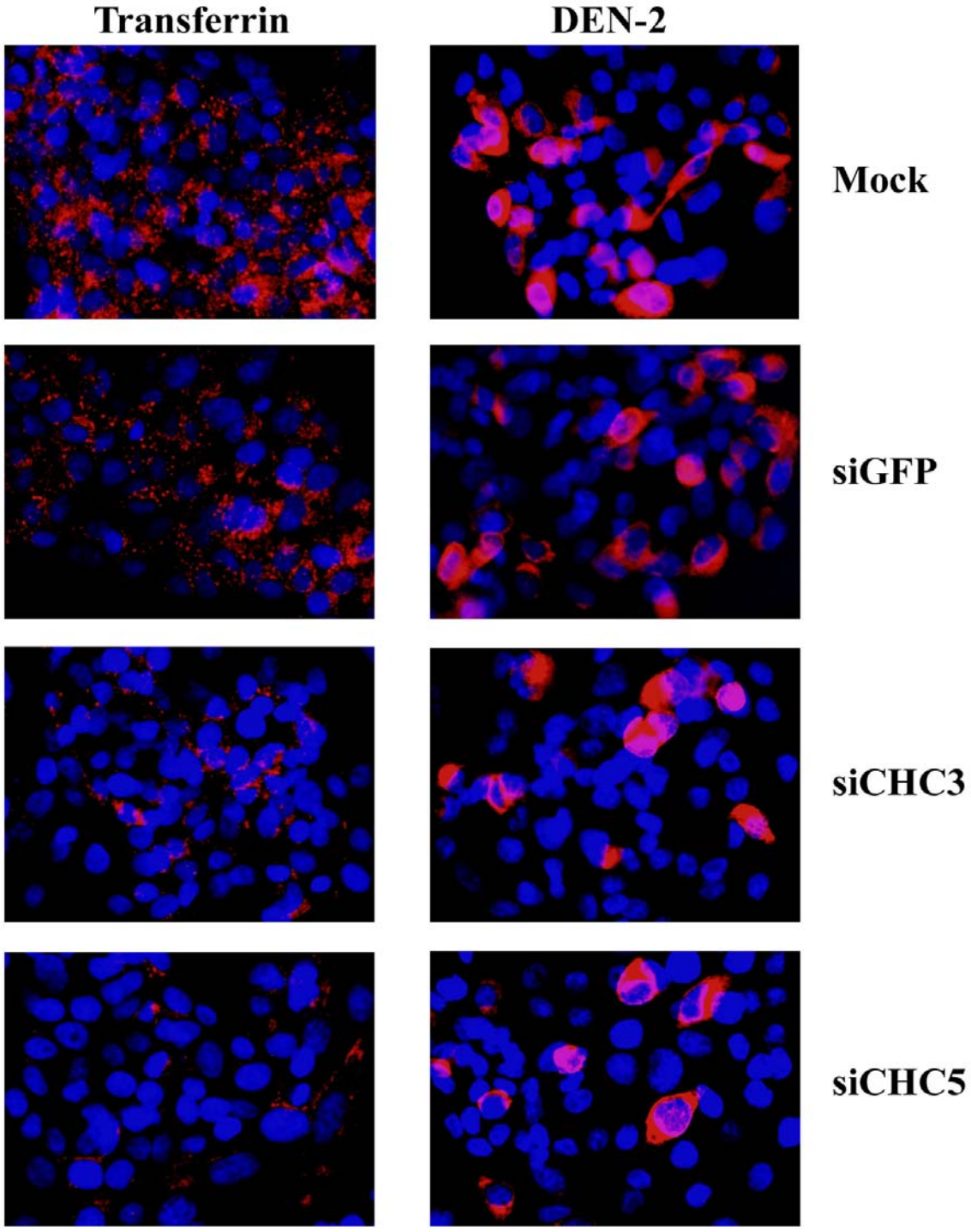

Figure 7
Dengue serotype 2 infection of siRNA silenced HepG2 cells. Indirect immunoflourescence of HepG2 cells either mock transfected or transfected with siGFP, siCHC3 or siCHC5 and subsequently either infected with the dengue virus (red) or incubated with transferrin (red). Cells were additionally stained with DAPI (blue) to show nuclei. Merged images are shown.

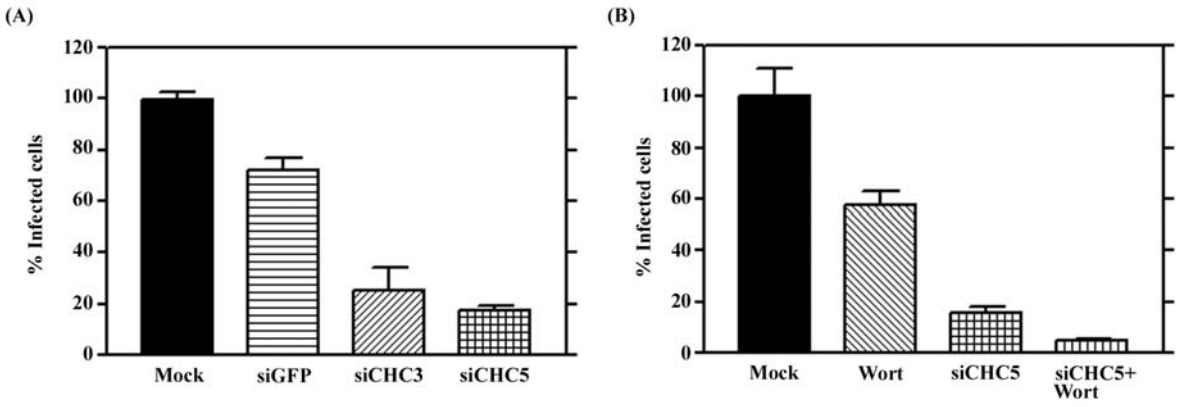

Figure 8
Infection of siRNA silenced HepG2 cells. A. HepG2 cells either mock transfected (mock) or transfected with siGFP, siCHC3 or siCHC5 were infected with dengue virus serotype 2 at MOI 20 and the number of infected cells determined by our adaptation of the standard plaque assay [15]. Results are expressed as a percentage of mock infection and error bars represent the SEM of three independent experiments assayed in duplicate. B. HepG2 cells were either mock transfected or transfected with siCHC5 and either treated or not treated with wortmannin prior to infection with the dengue virus serotype 2 at MOI 20. Results are expressed as a percentage of mock infection and error bars represent the SEM of three independent experiments assayed in duplicate.

dependent endocytosis

To determine whether the approximately 20% virus entry seen in cells in which clathrin mediated endocytosis has been inhibited is a result of background, or the result of dengue virus entry by macropinocytosis, we sought to simultaneously inhibit both pathways, clathrin mediated endocytosis through siRNA mediated RNA inhibition and macropinocytosis through biochemical inhibition using wortmannin.

Cells were therefore transfected with siCHC5 to silence clathrin heavy chain or mock transfected and on day 3 post-transfection were either treated or not treated with wortmannin for 1 hour before being either incubated with transferrin or infected with dengue serotype 2 at an MOI of 20. Following acid glycine treatment of dengue infected cells, cells were incubated for 15 hours before being either examined by microscopy or the number of infected cells determined by our adaptation of the standard plaque assay [15]. Experiments were all undertaken independently in triplicate.

Results (Figure 9) show that transfection with siCHC5, but not treatment with wortmannin significantly excluded transferrin and a similar level of transferrin exclusion was seen between cells treated with siCHC5 alone and cells treated with siCHC5 and wortmannin in combination. HepG2 cells treated with either siCHC5 or wortmannin both showed a reduction in levels of dengue infected cells as compared to control, but a significant number of dengue infected cells was observed in each case. The combination of siCHC5 and wortmannin treatment resulted in the infection of rare, single scattered cells (Figure 8, Panel B).

Results from our adaptation of the plaque assay (Figure 7, Panel B) provided consistent data, with a significant reduction in the number of dengue serotype infected cells seen in the cells treated with a combination of siCHC5 transfection and wortmannin as compared to the siCHC5 transfected cells alone.

Discussion

Despite flaviviral infections representing a significant world wide public health threat, little advance has been made in dissecting out the mechanism by which flaviviruses enter into either mammalian or insect cells. Studies on Japanese encephalitis virus and West Nile virus with either Vero (African Green monkey cells) or C6/36 cells have suggested that these two viruses enter by clathrin coated pit mediated endocytosis [8-10]. With the dengue virus however, data to date, which has been predominantly generated through electron microscopy studies [4-6], has suggested that direct fusion with the plasma membrane is the standard mode of entry of the dengue viruses.

Recently Chu et al., [9] provided evidence that West Nile virus enters into Vero cells via clathrin mediated endocy-

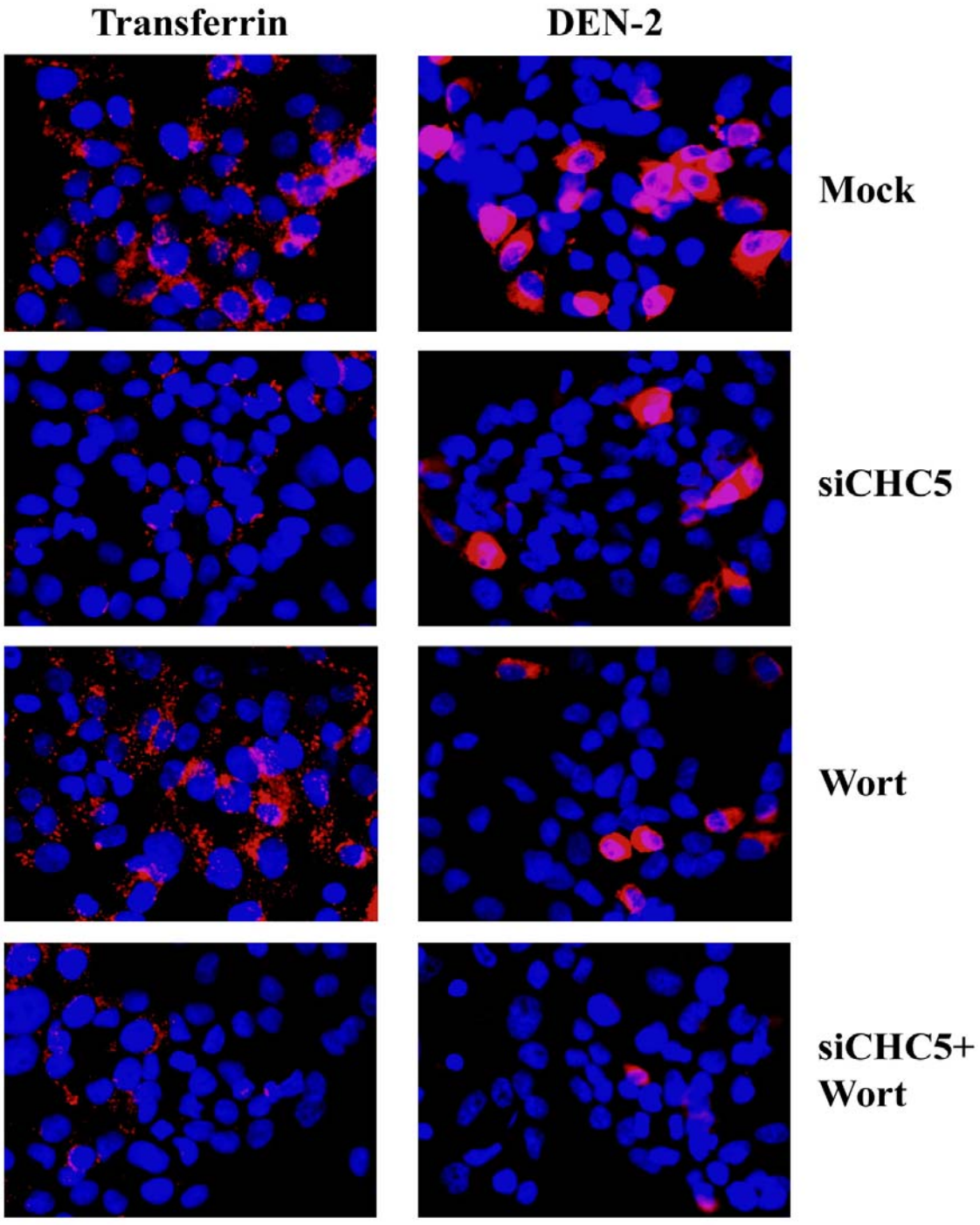

Figure 9
Simultaneous inhibition of macropinocytosis and clathrin mediated endocytosis in HepG2 cells and infection with dengue virus serotype 2. Indirect immunoflourescence of HepG2 cells either mock transfected or transfected with siCHC5 and subsequently either treated or not treated with wortmannin prior to infection with the dengue virus (red) at MOI 20 or incubated with transferrin (red). Cells were additionally stained with DAPI (blue) to show nuclei. Merged images are shown.

tosis [9]. The authors however noted that pre-treatment of Vero cells with cytochalasin D (an inhibitor of macropinocytosis) resulted in an inhibition of infection and the authors proposed that this was possibly due to an effect upon virus trafficking due to cytochalasin D mediated depolymerization of actin filaments [9]. In light of the results seen here it is possible that West Nile virus also enters via multiple pathways and the reduction seen in West Nile virus entry in the presence of cytochalasin D is a consequence of ablation of the macropinocytosis pathway rather than a consequence of altering virus trafficking. Further support for this is seen that reduction of West Nile virus entry in the presence of an Eps15 dominant negative mutant is some 80%, giving some 20% virus entry in the presence of the dominant negative mutant [9] – a figure comparable with the data presented here for the dengue virus.

Interestingly Chu and colleagues also investigated the entry of West Nile Virus into the aedes albopictus cell line C6/36 using the same dominant negative mutant of Eps15 [8] and similarly saw 15 to 20% entry of the virus in the presence of the mutant suggesting that West Nile virus may similarly enter into cells of both an insect and a mammalian origin by multiple pathways.

More recently Krishnan and colleagues have investigated the entry of the dengue virus into HeLa cells [7]. This study also used dominant negative mutants of Eps15 to ablate clathrin mediated endocytosis, and similarly concluded that the dengue virus entered by clathrin coated pit mediated endocytosis. Similar to Chu and Ng [9] however, some 20% virus entry as compared to wild type levels was observed, again giving the possibility that alternate pathways are responsible for the entry of some dengue virus into cells, and indeed, all four studies, this study and those of Chu and Ng [9], Chu and colleagues [8] and Krishnan and colleagues [7] suggest that ablation of clathrin coated pit mediated endocytosis only reduces virus entry by 80%.

Our data suggests that the remaining 20% virus entry observed is not the results of incomplete ablation of clathrin mediated endocytosis but represents virus entry by a viable, independent pathway, macropinocytosis. Entry of the dengue viruses (and more possibly flaviviruses in general) by multiple pathways as shown here raises some interesting questions, particularly with respect to the initial flavivirus: host cell interaction and may require a significant re-evaluation of our understanding of flavivirus entry into host cells.

Conclusion

Consistently, inhibition of clathrin mediated endocytosis using dominant negative mutants of Eps 15 results in a reduction of dengue virus entry of approximately 80% as shown by this study and others [7-9]. Our data shows that the incomplete ablation of virus entry is not a result of incomplete knock down of clathrin mediated endocytosis, but rather reflects entry via an alternate pathway.

Competing interests

The authors declare that they have no competing interests.

Authors' contributions

LS undertook the biochemical inhibition studies and Eps15 transfections and analyzed and interpreted the data. TS undertook the siRNA mediated silencing studies and analyzed and interpreted the data. DRS was responsible for design and implementation of the study as well as drafting the manuscript. All authors read and approved the final version.

Acknowledgements

This work was supported by the Thailand Research Fund Grant number 49800010 and Mahidol University. LS was the recipient of a Royal Golden Jubilee of Thailand Fund PhD scholarship and a Research Assistantship from the Faculty of Graduate Studies, Mahidol University. ST was supported by a Research Assistantship from the Faculty of Graduate Studies, Mahidol University. The authors would like to thank Mr. Umnaj Chanama for assistance with microscopy and Nitwara Wikan for flow cytometry experiments.

References

1. Pelkmans L, Helenius A: **Insider information: what viruses tell us about endocytosis.** *Curr Opin Cell Biol* 2003, **15:**414-422.
2. Halstead SB, Heinz FX, Barrett AD, Roehrig JT: **Dengue virus: molecular basis of cell entry and pathogenesis, 25–27 June 2003, Vienna, Austria.** *Vaccine* 2005, **23:**849-856.
3. Hase T, Summers PL, Cohen WH: **A comparative study of entry modes into C6/36 cells by Semliki Forest and Japanese encephalitis viruses.** *Arch Virol* 1989, **108:**101-114.
4. Hase T, Summers PL, Eckels KH: **Flavivirus entry into cultured mosquito cells and human peripheral blood monocytes.** *Arch Virol* 1989, **104:**129-143.
5. Lim HY, Ng ML: **A different mode of entry by dengue-2 neutralisation escape mutant virus.** *Arch Virol* 1999, **144:**989-995.
6. Se-Thoe SY, Ling AE, Ng MM: **Alteration of virus entry mode: a neutralisation mechanism for Dengue-2 virus.** *J Med Virol* 2000, **62:**364-376.
7. Krishnan MN, Sukumaran B, Pal U, Agaisse H, Murray JL, Hodge TW, Fikrig E: **Rab 5 is required for the cellular entry of dengue and West Nile viruses.** *J Virol* 2007, **81:**4881-4885.
8. Chu JJ, Leong PW, Ng ML: **Analysis of the endocytic pathway mediating the infectious entry of mosquito-borne flavivirus West Nile into Aedes albopictus mosquito (C6/36) cells.** *Virology* 2006, **349:**463-475.
9. Chu JJ, Ng ML: **Infectious entry of West Nile virus occurs through a clathrin-mediated endocytic pathway.** *J Virol* 2004, **78:**10543-10555.
10. Nawa M, Takasaki T, Yamada K, Kurane I, Akatsuka T: **Interference in Japanese encephalitis virus infection of Vero cells by a cationic amphiphilic drug, chlorpromazine.** *J Gen Virol* 2003, **84:**1737-1741.
11. Sithisarn P, Suksanpaisan L, Thepparit C, Smith DR: **Behavior of the dengue virus in solution.** *J Med Virol* 2003, **71:**532-539.
12. Thepparit C, Phoolcharoen W, Suksanpaisan L, Smith DR: **Internalization and propagation of the dengue virus in human hepatoma (HepG2) cells.** *Intervirology* 2004, **47:**78-86.
13. Thepparit C, Smith DR: **Serotype-specific entry of dengue virus into liver cells: identification of the 37-kilodalton/67-kilodalton high-affinity laminin receptor as a dengue virus serotype 1 receptor.** *J Virol* 2004, **78:**12647-12656.

14. Hung SL, Lee PL, Chen HW, Chen LK, Kao CL, King CC: **Analysis of the steps involved in Dengue virus entry into host cells.** *Virology* 1999, **257:**156-167.
15. Chingsuwanrote P, Suksanpaisan L, Smith DR: **Adaptation of the plaque assay methodology for dengue virus infected HepG2 cells.** *J Virol Methods* 2004, **116:**119-121.
16. Henchal EA, Gentry MK, McCown JM, Brandt WE: **Dengue virus-specific and flavivirus group determinants identified with monoclonal antibodies by indirect immunofluorescence.** *Am J Trop Med Hyg* 1982, **31:**830-836.
17. Cabrera-Hernandez A, Thepparit C, Suksanpaisan L, Smith DR: **Dengue virus entry into liver (HepG2) cells is independent of hsp90 and hsp70.** *J Med Virol* 2007, **79:**386-392.
18. Jindadamrongwech S, Thepparit C, Smith DR: **Identification of GRP 78 (BiP) as a liver cell expressed receptor element for dengue virus serotype 2.** *Arch Virol* 2004, **149:**915-927.
19. Phoolcharoen W, Smith DR: **Internalization of the dengue virus is cell cycle modulated in HepG2, but not Vero cells.** *J Med Virol* 2004, **74:**434-441.
20. Suksanpaisan L, Cabrera-Hernandez A, Smith DR: **Infection of human primary hepatocytes with dengue virus serotype 2.** *J Med Virol* 2007, **79:**300-307.
21. Benmerah A, Bayrou M, Cerf-Bensussan N, Dautry-Varsat A: **Inhibition of clathrin-coated pit assembly by an Eps15 mutant.** *J Cell Sci* 1999, **112(Pt 9):**1303-1311.
22. Benmerah A, Lamaze C, Begue B, Schmid SL, Dautry-Varsat A, Cerf-Bensussan N: **AP-2/Eps15 interaction is required for receptor-mediated endocytosis.** *J Cell Biol* 1998, **140:**1055-1062.
23. Carbone R, Fre S, Iannolo G, Belleudi F, Mancini P, Pelicci PG, Torrisi MR, Di Fiore PP: **eps15 and eps15R are essential components of the endocytic pathway.** *Cancer Res* 1997, **57:**5498-5504.
24. Nichols BJ, Lippincott-Schwartz J: **Endocytosis without clathrin coats.** *Trends Cell Biol* 2001, **11:**406-412.
25. Kirchhausen T: **Clathrin.** *Annu Rev Biochem* 2000, **69:**699-727.

VERSITA

CELLULAR & MOLECULAR BIOLOGY LETTERS
http://www.cmbl.org.pl

Received: 07 August 2007
Revised form accepted: 25 January 2008

DOI: 10.2478/s11658-008-0017-6

Research article

siRNA-MEDIATED SILENCING OF THE 37/67-kDa HIGH AFFINITY LAMININ RECEPTOR IN Hep3B CELLS INDUCES APOPTOSIS

THARINEE SUSANTAD and DUNCAN R. SMITH*
Molecular Pathology Laboratory, Institute of Molecular Biology and Genetics, Mahidol University, Salaya Campus, 25/25 Phuttamonthol Sai 4, Salaya, Nakorn Pathom, Thailand 73170

Abstract: The laminin-binding protein, variously called the 37/67-kDa high affinity laminin receptor or p40, mediates the attachment of normal cells to the laminin network, and also has a role as a ribosomal protein. Over-expression of this protein has been strongly correlated with the metastatic phenotype. However, few studies have investigated the cellular consequence of the ablation of this gene's expression. To address this issue, the expression of the 37/67-kDa high affinity laminin receptor was knocked out with several siRNA constructs via RNA interference in transformed liver (Hep3B) cells. In each case where the message was specifically ablated, apoptosis was induced, as determined by annexin V/propidium iodide staining, and by double staining with annexin V and an antibody directed against the 37/67-kDa high affinity laminin receptor. These results suggest that this protein plays a critical role in maintaining cell viability.

Key words: siRNA, RNA interference, Laminin receptor, p40, Ribosomal, Liver, Silencing, LAMR1

INTRODUCTION

The multifunctional protein which we here designate the 37LBP/67LR protein has been variously called the 37/67-kDa high affinity laminin receptor protein, the 37-kDa laminin-binding protein (37LBP), the laminin receptor precursor

* Author for correspondence; e-mail: duncan_r_smith@hotmail.com, tel.: (662) 800 3624-8, fax: (662) 441 9906

Abbreviations used: GAPDH – glyceraldehyde 3-phosphate dehydrogenase; LBP-p40 – laminin-binding protein precursor p40; LRP – laminin receptor precursor; PrP^c – cellular prion protein; siRNA – small interfering RNAs; 37LBP – 37-kDa laminin binding protein; 67LR – 67-kDa laminin receptor

(LRP), the 67-kDa laminin receptor (67LR), LAMR1, and the laminin-binding protein precursor p40 (LBP-p40). It was initially identified as a 67-kDa protein through its high affinity interaction with laminin [1-3], a predominant glycoprotein component of the extracellular matrix that mediates cell attachment, movement, growth and differentiation. The screening of human cDNA libraries using antibodies directed against the purified protein enabled the isolation of a full-length cDNA encoding a protein with a calculated molecular mass of 32 kDa and an apparent molecular weight of 37 kDa, after *in vitro* translation of hybrid-selected mRNA and SDS-PAGE analysis [4]. Highly homologous cDNAs were subsequently isolated from human colon cancer cell lines [5] and obtained in a study on the structure and sequence determination of the rat 40S ribosomal subunit [6]. LPB-p40 was localized on 40S ribosomes [7] and in the nucleus [8], while 67LR was located on the cell surface, where, in addition to its role as a high affinity laminin receptor, it was shown to function as the receptor for elastin [9] and as a positional marker for the differentiation of the fetal eye organ [10]. 37-kDa LRP was identified as a PrP^c accomplice [11], and 37LBP/67LR acts as a receptor for PrP^c [12] and infectious prions [13], as extensively reviewed elsewhere [14-16]. Additionally, 37LBP/67LR acts as a receptor for a number of viruses, including sindbis [17], dengue [18], and the adeno-associated virus serotypes 8, 2, 3, and 9 [19]. Although expression of the mature 67-kDa form of the protein was detected on many normal cells, the immature, 37-kDa form was identified as an oncofetal antigen [20, 21], and its over-expression directly correlated with the increased invasiveness and metastatic potential of a number of different tumours (reviewed in [22]). Although a clear precursor-product relationship between the 37-kDa (or 40-kDa) and 67-kDa forms was established [23], the exact mechanism by which the 37-kDa form gives rise to the 67-kDa form has yet to be established, although post-translational modification involving acylation [23], specifically via palmitoylation [24], has been implicated. Inhibiting 37LBP/67LR with a specific immunoreactive polyclonal antibody inhibited the attachment of a human fibrosarcoma cell line in a dose-dependent manner, and inhibited the formation of pulmonary metastases in a mouse model system [25]. Down-regulation of 37LBP using antisense cDNA constructs was shown to induce apoptosis in HeLa cells [26]. Down-regulation of 37LBP/67LR expression using an siRNA approach resulted in a reduction in PrP^{sc} propagation in Scrapie-infected neuronal cells [27]. More recently, 37LBP/67LR expression was knocked down in the mouse brain using an antisense-LRP RNA approach [28]. One anecdotal report suggested that inhibiting 37LBP/67LR using small interfering RNAs (siRNAs) may induce apoptosis in several cell types [29]. Given the multifunctional nature of this protein, we sought to formally verify whether siRNA-mediated knock-down of expression resulted in the induction of apoptosis in transformed liver cells.

MATERIALS AND METHODS

Cell culture

The human hepatoma cell line Hep3B [30] was cultivated at 37ºC under 5% CO_2 in Dulbecco's modified Eagle's medium (DMEM; HyClone, Logan, Utah) supplemented with 10% heat-inactivated fetal bovine serum (FBS; Gibco BRL, Gaitherburg, MD) and 100 U of penicillin-streptomycin (HyClone) per ml.

siRNA design and generation

The target sites on the human 37LBP/67LR (GenBank accession number NM_002295) and the green fluorescent protein (GFP; GenBank accession number U50974) were determined using the online tool from Ambion, Austin, TX (http://www.ambion.com/techlib/misc/siRNA_finder.html). The selected sequences were subjected to siRNA template design to generate DNA oligonucleotide sequences for use with the Silencer™ siRNA Construction kit (Ambion). Six templates for siRNA generation were selected:
siLRP1: 5'-AATTTCAGGGTGAATGGACTG-3' (nt 762-782);
siLRP2: 5'-AAATTTTCACAATGTCCGGAG-3' (nt 75-95);
siLRP3: 5'-AAATCTCAAGAGGACCTGGGA-3' (nt 232-252);
siLRP4: 5'-AACCTTCACTAACCAGATCCA-3' (nt 403-423);
siLRP5: 5'-AACAACAAGGGAGCTCACTCA-3' (nt 575-595);
siGFP: 5'-AAAGATGACGGGAACTACAAG-3' (nt 295-315).
The numbering indicates the corresponding position of the selected 21-nucleotide sequence in the open-reading frame of NM_002295 (siLRP1 to siLRP5) or U50974 (siGFP). All the sequences were searched against the NCBI database to confirm specificity to human 37LBP/67LR or GFP. Sense and antisense DNA templates were chemically synthesized (BioBasic, Canada), and following the kit instructions based on *in vitro* transcription, the siRNAs were produced and quantified by spectrophotometry. To confirm that the generated siRNAs were double-stranded, an aliquot of each siRNA was digested individually with RNaseIII or RNaseA. For RNaseIII treatment, 3 µg of siRNA, 1x $MnCl_2$, 1x ShortCut reaction buffer (50 mM Tris-HCl, 1mM DTT, pH 7.5) and 3 µl of ShortCut® RNaseIII (New England Biolabs, Inc. Ipswich, MA) were combined in a total volume of 20 µl, and incubated at 37ºC for 20 min. The reaction was stopped with the addition of EDTA. For the RNaseA treatment, 3 µg of siRNA, 1x RNaseA buffer (300 mM NaOAC, 10 mM Tris-HCl, pH 7.5 and 5 mM EDTA) and 0.01 µg/µl of RNaseA were mixed in a total volume of 20 µl, and the reaction mixture was incubated at 37ºC for 5 min before being terminated on ice. All the samples were analyzed by gel electrophoresis.

siRNA labeling

GAPDH-siRNA provided in the *Silencer*™ siRNA Labeling kit (Ambion) was end-labeled with the provided Cy3 by mixing the GAPDH-siRNA with the provided 10x labeling buffer and Cy3 labeling reagent. The reaction mixture was then incubated in the dark at 37ºC for 1 h, and excess label was removed via

ethanol precipitation by the addition of 0.1 volumes of 5 M NaCl and 2.5 volumes of 100% ethanol, with incubation at -20ºC for 1 h. The Cy3-labeled GAPDH-siRNA was pelleted by centrifugation at 10,000 g for 20 min, and the pellet was washed with 70% ethanol. Finally, the pellet was air-dried and dissolved in nuclease-free water. The concentration and base:dye ratio of the labeled siRNA was measured by spectrophotometry.

siRNA transfection

Hep3B cells were maintained in Dulbecco's modified Eagle's medium (DMEM) supplemented with 10% heat-inactivated fetal bovine serum without antibiotics. Reverse transfections were performed with Lipofectamine™RNAiMAX (Invitrogen, Carlsbad, CA) according to the manufacturer's protocols, by mixing the respective siRNA and 1.2 µl of Lipofectamine™RNAiMAX, and adding to a single well of a 24-well plate. After 20 min of incubation at room temperature, a suspension of $5x10^4$ Hep3B cells was added, and the cell:complex mixtures were incubated under standard conditions. Mock transfections (lipofectamine only) were performed in parallel. To assess transfection efficiency using Cy3-labeled GAPDH-siRNA, a glass cover slip was placed in the well prior to the transfection mix. All the transfections were undertaken in a final volume of 600 µl with siRNA at a final concentration of 50 nM. The cells transfected with Cy3-labeled GAPDH-siRNA were analyzed via fluorescent microscopy at 24 h post-transfection, while other transfections were harvested 1 to 4 days post-transfection. For the analysis of apoptosis, a total of $1x10^5$ Hep3B cells were reverse-transfected in a 6-well plate using the same final siRNA concentration and 2.4 µl of the transfection agent. All the transfections were undertaken independently in triplicate.

Fluorescent microscopy

After 24 h, the cells transfected with Cy3-labeled GAPDH-siRNA were fixed with 4% paraformaldehyde in PBS at room temperature for 30 min, and then permeabilized by incubation with 0.3% TritonX-100 in PBS for 5 min at room temperature. The coverslips were incubated with 1:500 DAPI in 0.3% TritonX-100/PBS for 10 min at room temperature, followed by two washes with PBS. They were then mounted on glass slides with Vectashield (Vector Laboratories, Inc.) mounting medium. The fluorescent signal was visualized under an Olympus BX61 fluorescent microscope.

RNA extraction and RT-PCR analysis

Transfected cells from a single well of a 24-well plate were homogenized in 0.5 ml Trizol reagent (Molecular Research Center, Cincinnati, OH) and allowed to stand at room temperature for 5 min. The cell lysate was vigorously shaken for 15 s in the presence of 0.1 ml chloroform, and allowed to stand at room temperature for 3 min, followed by centrifugation at 12,000 *g* and 4ºC for 15 min. The aqueous phase solution was transferred to a new tube and precipitated with 0.25 ml isopropanol at room temperature for 10 min, followed

by centrifugation at 12,000 *g* and 4ºC for 10 min. The RNA pellets were washed with 75% ethanol with subsequent centrifugation at 7,500 *g* and 4ºC for 5 min. They were air-dried. Finally, the RNA was dissolved in DEPC-treated water. For the RT-PCR analysis, an oligo$(dT)_{17}$ primer was used to synthesize the first strand cDNA using ImpromII™ reverse transcriptase (Promega, Madison, WI). The cDNA was then amplified in a multiplex reaction with 2 specific primer pairs for 37LBP/67LR (LRPf: 5'-TCACTCAGTGGGTTTGATGTG-3'; LRPr: 5'-TTCAGACCAGTCTGCAACCTC-3'), with GAPDH (GAPDHf: 5'-TTG GTATCGTGGAAGGACTCA-3'; GAPDHr: 5'-ACCACCTGGTGCTCAG TGTAG-3') as an internal control. The expected products were 343 bp (GAPDH) and 247 bp (37LBP/67LR). The cycle conditions were 94ºC for 3 min, followed by 20 cycles of 94ºC for 30 s, 58ºC for 45 s and 72ºC for 45 s, followed by a final extension of 72ºC for 7 min. The PCR products were analyzed on 1.8% agarose gels containing ethidium bromide.

Protein extraction and Western blot analysis

A total of $2.5x10^5$ Hep3B cells were reverse transfected in 6-well plates using a final siRNA concentration of 50 nM and 6 µl of transfection agent. On days 3 and 4 post-transfection, the transfected cells were harvested by scraping from the tissue culture plates, and transferred into 1.5-ml tubes followed by centrifugation at 1,500 rpm for 5 min to pellet the cells. The culture medium was then discarded, and the cell pellets were resuspended in ice-cold 1x PBS (137 mM NaCl, 2.7 mM KCl, 4.3 mM Na_2HPO_4 and 1.4 mM KH_2PO_4). After centrifugation at 1,500 rpm for 5 min, 1x PBS was removed, and the cells were lysed by vigorous vortexing in RIPA lysis buffer (1x PBS with 1% Nonidet P-40, 0.5% Sodium Deoxycholate and 0.1% SDS), followed by sonication for 15 min on ice. Finally, the supernatant was collected after centrifugation at 12,000 rpm for 15 min at 4ºC, and the protein concentration was determined using the Bradford assay (Bio-Rad). A total of 60 µg of total proteins was subjected to electrophoresis through 12% sodium dodecyl sulfate-polyacylamide gels in Tris-glycine buffer (25 mM Tris-HCl, pH 8.3, 192 mM glycine, 0.1% SDS) at a constant voltage of 100 volts at room temperature. The separated samples were then transferred to nitrocellulose membranes in a transfer buffer (15.6 mM Tris Base, 120 mM glycine) at a constant voltage of 30 volts at 4ºC for 16 h. The membrane containing the transferred proteins was blocked with 5% skimmed milk in TBS (20 mM Tris-HCl, pH 7.5, 140 mM NaCl) at room temperature for 1 h, and incubated with a mixture of a goat polyclonal antibody against the 37/67-kDa high-affinity laminin receptor (SC-21534, Santa Cruz Biotechnology, Inc., Santa Cruz CA) at a dilution of 1:500, and with a 1:500 dilution of goat polyclonal antibody against actin (SC-1616, Santa Cruz Biotechnology Inc.) in 5% skimmed milk in TBS at room temperature for 2 h. After three washes with TBS-T, the membrane was further incubated with a 1:3000 dilution of HRP-conjugated rabbit anti-goat IgG (31402, Pierce,

Rockford Il.) in 5% skimmed milk in TBS for 1 h at room temperature. The signal was developed using an ECL Plus™ Western blotting detection kit (Amersham Biosciences), followed by exposure to autoradiography film.

Flow cytometry analysis

Transfected cells in a single well of a 12-well plate were collected by treatment with trypsin (0.25% trypsin/1 mM EDTA in Hank's balance salt solutions) for 3 min at 37ºC, and transferred to a new tube. The collected cells were pelleted by centrifugation at 2,000 rpm for 3 min, and the supernatant was discarded. An ApoAlert® AnnexinV Apoptosis kit (Clontech, PaloAlto, CA) was used to assess the level of apoptosis in the LRP-silenced Hep3B cells. Following the manufacturer's protocols, the cell pellets were resuspended in 400 µl 1x Binding buffer and incubated for 15 min with 5 µl FITC-conjugated annexinV and 10 µl propidium iodide at room temperature in the dark. Finally, the cells were analyzed by flow cytometry using a FacsScan equipped with Cell Quest software (Becton-Dickinson). For double staining with an antibody against LRP and annexinV, the cell pellets were washed with 200 µl ice-cooled FACS buffer (1x PBS with 2% FBS, freshly prepared) followed by centrifugation at 2,000 rpm for 3 min. Then they were incubated with a 1:50 dilution of rabbit polyclonal antibody against the 37/67-kDa high-affinity laminin receptor (SC-20979, Santa Cruz Biotechnology Inc.) for 1 h on ice. The cells were then washed twice in FACS buffer and labeled with PE-conjugated donkey anti-rabbit secondary antibody (711-116-152; Jackson ImmunoResearch Laboratories, Inc. West Grove, PA) diluted 1:100 in FACS buffer for 45 min on ice in the dark. After two washes, the cells were resuspended in 400 µl FACS buffer, incubated with 5 µl FITC-conjugated annexinV for 15 min in the dark, and subjected to flow cytometry analysis.

RESULTS AND DISCUSSION

Small interfering RNAs (siRNAs) are double-stranded RNAs (dsRNAs) of approximately 19 to 21 bp in length that specifically induce the degradation of cellular mRNAs containing complementary nucleotide sequences [31] by activating the cellular RNA interference (RNAi) pathway [32]. As such, they can be used to specifically ablate the expression of single target genes. To down-regulate the expression of 37LBP/67LR, 5 different siRNAs against the human 37LBP/67LR gene (GenBank accession number NM_002295) were generated using *in vitro* transcription, together with 1 siRNA targeted to the green fluorescent protein gene (GFP; GenBank accession number U50974) for use as a control. To confirm that all the siRNAs were double-stranded, an aliquot of each siRNA was treated with RNaseIII, which digests double-stranded RNA, or RNaseA, which digests single-stranded RNA. All the siRNA constructs were confirmed to be of the appropriate size and to consist of dsRNA. Examples (siLRP2 and siLRP4) of the RNase treatment are shown in Fig. 1A. The optimal siRNA transfection conditions using lipofectamine were established using

commercially available siRNAs directed against GAPDH and subsequently labeled with Cy3. The optimal transfection conditions routinely resulted in transfection efficiencies of 80 to 90% (Fig. 1B).

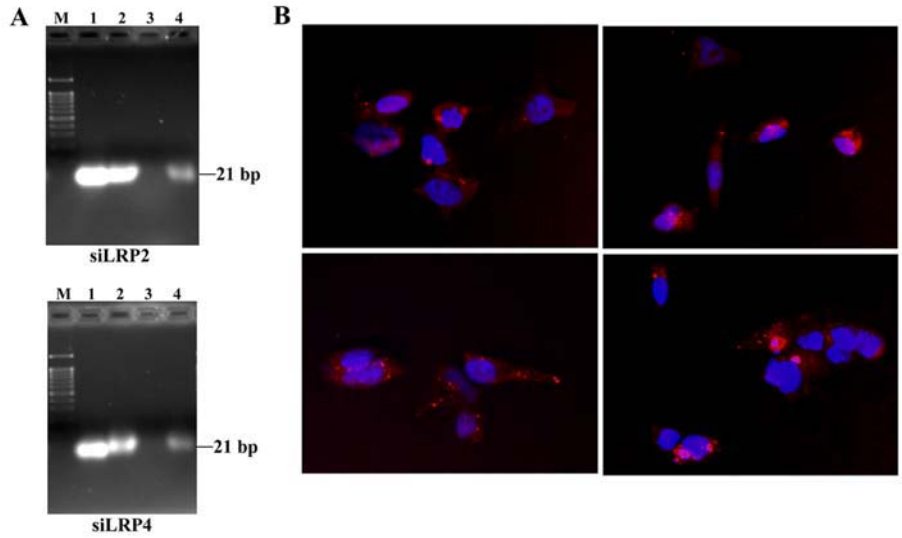

Fig. 1. siRNA analysis and transfection. A – Examples (siLRP2 and siLRP4) of RNAaseA- and RNaseIII-treated siRNAs. In both, lane M: 100-bp ladder, lane 1: dsDNA 21 bp, lane 2: siRNA, lane 3: RNaseIII-treated siRNA, lane 4: RNaseA-treated siRNA. B – Merged images of Hep3B cells transfected with Cy3-labeled siGAPDH (red signal). The nuclei are stained with DAPI (blue). Four representative individual fields are shown.

Silencing human 37LBP/67LR in cultured Hep3B cells

To silence the expression of 37LBP/67LR, 5 different siLRPs were transfected into Hep3B cells in parallel with transfections of siGFP and lipofectamine alone (mock control). On days 1 to 4 post-transfection, the cells were harvested and the RNA extracted. Multiplex RT-PCR was done to detect messages from GAPDH and 37LBP/67LR simultaneously, and the results were analyzed by agarose gel electrophoresis. The experiments were done independently in triplicate. The results (Fig. 2) showed a constant signal for GAPDH and 37LBP/67LR for the mock, siGFP and siLRP1 transfections. By contrast, a significant reduction in the level of expression for both genes was observed in the siLRP2 to siLRP5 transfections by day 3 to 4 post-transfection, with transfections for siLRP2 and siLRP4 showing a complete silencing of both genes, suggesting that cell death was occurring in response to the silencing of 37LBP/67LR.

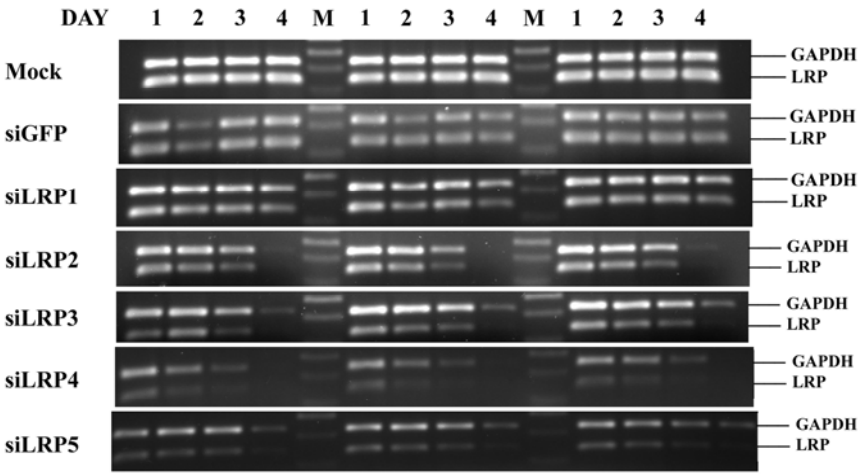

Fig. 2. siLRP-silencing profiles. Multiplex PCR products of GAPDH (upper band) and LRP (lower band), respectively (top to bottom) from mock, siGFP-, siLRP1-, siLRP2-, siLRP3-, siLRP4- and siLRP5-transfected Hep3B cells, from days 1 to 4 post-transfection. M: 100-bp ladder. The transfections were done independently in triplicate.

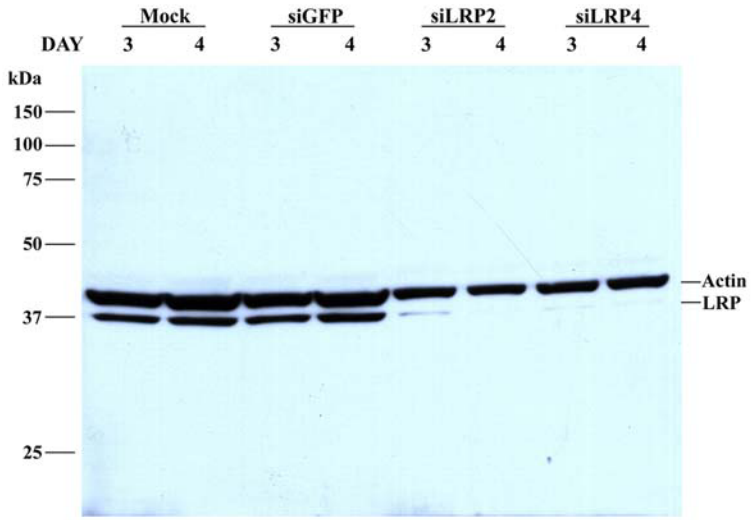

Fig. 3. Western blot analysis of the expression of 37LBP/67LR and actin. The expression levels of 37LBP/67LR and actin were simultaneously assessed by Western blot analysis for mock, siGFP-, siLRP2- and siLRP4-transfected Hep3B cells on days 3 and 4 post-transfection. The molecular weight in kDa is indicated. A representative gel of a duplicate experiment is shown.

Down-regulation of the 37LBP/67LR protein on days 3 and 4 post-transfection for mock, siGFP, siLRP2 and siLRP4 was investigated by Western blot analysis using a mixture of antibodies directed against actin and 37LBP/67LR. The experiment was done independently in duplicate. The results (Fig. 3) show a very significant reduction in the level of 37LBP/67LR protein in the cells transfected with siLRP2 and siLRP4 compared to the level seen in mock and siGFP-transfected cells. Notably, the level of actin was also reduced in siLRP2- and siLRP4-transfected cells as compared to mock and siGFP-transfected cells, again consistent with a loss of cells as a result of transfection with siLRP2 and siLRP4.

Observation of apoptosis in 37LBP/67LR knock-down Hep3B cells

To investigate whether silencing 37LBP/67LR was triggering apoptosis, both siLRP2 and siLRP4 were again transfected into Hep3B cells in parallel with a mock transfection as a control. On days 1 to 4 post-transfection, the samples were again harvested, and this time double-labeled with FITC-labeled annexinV and propidium iodide followed by analysis by flow cytometry (Fig. 4). The experiment was done independently in triplicate. The results showed a significant increase in Annexin V/propidium iodide-positive cells in cultures transfected with either siLRP2 or siLRP4 as compared to the mock transfected cultures, confirming that silencing 37LBP/67LR induces apoptosis in Hep3B cells. To confirm that the increase in the amount of apoptotic cells was associated with a loss in 37LBP/67LR protein, mock, siGFP-, siLRP2- and siLRP4-transfections were again undertaken, and this time, the cells were analyzed by flow cytometry on days 1 to 4 post-transfection by double staining with annexinV and an antibody directed against the 37LBP/67LR protein. This experiment was done independently in triplicate. The results (Fig. 5) show a significant increase in the percentage of AnnexinV+/37LBP/67LR- cells in the siLRP2 and siLRP4 transfections as compared to the mock and siGFP transfections, confirming that the cells undergoing apoptosis are those that have had the 37LBP/67LR protein down-regulated.

Besides its normal roles in mediating cellular adhesion and functioning as a member of the ribosomal translational machinery, the 37LBP/67LR protein has been implicated in a number of a pathological processes including metastasis (reviewed in [22]). It also functions as a receptor protein for a number of pathogenic agents including the prion protein [12] and several viruses [17-19]. As such, modulating the expression of 37LBP/67LR is an attractive prophylactic or therapeutic target. However, the induction of apoptosis in response to complete silencing of 37LBP/67LR, as shown here and previously for HeLa cells [26], suggests that this may not be a viable approach without specific targeting to avoid inducing apoptosis in non-tumorigenic cells. However, it should be noted that the induction of apoptosis in response to the down-regulation of 37LBP/67LR is limited to a small number of cell lines investigated, and this may not be the case for all cell types. In particular, the down-regulation

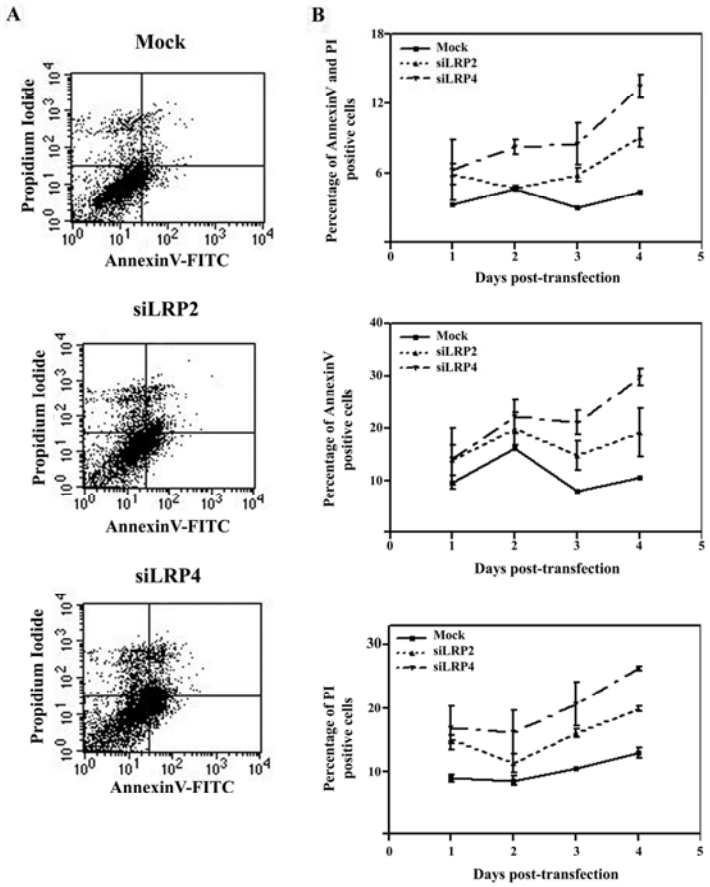

Fig. 4. Apoptosis detection by flow cytometry. A – Scattergrams of Hep3B cells 4 days after mock, siLRP2- or siLRP4-transfection, with double staining with annexinV and propidium iodide and analysis by flow cytometry. B – The results over days 1 through 4 of the flow cytometry analysis of Hep3B cells transfected with siLRP2 (dotted line) or siLRP4 (dashed line with one dot), or mock transfected (solid line), and stained with annexinV and propidium iodide. The graphs show the percentage of positive cells against the time point. The error bars represent the SEM of three experiments.

of 37LBP/67LR in the mouse brain is without apparent phenotypic abnormalities [28]. Given the high degree of over-expression of 37LBP/67LR in metastatic tumours [29], it is tempting to speculate that the expression of 37LBP/67LR is involved in maintaining a non-apoptotic state. As such, therapies that specifically target the cell surface-expressed protein [25], or that use viruses such as Sindbis, with 37LBP/67LR as their specific receptor protein [17], as the therapeutic agent [33] may well provide novel strategies for suppressing the growth of metastatic tumors.

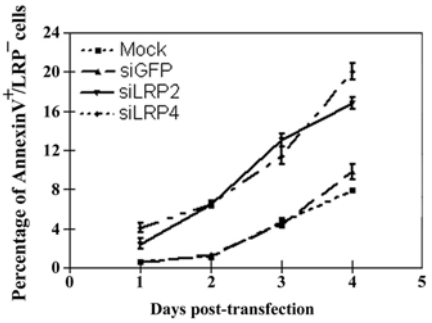

Fig. 5. Flow cytometric analysis of AnnexinV+/37LBP/67LR- cells. Flow cytometry was used to assess the percentage on days 1 through 4 of AnnexinV+/37LBP/67LR- cells of experimental populations that had been mock transfected, or transfected with siGFP, siLRP2 or siLRP4, and doubly stained with Annexin V and an antibody directed against the human 37LBP/67LR protein.

Acknowledgements. This study was supported by grants from Mahidol University and the Thailand Research Fund. Tharinee Susantad is the recipient of a Mahidol University Research Assistantship.

REFERENCES

1. Lesot, H., Kuhl, U. and Mark, K.V. Isolation of a laminin-binding protein from muscle cell membranes. **EMBO J.** 2 (1983) 861-865.
2. Malinoff, H.L. and Wicha, M.S. Isolation of a cell surface receptor protein for laminin from murine fibrosarcoma cells. **J. Cell Biol.** 96 (1983) 1475-1479.
3. Rao, N.C., Barsky, S.H., Terranova, V.P. and Liotta, L.A. Isolation of a tumor cell laminin receptor. **Biochem. Biophys. Res. Commun.** 111 (1983) 804-808.
4. Rao, C.N., Castronovo, V., Schmitt, M.C., Wewer, U.M., Claysmith, A.P., Liotta, L.A. and Sobel, M.E. Evidence for a precursor of the high-affinity metastasis-associated murine laminin receptor. **Biochemistry** 28 (1989) 7476-7486.
5. Yow, H.K., Wong, J.M., Chen, H.S., Lee, C.G., Davis, S., Steele, G.D., Jr. and Chen, L.B. Increased mRNA expression of a laminin-binding protein in human colon carcinoma: complete sequence of a full-length cDNA encoding the protein. **Proc. Natl. Acad. Sci. USA** 85 (1988) 6394-6398.
6. Tohgo, A., Takasawa, S., Munakata, H., Yonekura, H., Hayashi, N. and Okamoto, H. Structural determination and characterization of a 40-kDa protein isolated from rat 40 S ribosomal subunit. **FEBS Lett.** 340 (1994) 133-138.

7. Auth, D. and Brawerman, G. A 33-kDa polypeptide with homology to the laminin receptor: component of translation machinery. **Proc. Natl. Acad. Sci. USA** 89 (1992) 4368-4372.
8. Sato, M., Kinoshita, K., Kaneda, Y., Saeki, Y., Iwamatsu, A. and Tanaka, K. Analysis of nuclear localization of laminin binding protein precursor p40 (LBP/p40). **Biochem. Biophys. Res. Commun.** 229 (1996) 896-901.
9. Mecham, R.P., Hinek, A., Griffin, G.L., Senior, R.M. and Liotta, L.A. The elastin receptor shows structural and functional similarities to the 67-kDa tumor cell laminin receptor. **J. Biol. Chem.** 264 (1989) 16652-16657.
10. McCaffery, P., Neve, R.L. and Drager, U.C. A dorso-ventral asymmetry in the embryonic retina defined by protein conformation. **Proc. Natl. Acad. Sci. USA** 87 (1990) 8570-8574.
11. Rieger, R., Edenhofer, F., Lasmezas, C.I. and Weiss, S. The human 37-kDa laminin receptor precursor interacts with the prion protein in eukaryotic cells. **Nat. Med.** 3 (1997) 1383-1388.
12. Gauczynski, S., Peyrin, J.M., Haik, S., Leucht, C., Hundt, C., Rieger, R., Krasemann, S., Deslys, J.P., Dormont, D., Lasmezas, C.I. and Weiss, S. The 37-kDa/67-kDa laminin receptor acts as the cell-surface receptor for the cellular prion protein. **EMBO J.** 20 (2001) 5863-5875.
13. Gauczynski, S., Nikles, D., El-Gogo, S., Papy-Garcia, D., Rey, C., Alban, S., Barritault, D., Lasmezas, C.I. and Weiss, S. The 37-kDa/67-kDa laminin receptor acts as a receptor for infectious prions and is inhibited by polysulfated glycanes. **J. Infect. Dis.** 194 (2006) 702-709.
14. Ludewigs, H., Zuber, C., Vana, K., Nikles, D., Zerr, I. and Weiss, S. Therapeutic approaches for prion disorders. **Expert Rev. Anti. Infect. Ther.** 5 (2007) 613-630.
15. Vana, K., Zuber, C., Nikles, D. and Weiss, S. Novel aspects of prions, their receptor molecules, and innovative approaches for TSE therapy. **Cell. Mol. Neurobiol.** 27 (2007)107-128.
16. Zuber, C., Ludewigs, H. and Weiss, S. Therapeutic approaches targeting the prion receptor LRP/LR. **Vet. Microbiol.** 123 (2007) 387-393.
17. Wang, K.S., Kuhn, R.J., Strauss, E.G., Ou, S. and Strauss, J.H. High-affinity laminin receptor is a receptor for Sindbis virus in mammalian cells. **J. Virol.** 66 (1992) 4992-5001.
18. Thepparit, C. and Smith, D.R. Serotype-specific entry of dengue virus into liver cells: identification of the 37-kilodalton/67-kilodalton high-affinity laminin receptor as a dengue virus serotype 1 receptor. **J. Virol.** 78 (2004) 12647-12656.
19. Akache, B., Grimm, D., Pandey, K., Yant, S.R., Xu, H. and Kay, M.A. The 37/67-kilodalton laminin receptor is a receptor for adeno-associated virus serotypes 8, 2, 3, and 9. **J. Virol.** 80 (2006) 9831-9836.
20. Coggin, J.H. Jr., Barsoum, A.L. and Rohrer, J.W. 37 kiloDalton oncofetal antigen protein and immature laminin receptor protein are identical,

universal T-cell inducing immunogens on primary rodent and human cancers. **Anticancer Res.** 19 (1999) 5535-5542.
21. Zelle-Rieser, C., Barsoum, A.L., Sallusto, F., Ramoner, R., Rohrer, J.W., Holtl, L., Bartsch, G., Coggin, J.J. and Thurnher, M. Expression and immunogenicity of oncofetal antigen-immature laminin receptor in human renal cell carcinoma. **J. Urol.** 165 (2001) 1705-1709.
22. Castronovo, V. Laminin receptors and laminin-binding proteins during tumor invasion and metastasis. **Invasion Metastasis** 13 (1993) 1-30.
23. Castronovo, V., Claysmith, A.P., Barker, K.T., Cioce, V., Krutzsch, H.C. and Sobel, M.E. (1991). Biosynthesis of the 67 kDa high affinity laminin receptor. **Biochem. Biophys. Res. Commun.** 177 (1991) 177-183.
24. Buto, S., Tagliabue, E., Ardini, E., Magnifico, A., Ghirelli, C., van den Brule, F., Castronovo, V., Colnaghi, M.I., Sobel, M.E. and Menard, S. Formation of the 67-kDa laminin receptor by acylation of the precursor. **J. Cell. Biochem.** 69 (1998) 244-251.
25. Narumi, K., Inoue, A., Tanaka, M., Isemura, M., Shimo-Oka, T., Abe, T., Nukiwa, T. and Satoh, K. Inhibition of experimental metastasis of human fibrosarcoma cells by anti-recombinant 37-kDa laminin binding protein antibody. **Jpn. J. Cancer Res.** 90 (1999) 425-431.
26. Kaneda, Y., Kinoshita, K., Sato, M., Saeki, Y., Yamada, R., Wataya-Kaneda, M., and Tanaka, K. The induction of apoptosis in HeLa cells by the loss of LBP-p40. **Cell Death Differ.** 5 (1998) 20-28.
27. Leucht, C., Simoneau, S., Rey, C., Vana, K., Rieger, R., Lasmezas, C.I. and Weiss, S. The 37 kDa/67 kDa laminin receptor is required for PrP(Sc) propagation in scrapie-infected neuronal cells. **EMBO Rep.** 4 (2003) 290-295.
28. Leucht, C., Vana, K., Renner-Muller, I., Dormont, D., Lasmezas, C.I., Wolf, E. and Weiss, S. Knock-down of the 37-kDa/67-kDa laminin receptor in mouse brain by transgenic expression of specific antisense LRP RNA. **Transgenic Res.** 13 (2004) 81-85.
29. Ardini, E., Pesole, G., Tagliabue, E., Magnifico, A., Castronovo, V., Sobel, M.E., Colnaghi, M.I. and Menard, S. The 67-kDa laminin receptor originated from a ribosomal protein that acquired a dual function during evolution. **Mol. Biol. Evol.** 15 (1998) 1017-1025.
30. Knowles B.B., Howe, C.C. and Aden D.P. Human hepatocellular carcinoma cell lines secrete the major plasma proteins and hepatitis B surface antigen. **Science** 209 (1980) 497-499.
31. Elbashir, S.M., Harborth, J., Lendeckel, W., Yalcin, A., Weber, K. and Tuschl, T. Duplexes of 21-nucleotide RNAs mediate RNA interference in cultured mammalian cells. **Nature** 411 (2001) 494-498.
32. Hannon, G.J. RNA interference. **Nature** 418 (2002) 244-251.
33. Hurtado, A., Tseng, J.C. and Meruelo, D. Gene therapy that safely targets and kills tumor cells throughout the body. **Rejuvenation Res.** 9 (2006) 36-44.

Journal of Virological Methods 151 (2008) 325–328

Contents lists available at ScienceDirect

Journal of Virological Methods

journal homepage: www.elsevier.com/locate/jviromet

Short communication

Identification of dengue virus binding proteins using affinity chromatography

Supranee Upanan, Atichat Kuadkitkan, Duncan R. Smith*

Molecular Pathology Laboratory, Institute of Molecular Biology and Genetics, Mahidol University, Salaya Campus, 25/25 Phuttamonthol Sai 4, Salaya, Nakorn Pathom 73170, Thailand

ARTICLE INFO

Article history:
Received 16 January 2008
Received in revised form 26 March 2008
Accepted 6 May 2008
Available online 17 June 2008

Keywords:
Flavivirus
GRP78
Liver
Receptor
37/67 kDa high affinity laminin receptor

ABSTRACT

Several studies have identified putative dengue virus receptors using virus overlay protein binding assays (VOPBA) with some apparent success. Given that this technique relies upon the use of electrophoresis of proteins through polyacrylamide gels with varying amounts of protein denaturation, the physiological relevance of the proteins isolated is open to question. To address this issue a Sepharose 4B–dengue virus serotype 2-affinity column was constructed to selectively bind dengue virus binding proteins from HepG2 (liver) cell membrane preparations. Results show that GRP78, but not the 37/67 kDa high affinity laminin receptor, was specifically bound by the column. This result is consistent with earlier work and shows that while affinity chromatography may provide a useful adjunct to VOPBA based studies particularly in cases where proteins maybe sensitive to denaturation, proteins isolated by VOPBA can be physiologically relevant.

Dengue viruses are enveloped nucleocapsid spherical viruses of 40–50 nm in diameter that belong to the family *Flaviviridae*, genus *Flavivirus*, a genus that contains a number of important human pathogens (Leyssen et al., 2000). There are four antigenically distinct, but closely related, dengue virus serotypes (DEN-1, DEN-2, DEN-3, and DEN-4) with numerous virus strains found worldwide. Infection with any one of four dengue serotypes can causes either an asymptomatic infection or a spectrum symptomatic illness, ranging from an undifferentiated fever, dengue fever (DF), through to dengue hemorrhagic fever (DHF) or dengue shock syndrome (DSS).

The mature dengue virus virion contains three structural proteins: the core or capsid protein (C), a membrane-associated protein (M), and the envelope protein (E) and in order to infect target cells, the dengue virus utilizes its envelope glycoprotein or E protein, which contains the component responsible for target cell binding and fusion (Klasse et al., 1998; Modis et al., 2004), to interact with a specific receptor on the target cell surface.

Studies have suggested that monocytes, macrophages, B lymphocytes, T lymphocytes, hepatocytes, endothelial cells, epithelial cells, dendritic cells and fibroblasts are all potential targets for dengue virus infection and replication (Diamond et al., 2000; Kurane et al., 1990; Lin et al., 2000; Mentor and Kurane, 1997; Moreno-Altamirano et al., 2002; Palucka, 2000; Suksanpaisan et al., 2007; Tassaneetrithep et al., 2003; Wei et al., 2003) and dengue viral antigens have been detected in tissues including liver, spleen, lymph node, thymus, kidney, lung, and skin (Bhoopat et al., 1996; Jessie et al., 2004; Rosen et al., 1999). The liver seems to be a major target organ for dengue virus infection in humans since hepatomegaly, liver dysfunction, and pathologic findings including centrilobular necrosis, fatty change, Kupffer cell hyperplasia, acidophilic bodies, and monocyte infiltration of the portal tract have been detected in the livers of DHF/DSS patients (Bhamarapravati, 1989; Bhamarapravati et al., 1967; Burke, 1968; Wahid et al., 2000). The abnormal elevation of liver enzymes alanine aminotransferase (ALT) and aspartate aminotransferase (AST) levels observed in DHF patients is also suggestive of liver dysfunction (Nguyen et al., 1997; Wahid et al., 2000). In addition both dengue virus antigens (Huerre et al., 2001) as well as dengue virus RNA (Rosen et al., 1999) have been documented in liver specimens from fatal DHF cases (Rosen et al., 1999). The virus itself has been recovered from the liver of fatal cases of dengue infections (Rosen et al., 1989) and recently the productive infection of primary human hepatocytes with dengue virus serotype 2 has been documented (Suksanpaisan et al., 2007).

Two proteins, the 37/67-kDa high affinity laminin receptor (Thepparit and Smith, 2004) and GRP78 (Jindadamrongwech et al., 2004) have been identified as receptors on HepG2 (liver) cells for dengue virus serotypes 1 and 2 entry, respectively, although evidence suggests that GRP78 may not be the major receptor protein for dengue serotype 2 infection in HepG2 cells (Jindadamrongwech et al., 2004). Both of these proteins were identified initially through the use of virus overlay protein binding assays (VOPBA) a technique that relies on complete or partial denaturation of the proteins during the analysis, and as such can lead to doubts about the physiological relevance of the proteins isolated. To determine if VOPBA

* Corresponding author. Tel.: +66 2 800 3624; fax: +66 2 441 9906.
E-mail address: duncan_r_smith@hotmail.com (D.R. Smith).

0166-0934/$ – see front matter © 2008 Elsevier B.V. All rights reserved.
doi:10.1016/j.jviromet.2008.05.001

can indeed isolate physiologically relevant proteins a dengue virus serotype 2–Sepharose 4B affinity column was constructed to isolate binding proteins from membrane preparations of HepG2 (liver) cells. To ensure no contaminating cellular proteins were present in dengue virus preparations, dengue virus was initially concentrated through PEG precipitation and purified by discontinuous sucrose gradient centrifugation as described previously (Suksanpaisan and Smith, 2003). To construct the dengue virus serotype 2–Sepharose 4B affinity column, CNBr-activated Sepharose 4B freeze-dried powder (Amersham Biosciences, Piscataway, NJ) was prepared as recommended by the manufacturer. Subsequently 1.44×10^7 pfu of purified dengue virus serotype 2 (strain 16681) propagated in C6/36 cells was suspended in 2 ml of coupling buffer (0.1 M $NaHCO_3$ pH 8.3 containing 0.5 M NaCl). An aliquot of 30 μl of the dengue virus serotype 2-coupling solution was kept before the coupling solution was mixed with 0.4 g (approximately 1.5 ml of column volume) of the activated Sepharose 4B. The DEN-2–Sepharose 4B mixture was incubated at 4 °C for 6 h with gentle agitation. A further 30 μl of the DEN-2–Sepharose 4B coupling solution was removed at this point and coupling efficiency determined by quantitating the level of infectious virus in standard plaque assays (Sithisarn et al., 2003). Virus titers of 1.2×10^7 pfu/ml before coupling, and 4.4×10^5 pfu/ml after coupling suggested a coupling efficiency of approximately 90%. The amount of ligand (approximately 50 μg as assessed by Bradford assay) significantly lower than that recommended by the manufacturer was chosen to reduce non-specific protein–protein interactions. Under the coupling conditions used (pH, time, and temperature), approximately 20% natural loss of infectivity would be expected as determined previously (Sithisarn et al., 2003). Excess, unbound DEN-2 virus was washed away with 5 column volumes of coupling buffer, and any remaining active groups of CNBr-activated Sepharose 4B were blocked by adding 2 ml of 0.1 M Tris–HCl pH 8.0 and incubating at 4 °C for 6 h with gentle shaking. The DEN-2–Sepharose 4B column was washed with three cycles of alternating pH buffers (0.1 M sodium acetate pH 4.0 containing 0.5 M NaCl and 0.1 M Tris–HCl pH 8.0 containing 0.5 M NaCl) with 5 column volumes of each buffer. The column was further washed with 10 column volumes of binding buffer (0.1 M Tris–HCl pH 8.0) before use.

To prepare HepG2 membrane proteins, confluent HepG2 cells cultured as described elsewhere (Jindadamrongwech and Smith, 2004; Jindadamrongwech et al., 2004; Thepparit and Smith, 2004) were washed twice with PBS and the cells were detached by scraping in PBS. Cells were harvested by centrifugation at 1200 × *g* for 5 min at 4 °C in an Eppendorf tube. After discarding the supernatant, the cell pellet was resuspended in ice-cold modified buffer M (100 mM NaCl, 20 mM Tris–HCl pH 8.0, 2 mM $MgCl_2$, 1 mM EDTA, 0.2% Triton X-100, and 1× protease inhibitor cocktail) and lysed by vigorous vortexing. Subsequently organelle fractionation was performed by sequential differential velocity centrifugation as described previously (Jindadamrongwech and Smith, 2004; Jindadamrongwech et al., 2004; Thepparit and Smith, 2004). Briefly, nuclei and debris were removed by centrifugation at 600 × *g* for 3 min at 4 °C. The supernatant was further centrifuged at 6000 × *g* for 5 min at 4 °C to pellet membranous organelles and finally the supernatant was centrifuged at 24,000 × *g* for 10 min at 4 °C and from this step membrane proteins were pelleted and resuspended in modified buffer M. The proteins concentration was determined by the Bradford method (Bradford, 1976).

A total of 500 μg of HepG2 membrane proteins were dissolved in 2 ml of binding buffer, added onto the DEN-2–Sepharose 4B column, and incubated at 4 °C for 9 h with gentle agitation and unbound fractions were collected by washing the columns with 10 column volumes of binding buffer. Proteins were subsequently eluted from the column using 1 column volume of a step gradient of binding buffer containing NaCl concentrations of 0, 0.1, 0.5 and 1 M NaCl. Protein concentration of eluted fractions was too low to be measured directly by the Bradford method (Bradford, 1976) so fractions from the affinity column were concentrated by trichloroacetic acid (TCA) precipitation by adding bovine serum albumin fraction V (Research Organics, Cleveland, OH) to a final concentration of 5 μg/ml and TCA to 10% (v/v). The protein precipitates were placed on ice for 30 min and subsequently pelleted by centrifugation at 10,000 × *g* for 5 min at 4 °C. The pellet was finally resuspended in 0.1 M NaOH. Proteins were mixed with 1/5th volume of 5× loading buffer (62.5 mM Tris–HCl pH 6.8, 4% (w/v) SDS, 17.4% (v/v) glycerol, 100 mM DTT, and 0.1% (w/v) bromophenol blue), heated to 95 °C for 5 min and loaded onto 10% SDS-PAGE gels. After electrophoresis samples were transferred to solid matrix support (Schleicher & Schuell) before transfer using the Wet-Blot Electrophoretic Transfer cell (Bio-Rad, Hercules, CA). Nitrocellulose membrane was blocked with 5% skim milk in TBS for 1 h at room temperature and incubated with a 1:500 dilution of a rabbit polyclonal antibody directed against human GRP78 (H-129, Santa Cruz Biotechnology, Inc., Santa Cruz, CA) followed by incubation with a 1:2000 dilution of a horseradish peroxidase conjugated goat anti-rabbit IgG (31460 Pierce, Rockford, IL). Signal was developed using the ECL Plus western blotting analysis kit (Amersham Pharmacia Biotech, Piscataway, NJ). Western blot was run in parallel with a control nitrocellulose membrane with 150 μg membrane proteins transferred after electrophoresis through an identical gel system. Results (Fig. 1) show that a band of approximately 78 kDa was detected by the anti-GRP78 antibody in both the control strip and fractions E3 and E4 corresponding to elution with 0.5 and 1.0 M NaCl. To confirm proteins were still able to bind dengue serotype 2, filter was split between lanes E2 and E3 (to minimize amount of virus used) and used in a VOPBA reaction as described previously (Jindadamrongwech and Smith, 2004; Jindadamrongwech et al., 2004). Binding of the virus to the membrane fractions was consistent with previous reports (data not shown).

Filters were subsequently stripped and incubated with a 1:500 dilution of a goat polyclonal directed against the human 37/67 kDa high affinity laminin receptor (SC-21534, Santa Cruz Biotechnology, Inc.) for 2 h at room temperature followed by incubation with

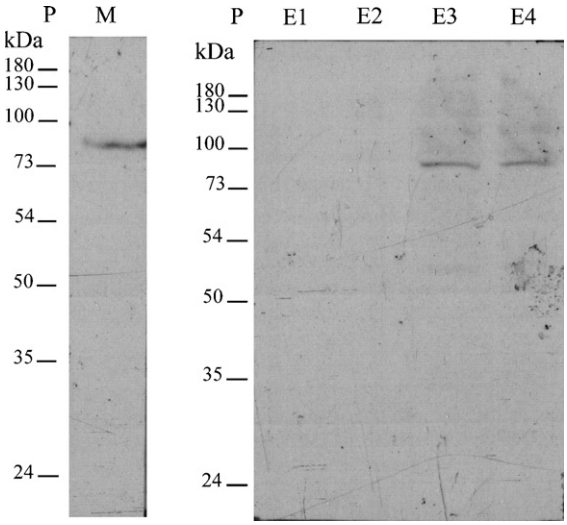

Fig. 1. Western blot of GRP78 after selection on a dengue serotype 2-affinity column. Nitrocellulose membranes with control membrane fraction (M) or elution fractions (E1, E2, E3, and E4) of a step gradient containing 0, 0.1, 0.5, and 1 M NaCl, were incubated with a polyclonal antibody directed against human GRP78 followed by a horseradish peroxidase labeled secondary antibody. Prestained protein marker (P) was used as a molecular mass marker as indicated.

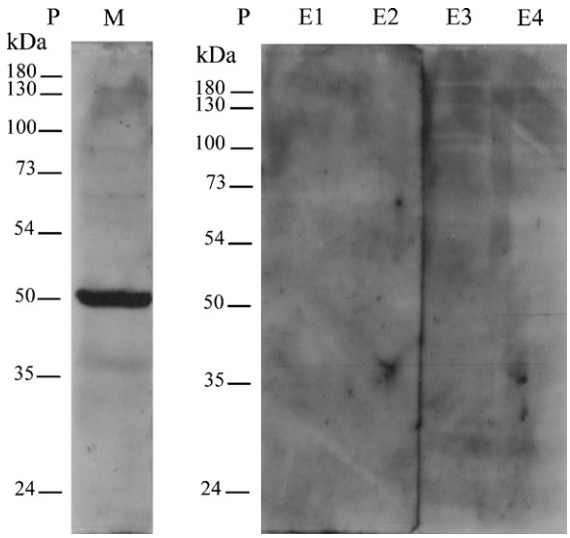

Fig. 2. Western blot of the 37/67 kDa high affinity laminin receptor after selection on a dengue serotype 2-affinity column. Filters used in Fig. 1 were stripped and re-probed with an antibody directed against the 37/67 kDa high affinity laminin receptor protein, followed by a horseradish peroxidase labeled secondary antibody. Prestained protein marker (P) was used as a molecular mass marker as indicated.

a horseradish peroxidase conjugated rabbit anti-goat IgG (31402, Pierce, Rockford, IL). Signal was developed as described previously. A single band of approximately 52 kDa was detected in the control strip with the antibody directed against the 37/67 kDa high affinity laminin binding protein while no band was seen in the NaCl eluted fractions (Fig. 2).

Virus overlay protein binding assays have previously identified GRP78 as a dengue virus serotype 2 receptor protein (Jindadamrongwech et al., 2004) and the 37/67 kDa high affinity laminin binding protein as a dengue virus serotype 1 receptor protein (Thepparit and Smith, 2004) expressed on the surface of HepG2 (liver) cells and shown that the interaction between the dengue virus and its cognate receptor is serotype specific (Jindadamrongwech et al., 2004; Thepparit and Smith, 2004). In this study affinity column chromatography was used to probe the interaction between dengue virus serotype 2 and HepG2 membrane proteins and results have again shown that there is a specific interaction between GRP78 and dengue virus serotype 2. As importantly, affinity chromatography again confirms the lack of an interaction between dengue virus serotype 2 and the 37/67 kDa high affinity laminin binding protein as proposed earlier (Thepparit and Smith, 2004) although other authors have proposed such an interaction occurs (Tio et al., 2005). This result suggests that while proteins maybe denatured as part of the virus overlay protein binding assay, the technique is still capable of selecting physiologically relevant binding molecules, possibly as a result of partial renaturation of the proteins during the overlay process. While column chromatography has been used by other to isolate putative dengue virus receptor proteins (Mercado-Curiel et al., 2006; Reyes-del Valle et al., 2005; Reyes-del Valle and del Angel, 2004) these studies have used significantly higher ligand concentrations (up to 10-fold higher) and as such have a much greater likelihood of isolating proteins through non-specific protein–protein interactions. The study here shows both that significantly lower ligand concentrations can be used to isolate dengue virus interacting proteins, and that the methodology is capable of discriminating serotype specific interactions. In contrast, previous studies (Mercado-Curiel et al., 2006; Reyes-del Valle et al., 2005; Reyes-del Valle and del Angel, 2004) have seen similar results for all four dengue serotypes. These results show that affinity chromatography can be used to investigate subtle interactions between the dengue viruses and their respective receptor or binding proteins and as such may play a role in future studies.

Acknowledgements

This work was supported by the Thailand Research Fund, Basic Research Grant number BRG4900010. AK is supported by a Thai Royal Golden Jubilee Research Scholarship.

References

Bhamarapravati, N., 1989. Hemostatic defects in dengue hemorrhagic fever. Rev. Infect. Dis. 11 (Suppl. 4), S826–S829.
Bhamarapravati, N., Tuchinda, P., Boonyapaknavik, V., 1967. Pathology of Thailand haemorrhagic fever: a study of 100 autopsy cases. Ann. Trop. Med. Parasitol. 61, 500–510.
Bhoopat, L., Bhamarapravati, N., Attasiri, C., Yoksarn, S., Chaiwun, B., Khunamornpong, S., Sirisanthana, V., 1996. Immunohistochemical characterization of a new monoclonal antibody reactive with dengue virus-infected cells in frozen tissue using immunoperoxidase technique. Asian Pac. J. Allergy Immunol. 14, 107–113.
Bradford, M.M., 1976. A rapid and sensitive method for the quantitation of microgram quantities of protein utilizing the principle of protein–dye binding. Anal. Biochem. 72, 248–254.
Burke, T., 1968. Dengue haemorrhagic fever: a pathological study. Trans. R. Soc. Trop. Med. Hyg. 62, 682–692.
Diamond, M.S., Edgil, D., Roberts, T.G., Lu, B., Harris, E., 2000. Infection of human cells by dengue virus is modulated by different cell types and viral strains. J. Virol. 74, 7814–7823.
Huerre, M.R., Lan, N.T., Marianneau, P., Hue, N.B., Khun, H., Hung, N.T., Khen, N.T., Drouet, M.T., Huong, V.T., Ha, D.Q., Buisson, Y., Deubel, V., 2001. Liver histopathology and biological correlates in five cases of fatal dengue fever in Vietnamese children. Virchows Arch. 438, 107–115.
Jessie, K., Fong, M.Y., Devi, S., Lam, S.K., Wong, K.T., 2004. Localization of dengue virus in naturally infected human tissues, by immunohistochemistry and in situ hybridization. J. Infect. Dis. 189, 1411–1418.
Jindadamrongwech, S., Smith, D.R., 2004. Virus overlay protein binding assay (VOPBA) reveals serotype specific heterogeneity of dengue virus binding proteins on HepG2 human liver cells. Intervirology 47, 370–373.
Jindadamrongwech, S., Thepparit, C., Smith, D.R., 2004. Identification of GRP 78 (BiP) as a liver cell expressed receptor element for dengue virus serotype 2. Arch. Virol. 149, 915–927.
Klasse, P.J., Bron, R., Marsh, M., 1998. Mechanisms of enveloped virus entry into animal cells. Adv. Drug Deliv. Rev. 34, 65–91.
Kurane, I., Kontny, U., Janus, J., Ennis, F.A., 1990. Dengue-2 virus infection of human mononuclear cell lines and establishment of persistent infections. Arch. Virol. 110, 91–101.
Leyssen, P., De Clercq, E., Neyts, J., 2000. Perspectives for the treatment of infections with Flaviviridae. Clin. Microbiol. Rev. 13, 67–82, table of contents.
Lin, Y.L., Liu, C.C., Lei, H.Y., Yeh, T.M., Lin, Y.S., Chen, R.M., Liu, H.S., 2000. Infection of five human liver cell lines by dengue-2 virus. J. Med. Virol. 60, 425–431.
Mentor, N.A., Kurane, I., 1997. Dengue virus infection of human T lymphocytes. Acta Virol. 41, 175–176.
Mercado-Curiel, R.F., Esquinca-Aviles, H.A., Tovar, R., Diaz-Badillo, A., Camacho-Nuez, M., Muñoz, M.L., 2006. The four serotypes of dengue recognize the same putative receptors in *Aedes aegypti* midgut and *Ae. albopictus* cells. BMC Microbiol. 6, 85.
Modis, Y., Ogata, S., Clements, D., Harrison, S.C., 2004. Structure of the dengue virus envelope protein after membrane fusion. Nature 427, 313–319.
Moreno-Altamirano, M.M., Sanchez-Garcia, F.J., Munoz, M.L., 2002. Non Fc receptor-mediated infection of human macrophages by dengue virus serotype 2. J. Gen. Virol. 83, 1123–1130.
Nguyen, T.L., Nguyen, T.H., Tieu, N.T., 1997. The impact of dengue haemorrhagic fever on liver function. Res. Virol. 148, 273–277.
Palucka, A.K., 2000. Dengue virus and dendritic cells. Nat. Med. 6, 748–749.
Reyes-del Valle, J., Chavez-Salinas, S., Medina, F., Del Angel, R.M., 2005. Heat shock protein 90 and heat shock protein 70 are components of dengue virus receptor complex in human cells. J. Virol. 79, 4557–4567.
Reyes-del Valle, J., del Angel, R.M., 2004. Isolation of putative dengue virus receptor molecules by affinity chromatography using a recombinant E protein ligand. J. Virol. Methods 116, 95–102.
Rosen, L., Drouet, M.T., Deubel, V., 1999. Detection of dengue virus RNA by reverse transcription-polymerase chain reaction in the liver and lymphoid organs but not in the brain in fatal human infection. Am. J. Trop. Med. Hyg. 61, 720–724.
Rosen, L., Khin, M.M., UT, 1989. Recovery of virus from the liver of children with fatal dengue: reflections on the pathogenesis of the disease and its possible analogy with that of yellow fever. Res. Virol. 140, 351–360.
Sithisarn, P., Suksanpaisan, L., Thepparit, C., Smith, D.R., 2003. Behavior of the dengue virus in solution. J. Med. Virol. 71, 532–539.
Suksanpaisan, L., Cabrera-Hernandez, A., Smith, D.R., 2007. Infection of human primary hepatocytes with dengue virus serotype 2. J. Med. Virol. 79, 300–307.

Suksanpaisan, L., Smith, D.R., 2003. Analysis of saturation binding and saturation infection for dengue serotypes 1 and 2 in liver cells. Intervirology 46, 50–55.
Tassaneetrithep, B., Burgess, T.H., Granelli-Piperno, A., Trumpfheller, C., Finke, J., Sun, W., Eller, M.A., Pattanapanyasat, K., Sarasombath, S., Birx, D.L., Steinman, R.M., Schlesinger, S., Marovich, M.A., 2003. DC-SIGN (CD209) mediates dengue virus infection of human dendritic cells. J. Exp. Med. 197, 823–829.
Thepparit, C., Smith, D.R., 2004. Serotype-specific entry of dengue virus into liver cells: identification of the 37-kilodalton/67-kilodalton high-affinity laminin receptor as a dengue virus serotype 1 receptor. J. Virol. 78, 12647–12656.
Tio, P.H., Jong, W.W., Cardosa, M.J., 2005. Two dimensional VOPBA reveals laminin receptor (LAMR1) interaction with dengue virus serotypes 1, 2 and 3. Virol. J. 2, 25.
Wahid, S.F., Sanusi, S., Zawawi, M.M., Ali, R.A., 2000. A comparison of the pattern of liver involvement in dengue hemorrhagic fever with classic dengue fever. Southeast Asian J. Trop. Med. Public Health 31, 259–263.
Wei, H.Y., Jiang, L.F., Fang, D.Y., Guo, H.Y., 2003. Dengue virus type 2 infects human endothelial cells through binding of the viral envelope glycoprotein to cell surface polypeptides. J. Gen. Virol. 84, 3095–3098.